THE EFFECTS OF SOIL STRENGTH AND SLOPE GEOMETRY PARAMETERS ON SLOPE STABILITY

TAN NIAN HAN

A project report submitted in partial fulfilment of the requirements for the award of Bachelor of Engineering (Honours) Civil Engineering

Lee Kong Chian Faculty of Engineering and Science
Universiti Tunku Abdul Rahman

May 2021

DECLARATION

I hereby declare that this project report is based on my original work except for citations and quotations which have been duly acknowledged. I also declare that it has not been previously and concurrently submitted for any other degree or award at UTAR or other institutions.

Signature :

Name : Tan Nian Han

ID No. : 1604932

Date : 8/5/2021

APPROVAL FOR SUBMISSION

I certify that this project report entitled **"THE EFFECTS OF SOIL STRENGTH AND SLOPE GEOMETRY PARAMETERS ON SLOPE STABILITY"** was prepared by **TAN NIAN HAN** has met the required standard for submission in partial fulfilment of the requirements for the award of Bachelor of Engineering (Honours) Civil Engineering at Universiti Tunku Abdul Rahman.

Approved by,

Signature : 

Supervisor : Dr. Chong Siaw Yah

Date : 8/5/2021

ACKNOWLEDGEMENTS

I would like to thank everyone who had contributed to the successful completion of this project. I would like to express my gratitude to my research supervisor, Dr. Chong Siaw Yah for her invaluable advice, guidance and her enormous patience throughout the development of the research.

In addition, I would also like to express my gratitude to my loving parents and friends who had helped and given me encouragement during my research.

ABSTRACT

Many slope failure incidents happened in Malaysia. One of the main causes of artificial slope failures was the inaccurate slope analysis due to the lack of understanding on the principles and factors affecting slope stability. In order to obtain an accurate prediction on the safety factor of slope (FS), correct slip surface prediction, proper soil strength and slope geometry parameters selection are essential. There are a lot of software programs available for slope stability analysis but excel spreadsheet is still commonly used in engineering practices as it is cheaper. The aim of this study was to study the factors affecting the slope stability. In this study, an Excel spreadsheet was developed for slope stability analysis using Simplified Bishop Method. Then, it was used to find the relationship between soil strength parameters and FS for the slope with a fixed surface of failure. Then, GEO5 software program was used to analyze minimum FS and determine the critical slip surface by applying different soil strength and slope geometry parameters. Lastly, results acquired were compared and discussed. It was found that with the increase of soil unit weight which acted as a driving force, the FS of slope decreased, the critical slip surface became larger and deeper with a longer length of failure arc. Whereas the soil cohesion and internal friction angle which contributed to the resisting force increased the FS of slope. Higher soil cohesion caused the critical slip surface to be larger and deeper; the length of failure arc also increased. As the soil internal friction angle increased, the critical slip surface became smaller and shallower, and length of failure arc decreased. Minimum FS increased significantly with the Beta, β angle but not much effect was observed for Alpha, α angle. The location and arc length of critical slip surface had not much difference with the increase of Beta, β angle. However, the critical slip surface became larger and deeper, and failure arc length increased when Alpha, α increased. When driving forces overcome resisting forces, the slope is unstable and will result in mass wasting. The dimensionless function λ which is related to γ, c, φ affected the slip surface. However, the slip surface remained unchanged with constant λ, although there was a change of shear strength parameter.

Keywords: Limit Equilibrium Method, Factor of Safety, Length of Failure Arc, Critical Failure Surface, Soil Slope Stability

TABLE OF CONTENTS

LIST OF TABLES

LIST OF FIGURES

LIST OF SYMBOLS / ABBREVIATIONS

AutoCAD	Automatic Computer Aided Design
c	Cohesion
FEM	Finite Elements Method
FLAC	Fast Lagrangian Analysis of Continua
FS	Factor of Safety
h	Height of Slope
L	Length of Failure Arc
le	Slope Surface Entry Distance
LEM	Limit Equilibrium Method
UW	Unit Weight
α	Angle of Slope
β	Angle of Slope
γ	Unit Weight
λ	Lambda
φ	Internal Friction Angle

CHAPTER 1

INTRODUCTION

1.1 General Introduction

Slope is generally divided into natural and artificial (man-made) slope. It is commonly encountered in construction project. The safety of people and state property badly threatened by slope failure. For the past decades, it was observed that there is increase of failure of slope in Malaysia. On 7 August 2011, in Kampung Sungai Ruil, Cameron Highlands happened a slope failure that brings devastating impact. On 21 May 2011, another major failure of slope took place in Hulu Langat. A reworked slope like in the Klang Valley Region (KVR) occurred slope failure which is in the urban areas. In the last 10 years, slope failures frequently happen and should be aware of (Thanapackiam & Khairulmaini, 2008).

An infinite slope is a slope that elongate for a comparatively long distance together with a consistent subsurface profile. For this case, the failure plane is parallel to the surface of slope. With that, method of limit equilibrium is applied readily. For designing a slope of constant with infinite extent, the term infinite slope is applied. An example of infinite slope is the long slope of the face of a mountain. On the other hand, slopes with limited extent are finite slopes. For example, the embankments and earth dams' slopes are finite slopes. For both two- and three-dimensions stability of slope, limit equilibrium method is most frequent approach applied to analyze. For a particular geotechnical situation, potential failure mechanisms are identified, and safety factor are derived by limit equilibrium method. The method of limit equilibrium are suitable for interpreting the stability of earth and rock dams, potential landslides, retaining walls, shallow and deep foundations, and surface mining sites.

At the beginning of this century, the investigations held in Sweden have clearly confirmed that the circular arc shape are resembled for the failure surface of earth slopes. It is called finite slope stability analysis with circular failure surface. A rotational slide is defined when soil slips along a circular surface. Rotational slide includes outward and downward movement of a slice of earth. Along the entire contact surface between the slice and its base, sliding occurred. Multiple two-dimensional stripes, or slices are divided for a slope are the method of slices. For each slice, the driving and resisting forces are computed. Both circular and planar slip surfaces are considered in this method such as Bishop, 1955. Slope stability analysis is a process of applying trial slip surface and calculating FS. Iterations were repeated until a smallest FS is obtained. Critical slip surface is surface of slip which produces the lowest safety factor.

Safety factor (FS) for stability of slope gives the meaning of the ratio of soil shear strength (resisting force) to maximum-armed shear stress (driving force) at potential failure surface. The soil strength parameters consist of cohesion, internal friction angle. Gravity and other factors (e.g. removal of load at slope's toe, additional loads at top of slope surface loads, seismic load, or seepage of water) contribute to the driving force in analysis of slope stability. The slope fails when the force of resistance is smaller than the force of driving (FS< 1).

Stability of slope is mainly governed by slope internal and external factors. Internal factors include soil strength at potential failure surface (e.g. cohesion and internal frictional angle) and slope geometry (e.g. slope height, slope inclination angle and slope shape). The external factors include the temperature and weathering changes, rainfall, earthquake, environment conditions of slope, tectonic stress, and artificial destruction (Wen, 2016).

Currently, many software programs (e.g. SLOPE/W, GEO5 and FLAC/SLOPE) are available for analysis of slope stability. However, it is essential to build up the knowledge on the principles of slope stability. Only if the correct slopes' critical slip surface and accurate soil parameters of shear strength are adopted in slope stability analysis, the FS for slope can be correctly predicted (Cheng, 2003). It is also important to understand the factors affecting the slope stability, especially the soil strength and slope geometry. If the factors affecting slope stability are well-considered during the design stage, an economical and sustainable design can be produced. With addition of the good understanding on external factors, it can help to predict the possible slope failure in future at the project planning and design stages.

1.2 Importance of Study

A spreadsheet to compute FS for the slope stability analysis applying Simplified Bishop method is developed. Although there is many softwares available, the development of this spreadsheet is considered important because it is a platform that is more user friendly and easy to understand by the engineers. It can help the user to understand better on the principles of slope stability analysis as detailed theory and steps are provided in the excel spreadsheet. Other than that, it is a cheaper alternative of the available software.

In this study, it increases the understanding on the factors governing the slope stability, especially soil strength and slope geometry. The relationship of each parameter on slope stability and slip surface are studied. With better understanding of influence of soil strength and slope geometry on slope stability, better consideration is taken during the planning and design stage to prevent or reduce slope failure. Sustainable and economical design can be produced with deeper understanding of factor affecting the slope stability.

1.3 Problem Statement

Even though many softwares are available, excel spreadsheet created are useful because of the license of software are usually expensive. Not only that, it is important to master the knowledge on the principles of slope stability. For producing accurate prediction of safety factor, only applicable when the correct slip surface and soil strength parameter are used. Without the further understanding of knowledge, a design will be costly and not environmentally friendly. Lack of understanding on slope stability principles will also cause the prediction of slope failure to be not accurate for future and some unforeseen effects may happen.

Many slope failure incidents happened in Malaysia nowadays. Internal factors and external factors are factors that affect the slope stability. The controlling factors of slope stability include shape of the structure surface, soil type, and the relationship with the slope surface. Slope are mostly destroyed by the rainfall. The slope stability is reduced by increasing the surface porosity, softening the soil, and reducing the intensity. Earthquake generates additional horizontal earthquake force that caused decrease of the slope stability. Human activity is the external cause of slope stability. Currently, changes in topography and natural vegetation are caused by improper use of slope. Digging, deforestation of natural vegetation and filling will have resulted in steepening of slope gradient. The slope collapse accident is accelerated due to loss of soil and water conservation function. The slope stability will be affected with poor maintenance and the slope protection facilities are not improper. With that, improvement on slope design and analysis should done. To solve the problem faced, understanding the internal factors (slope geometry and soil strength parameter) and external factors should be improved by geotechnical engineers.

1.4 Aim and Objectives

The aim of this study was to study the factors affecting the slope stability analysis. The objectives to achieve the aim were:

i) To develop an Excel Spreadsheet for slope stability analysis

ii) To investigate the effects of soil strength on safety factor of slope with fixed slip surface

iii) To investigate the effects of soil strength and slope geometry parameters on critical slip surface and minimum safety factor.

1.5 Contribution of the Study

Currently, many software products are accessible for analysis of slope stability. However, it is important to build up the knowledge on the principles of slope stability. Safety factor for slope only can be predicted correctly if the correct slopes' critical slip surface and accurate parameters of soil shear strength are adopted in analysis of slope stability using GEO5 software. If the factors affecting slope stability are well-determined during the design stage, an economical and sustainable design can be produced. So, it is important to understand the factors affecting the slope stability, especially the soil strength and slope geometry.

A Microsoft Excel spreadsheet to determine FS for analysis of slope stability using Simplified Bishop method was developed. It is a platform that is more user friendly and easy to be understood by the engineers. It can help the user to have a greater perception on principles of slope stability analysis as detailed theory and steps were provided in the excel spreadsheet. Other than that, it will be cheaper alternative of the available software. Moreover, it will help to predict the possible slope failure in future at the project planning and design stages with good understanding on external factors.

1.6 Scope and Limitation of the Study

The scope of this research included the development of an Excel spreadsheet to calculate the FS of a slope with fixed slip surface using Bishop Simplified Method. Parameters can be varied in the spreadsheet (e.g. soil layers, soil properties: unit weight, c, phi, slope angle etc.). Simplified Bishop Method is one of the simplest methods of limit equilibrium for analysis of slope stability. It assumes that the resultant of interslice force is in horizontal direction and there is no interslice shear force. Statistically equilibriums in vertical force and moment balance are fulfilled in this analysis. Choosing the Simplified Bishop method for this research for the convenience of this study, the general approach presented in this report may be applied to any other method.

By using the excel spreadsheet, the effect of soil strength on the slope stability for a fixed slip surface are studied. The parameters studied were cohesion, unit weight of soil, and angle of internal friction. Parameter effects are investigated by comparing the safety factor computed. The results obtained were tabulated and graph were generated to find the relationship between each parameters and safety factor. However, this study was limited to homogeneous soil. No groundwater table effect was studied as the groundwater table was assumed far below the slope level.

GEO5 software program was used to investigate the influence of soil strength parameter and slope geometry on critical surface of slip and FS. For this part, parameters studied were unit weight, cohesion, and angle of internal friction, slope angle together with combined effect of soil strength. By analyzing the safety factor, failure surface and failure arc length computed, the parameter effects are investigated. The results obtained were tabulated and graph are generated to find the relationship between each parameters and safety factor and critical surface. However, homogeneous soil was assumed in the study. Like the excel spreadsheet, the groundwater table was assumed far below the slope level and groundwater table effect was ignored.

1.7 Outline of the Report

This report consists of 5 chapters. Chapter 1 outlines the background of research, problem statements, objectives, importance of study, scope and limitation of the study.

Chapter 2 outlines the literature review of slope stability analysis for finite slope with circular failure, including FS and slip surface. Different analysis methods (e.g. Simplified Bishop method, Ordinary Method of Slices and Spencer method) are also discussed. For second part of this chapter, it covers the factors affecting slope stability which consist of the internal factors and external factors. Next, this chapter outlines unit weight, soil strength (cohesion, and internal friction angle), geometry parameter (e.g. Slope angle, Alpha and Beta) and combined influence of soil strength (λ) influence on slope stability and surface of failure. Introduction on the common software for slope stability analysis such as GEO5 and SLOPE/W are also covered in this chapter.

In Chapter 3, methods, excel spreadsheet, materials together with software programs which had been used in the study are demonstrated.

Chapter 4 outlines the modelling results of parameters’ effects on safety factor and critical slip surface (e.g. failure arc length) and discussion on them.

In Chapter 5, conclusions of the study are made. Lastly, references and research resources are presented.

CHAPTER 2

LITERATURE REVIEW

2.1 Introduction

This chapter shows a briefing introduction on slope stability analysis methods for finite slope with circular failure (method of slices). Factor of safety, slip surfaces, and some common software used for slope stability analysis are explained. Both internal (e.g. soil strength and slope geometry) and external factors affecting the slope stability are discussed. The influence of soil strength and slope geometry on slope stability are also critically reviewed.

2.2 Slope Stability Analysis for Finite Slope with Circular Failure

For analyzing the slope stability, several different methods are available to apply. Thus it all depends on engineer to choose the method to apply (Albataineh, 2006). Two major groups are divided by these methods (Finite Element Methods, FEM and Limit Equilibrium Methods, LEM). For safe design of constructed or natural earth slopes, slope stability analysis applying LEM is the basic principles. For certain situation of geotechnical, Limit Equilibrium Method are used to find mechanisms of potential failure and safety factors. LEM is a suitable way for analyzing the stability of surface mining sites, earth and rock dams, retaining walls, shallow and deep foundations, and potential landslides. Like LEM, Finite element methods uses a similar failure mechanism. However, these methods do not require the simplified assumptions by applying the power of finite element.

In the 1970s, Fredlund from the University of Saskatchewan developed a general limit equilibrium (GLE) formulation (Fredlund and Krahn 1977; Fredlund et al. 1981). Framework for understanding, describing, and discussing all methods are provided by formulation of GLE. By assuming range of interslice shear normal force, GLE is depends on 2 FS equations. 1 equation generates the FS depends on moment equilibrium (Fm). On the other hand, next equation generates FS depends on horizontal force equilibrium (Ff). Following the work of Spencer, the concept of applying two equations of safety factor are applied (Spencer, 1967). Equation introduced by Morgenstern and Price (1965) are used for forces of interslice shear in GLE formulation. The equation is:

$$X = E\lambda f(x) \tag{2.1}$$

X = Shear force of interslice, kN

E = Normal force of interslice, kN

λ = The percentage of the function used (in decimal form)

f(x) = A function

The GLE safety factor equation depends on moment equilibrium is:

$$F_m = \frac{\sum(c'\beta R+(N-u\beta)R\ tan\varphi'}{\sum Wx-\sum Nf\pm\sum Dd} \tag{2.2}$$

FS equation depends on horizontal force equilibrium is:

$$FS = \frac{\sum(c'\beta cos\alpha+(N-u\beta)tan\varphi'\ cos\alpha}{\sum Nsin\alpha-\sum Dcos\omega} \tag{2.3}$$

c' = Effective cohesion, kPa

f, d, x, ω, β, R = Parameters of geomtery

N = Normal force of slice base, kN

W = Slice weight, kN

φ' = Effective internal friction angle, °

D = Concentrated point load, kN

u: Pore-water pressure

α: Inclination of slice base, °

Over the years, for the method of slices, many different solution techniques are developed. However, all methods are very similar basically.

Depending on statics equation included, there are differences between methods. Not only that, the relationship between the normal forces and interslice shear are also one of the differences. A particular sliding mass was sliced and possible forces performed on the slice is shown in Figure 2.1.

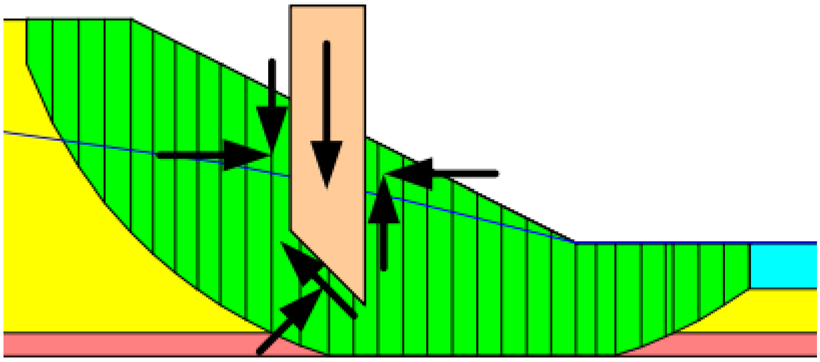

Figure 2.1: Slice forces and slice discretization in a sliding mass (Kramer, 1996).

First method developed was Fellenius or Ordinary method. However, it satisfied only equilibrium of moment and ignored forces of interslice. Using hand calculations, it is possible to calculate a safety factor by applying these simplified assumptions. It is important when there were no availability of computers. After that, Bishop (1955) ignored the interslice shear forces and devised a concept included interslice normal forces. Same to previous method, only moment equilibrium is satisfied by Bishop's Simplified method. The safety factor equation became nonlinear. To compute safety factor, an iterative procedure was needed by including normal interslice forces. Janbu's Simplified method like Bishop's Simplified method, ignored forces of interslice shear and included forces of normal interslice. However, opposed to moment equilibrium in Simplified Bishop method, Janbu's Simplified methods satisfied only equilibrium of horizontal force.

Later, iterative process in LEM are easier to compute by computers. With that, it brought to mathematically more rigorous formulations that satisfied all equations of statics and included all interslice forces. Morgenstern-Price and Spencer methods are two of the methods. However, for this study, Simplified

Bishop method are discussed in this section due to the method are easier to apply in excel spreadsheet created. To make it standardize, Simplified Bishop method are also used in the analysis using GEO5 software.

2.2.1 Ordinary Method of Slices

Ordinary method of slices technique is "Fellenius' Technique", developed by Fellenius in year 1927 (Budhu, 2010). This method satisfied the moment equilibrium but does not satisfy horizontal or vertical forces equilibrium. In this method, the resultant of inter-slices forces is ignored. This method solution can be completing by using calculator. Figure 2.2 shows the slip surface and forces in a slice for Ordinary method of slices.

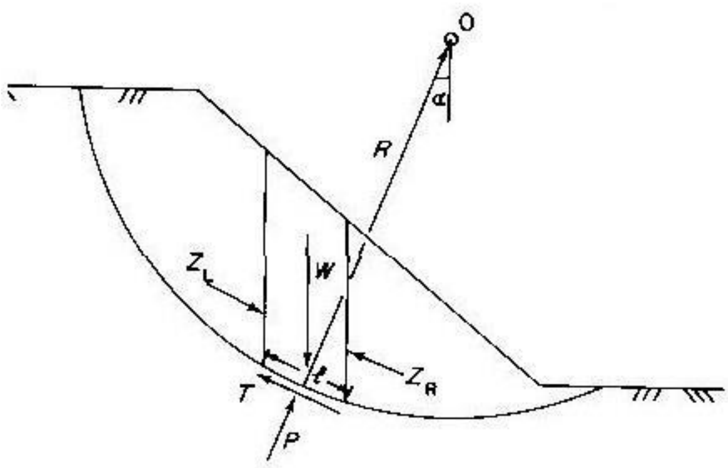

Figure 2.2: Ordinary Method of Slices (Anderson and Richards, 1987).

Based on failure criterion of Mohr-Coulomb, shear strength is defined in Equation 2.4.

$$s = c' + (\sigma - u)\ \tan\varphi' \qquad (2.4)$$

Where,

s = Shear strength

c' = Cohesive strength, kPa

φ' = Angle of internal friction, °

u = Pore water pressure

σ = Total stress, kPa

Let $t = s/F$, $p = s \times l$ and $T = t \times l$. By adding a factor of safety, FS to Equation 2.5 :

$$T = \frac{1}{FS}\ (c'\ l + (p - ul)\ \ tan\varphi') \qquad (2.5)$$

Where,

t = Tolerance of soil

T = Tangent force, kN

l = Slice length, m

p = Normal force, kN

FS = Safety factor

By neglecting forces of interslice, normal forces on the slice base were computed by using Equation 2.6:

$$P = wcos\alpha \qquad (2.6)$$

Where,

P = Normal force, kN

α = The angle between slice base's tangent center and global horizontal, °

W = The slice's weight, kN

The moment at the center of the slope failure shape were computed by Equation 2.7:

$$\sum WRsin\alpha = \sum TR \qquad (2.7)$$

W = Slice's weight, kN

R = Radius, m

Hence the safety factor (FS) were computed by using Equation 2.8:

$$FS = \frac{\sum(c\prime\, l+(wcos\alpha-ul)\ tan\varphi\prime)}{\sum Wsin\alpha} \tag{2.8}$$

It is necessarily to know failure surface before Ordinary method is applied to compute the slope's safety factor (Anderson and Richards, 1987). According to Whitman and Bailey (1967), this method is more conservative; the FS of slope calculated by using this method is 60 % smaller compared to other methods. As a result, nowadays this technique is less applied.

2.2.2 Simplified Bishop Method

Acknowledged by all those engineering professions, the most widely applied analysis of slope stability method is the Simplified Bishop method (Bishop, 1955). It assumed that rotation of a circular mass of soil caused the slope failure, as shown in Figure 2.3. The forces between the slices are also assumed acting at horizontal direction. Between slices, there is no active shear stress. The effective normal force, N′ or P, are discovered although magnitude on both sides of slide for the horizontal forces is not known, even by taking into each slice's vertical equilibrium. Normal force of each slice, P, can be computed using Equation 2.9 and is assumed to act at each base's center.

$$P = \frac{[W-\frac{1}{FS}(c\prime\, lsin\alpha-ultan\varphi\prime\, sin\alpha)]}{m\alpha} \tag{2.9}$$

Where,

$$m\alpha = cos\alpha + \frac{(sin\alpha tan\varphi')}{FS} \tag{2.10}$$

W = Slice Weight, kN

α = The angle between slice base's tangent center and global horizontal, °

FS = Safety factor

c' = Cohesive strength, kPa

u = Pore water pressure

φ' = Internal friction angle, °

l = Slice length, m

Moment are taken about center of circle:

$$FS = \frac{\sum[\frac{c' \, lcos\alpha + (w - ulcos\alpha) \, tan\varphi'}{cos\alpha + \frac{sin\alpha tan\varphi'}{FS}}]}{\sum W sin\alpha} \tag{2.11}$$

In Equation 2.11, FS appears on both sides of equation. FS in simplified Bishop method can only be solved iteratively. Hand calculations is satisfactory for this method. The benefit of this procedure is that it is normally fast and provides a relatively precise answer. Compare to FEM methods, the accuracy is also high with 5 percent of dissimilarity only. (Anderson and Richards, 1987).

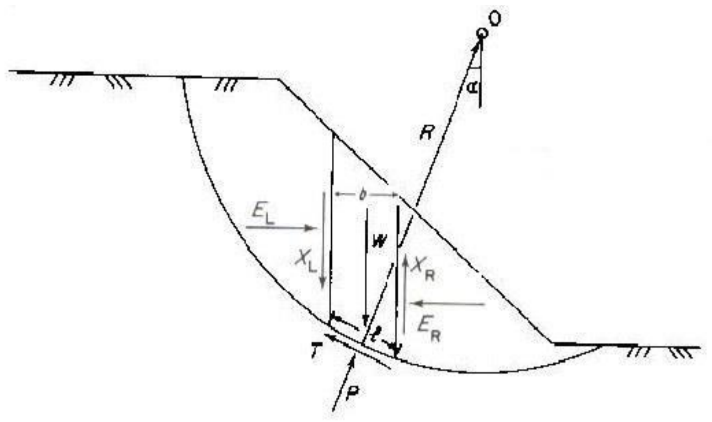

Figure 2.3: Simplified Bishop Method (Anderson and Richards, 1987).

First, it needs to design the failure surface just like the other methods. At the vertical direction, all forces are achieved statical equilibrium. Figure 2.4 shows the forces acting on slice for Simplified Bishop method and reveals one of the slices to be analyzed. The effective normal forces are calculated applying Equation 2.12.

$$N' = \frac{FS(W' + Lsin\alpha) - c' \, btan\theta}{FScos\theta + sin\theta tan\varphi'} \tag{2.12}$$

Where,

W’ = W – ub

N’ = Normal force, kN

W’ = Slice Weight, kN

Ub = uniform force acts on slope, kN/m

θ = Angle of slope horizontal, °

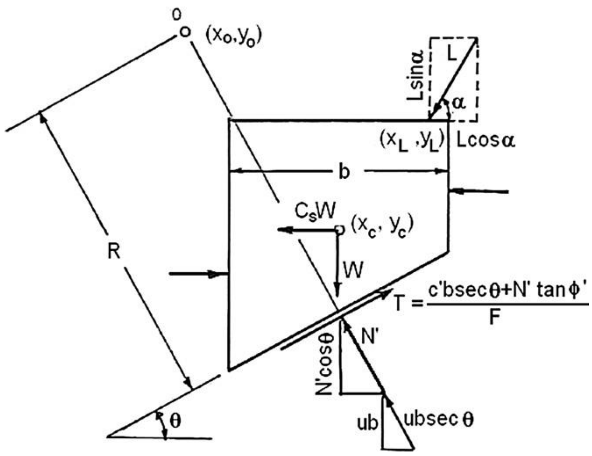

Figure 2.4: Forces on a slice for simplified Bishop method (Anderson and Richards, 1987).

For W′ = W – ub, Safety factor (FS) are determined for non-circular and circular failure surfaces by knowing N′. In Equation 2.12, tan ϕ′ should be changed to 0 if N′ is negative. Factor of safety (FS) based on N′ in Equation 2.12. An iteration method were applied to solve the safety factor, FS. First, a trial FS is assumed to compute N′ by using Equation 2.12. Then, a new computed FS is obtained and compared with the assumed FS. The process were repeated until assumed safety factor was similar with computed FS. With help of Newton's method of tangent, FS came together very fast. It usually can be obtained in two or three iterations (Wang, 2020).

2.2.3 Spencer's Method

The most clarified method is the Spencer method (Spencer, 1973). All the equations of equilibrium are satisfied. For the right-hand side of the slice, the normal case with shear force, S and normal force, E was shown in Figure 2.5. ΔE and ΔS are the left and right-hand sides' dissimilarity in normal and shear forces. Although same to original Spencer method, assumption of S = E tan δ. However, the base of each slice at the midpoint, the moment is taken. S = 0 is assumed. Determine the tangential force, T, the normal forces, E and N′, and safety factor, FS depend on force equilibrium. Calculate shear forces, S new set and the angle of inclination, δ depend on the equilibrium of force.

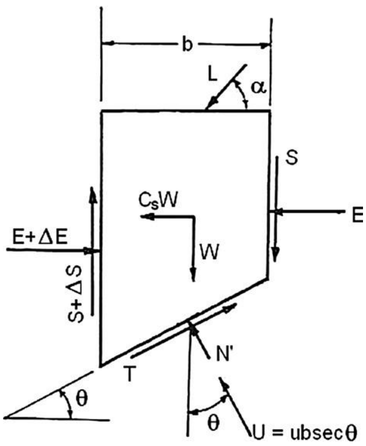

Figure 2.5: General case of forces on a slice (Anderson and Richards, 1987).

Until safety factor come together, process is repeated by using new set of S and the FS obtained. Close to the Morgenstern-Price Method (Morgenstern and Price, 1965), presumed shear forces, S by the Spencer method, based on function f(x), change from slice to slice, not different with the normal forces, E only but between the slices shown in Equation 2.13.

$$S = \lambda f(x)E \qquad (2.13)$$

Where,

S = Shear force, kN

E = Normal force, kN

in which *f(x)* be constant and unknown constant λ to find out. At each vertical side, it can either numerical value, linear function, or sine curve. With *f(x)* = 1 and λ = tan δ, an exceptional case of Morgenstern-Price is the Spencer method. However, there are more flexibility in the assumptions of Morgenstern-Price Method for interslice forces' inclination compared to the Spencer Method. On computed safety factor, during static equilibrium is fulfilled, there is very little effect for the assumption.

Originally, in circular failure surface, Spencer's method was applied. However, for non-circular slips, with the assumption of a frictional center of rotation, it has been easily extended. They will have same inclination by assuming parallel interslice forces in Equation 2.14:

$$tan\theta = \frac{X_1}{E_1} = \frac{X_R}{E_R} \qquad (2.14)$$

Where,

θ = Interslice forces angle from horizontal, °

In Equation 2.15, the normal force on slices base which perpendicular to forces of interslice was summed will be:

$$P = \frac{W-(E_R-E_1)tan\theta-1/FS(c\prime\ lsin\alpha-ultan\varphi\prime\ sin\alpha)}{m\alpha} \qquad (2.15)$$

Where,

$$m\alpha = cos\alpha\ (1 + tan\alpha \frac{tan\varphi\prime}{FS}) \qquad (2.16)$$

E_R = Normal force, kN

FS = Safety Factor

c' = Cohesion, kPa

φ' = Internal Friction Angle, °

l = Length of each slice, m

In Figure 2.6, 2 different factors of safety will be derived by considering overall moment and force equilibrium. This is due to total assumptions are made for the problem is over specified. FS from equilibrium of moment, by taking moment about O in Equation 2.17:

$$\sum WR sin\alpha = \sum TR \quad (2.17)$$

Where,
P = Normal force, kN
u = Pore water pressure

$$T = \frac{1}{FS}(c'\, l + (p - ul)\ tan\varphi') \quad (2.18)$$

$$FS = \frac{\sum(c'\, l + (p - ul)\ tan\varphi')}{\sum W sin\alpha} \quad (2.19)$$

By considering ΣFH=0, the safety factor from force equilibrium:

$$T cos\alpha - P sin\alpha + ER - EL = 0 \quad (2.20)$$

$$\sum ER - EL = \sum P sin\alpha - 1/FS \sum(c'\, l + (P - ul)\ tan\varphi')\ cos\alpha \quad (2.21)$$

In absence of surface loading, using the Spencer's assumption (tanθ=Xl/El=cte) and $\Sigma XR - XL$=0 in Equation 2.22:

$$FS = \frac{\sum(c'\, l + (P - ul)\ tan\varphi')\ sec\alpha}{\sum(W - (X_R - X_L))\ tan\alpha} \quad (2.22)$$

According to Spencer (1967), with satisfying both equations for determination of the safety factor, trial and error method applied. Both equations obtained FS values that is equal, which was examined by Spencer and showed interslice forces' proper angle. The safety factor will be considered for the value. Most importantly, having the correct failure surface in this method.

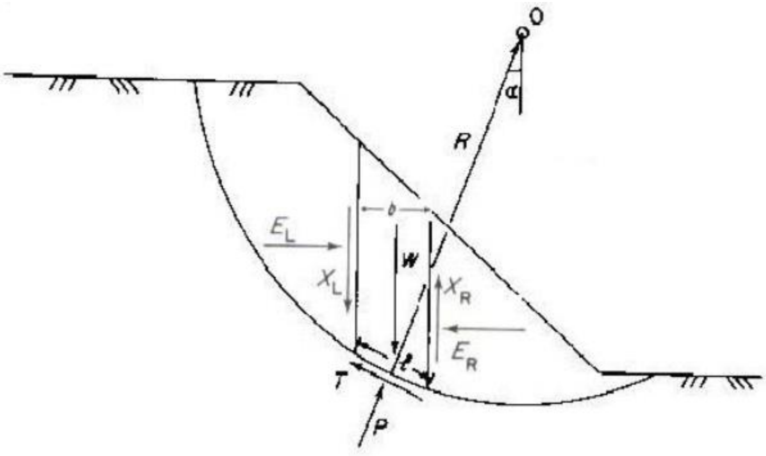

Figure 2.6: Spencer's Method (Anderson and Richards, 1987).

Force Equilibrium of Each Slice

For direction of vertical, equilibrium forces,

$$N' = (W' - \Delta S)sec\theta - Ttan\theta + Lsin\alpha sec\theta \qquad (2.23)$$

Where,

N' = Normal force, kN

W' = W – ub

W = Slice weight, kN

T = Tangential shear force, kN

L = Length of slice, m

ΔS = Right-hand sides' dissimilarity in normal and shear forces

Equation can be rewritten without subscript i as,

$$T = \frac{c' bsec\theta + N' tan\varphi'}{FS} \qquad (2.24)$$

Shear force, *T*, are determined from Equation 2.24,

$$T = \frac{c' bsec\theta + [(W' - \Delta S)sec\theta + Lsin\alpha sec\theta]tan\varphi'}{FS + tan\theta tan\varphi'} \qquad (2.25)$$

In horizontal direction, equilibrium forces,

$$\Delta E = (W - \Delta S)tan\theta - Tsec\theta + CsW + L(sin\alpha tan\theta + cos\alpha) \qquad (2.26)$$

Since, it must satisfy the overall horizontal force equilibrium,

$$\sum \Delta E = P2 - P1 \qquad (2.27)$$

Where,
P1 & P2: Pressure force, Pa

At both ends, if there is no water pressure, *P1* and *P2* may be zero.

$$FS = \frac{\sum\{c' bsec\theta + [(W' - \Delta S)sec\theta - Ttan\theta + Lsin\alpha sec\theta]tan\varphi' \}sec\theta}{\sum(W - \Delta S)tan\theta + Cs\sum W + \sum L(sin\alpha tan\theta + cos\alpha) - (P2 - P1)} \qquad (2.28)$$

For determination of safety factor in Spencer method, Equation 2.25 in conjunction with Equation 2.28 can be used. From the moment equilibrium, the evaluation of unknown ΔS, which contained in both equations was done. From Equation 2.25, the value of *T* obtained must not be negative. tan $\phi' = 0$ in Equation 2.25 and Equation 2.28, if $T < 0$.

Moment Equilibrium of Each Slice

Forces involved in moment equilibrium is shown in Figure 2.7. It is assumed that the side forces, Z_1 and Z_2, are applied at h_1 and h_2 above the base. Obtained the following equation by calculating the moment at the base midpoint:

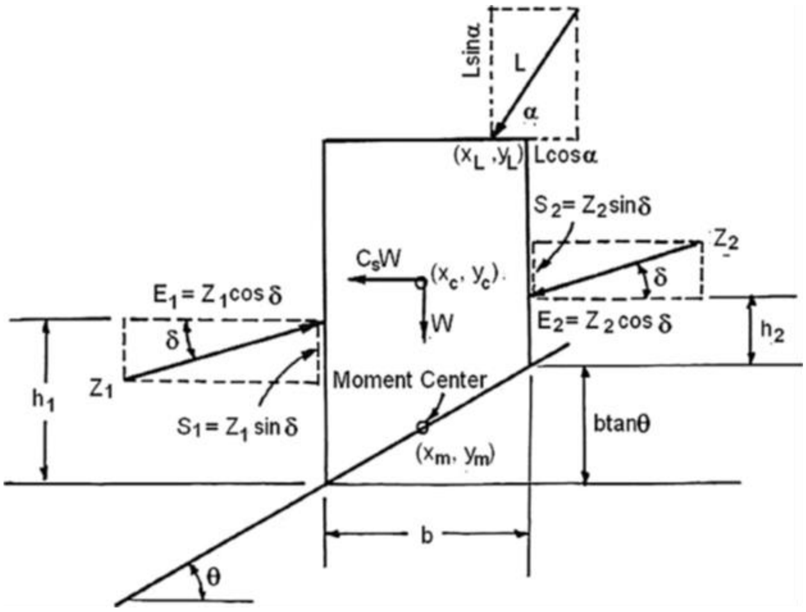

Figure 2.7: Forces for moment equilibrium based on the Spencer method (Anderson and Richards, 1987).

$$Z_1 cos\delta(h_1 - \frac{b}{2}\, tan\theta) + \frac{b}{2}\,(Z_1 sin\delta + Z_2 sin\delta) + Lsin\alpha(x_L - x_m)$$
$$-Lcos(y_L - y_m) - CsW(y_c - y_m) - Z_2 cos\delta(h_2 + \frac{b}{2}\, tan\theta) = 0 \tag{2.29}$$

Where,

B = Base length, m

h = Height, m

Z_1 & Z_2 = Acting force from left and right, kN

E_1& E_2 = Normal force from left and right, kN

Δ = Angle from horizontal, °

Moving h_2 to one side and substituting Z_1 by $E_1/\cos\delta$ and Z_2 by $E_2/\cos\delta$,

$$h_2 = \left(\frac{E_1}{E_2}\right)h_1 + \frac{b}{2}\left(1 + \frac{E_1}{E_2}\right)(tan\delta - tan\theta) - \frac{CsW(y_c - y_m)}{E_2} + \frac{L[sin\alpha(x_L - x_m) - cos\alpha(y_L - y_m)]}{E_2} \tag{2.30}$$

According to the known or computed value of h_1, to determine h_2, Equation 2.30 can be applied for all intermediate slices. Equation 2.30 should be modified for the first slice shown in Figure 2.8(a):

$$h_2 = \left(\frac{P_1}{E_2}\right)h_1 - \frac{b}{2}\left(1 + \frac{P_1}{E_2}\right)tan\theta + \frac{b}{2}\,tan\delta - \frac{CsW(y_c - y_m)}{E_2} + \frac{L[sin\alpha(x_L - x_m) - cos\alpha(y_L - y_m)]}{E_2} \tag{2.31}$$

On slope surface, when there is no pounding of water, P_1 and h_1 are both zero in most cases. On the slope surface $h_1 = d_1/3$ if water is pounded, where d is water table:

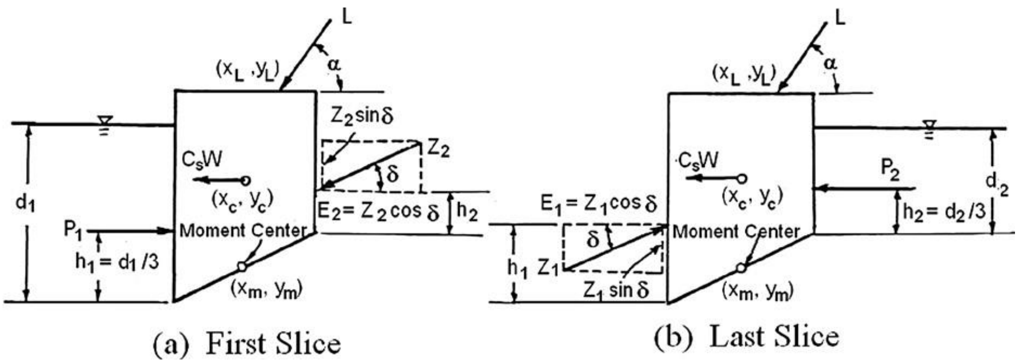

Figure 2.8: Forces for moment equilibrium of first and last slices (Anderson and Richards, 1987).

For first slice, d_1 is the water table that was placed on upper failure surface. In Figure 2.8(b), the last slice is shown:

$$h_2 = \left(\frac{E_1}{P_2}\right) h_1 - \frac{b}{2}\left(1 + \frac{E_1}{P_2}\right) tan\theta + \frac{b}{2}\ (\frac{E_1}{E_2}) tan\delta - \frac{CsW(y_c - y_m)}{P_2} + \frac{L[sin\alpha(x_L - x_m) - cos\alpha(y_L - y_m)]}{P_2} \tag{2.32}$$

Until h_2 of last slice is obtained, the first slice is started with given values of P_1 and h_1, Equation 2.30, 2.31, and 2.32 are applied successively. By trial and error until $h_2 = d_2/3$, it can be adjusted gradually the value of δ. The water table on upper of failure surface for last slice is d_2. h_1 in last slice can be determined when $P_2 = 0$:

$$h_1 = \frac{b}{2} tan\theta - \frac{b}{2} tan\delta + \frac{CsW(y_c - y_m)}{E_1} - \frac{L[sin\alpha(x_L - x_m) - cos\alpha(y_L - y_m)]}{E_1} \tag{2.33}$$

As obtained from Equation 2.31, selected value of δ that h_2 of the last slice from next slide, is same to h_1 of the last slice from Equation 2.33.

As follows, Spencer method can be summarized:

1. From Equation 2.25, determine T and from Equation 2.28, a new value of FS depend on starting FS by like S = ΔS = 0, the normal method and δ = 0. Until FS converges, repeat the process applying the new FS as the assumed FS.

2. By Equation 2.25, compute T and by Equation 2.26, compute ΔE depends on the value of FS and ΔS = 0 and obtained in step 1. Then, compute E_2 on right side of 1st slice by $E_2 = E_1 - \Delta E$, which began from left side of 1st slice where $E_1 = 0$ or P_1. Until the last slice is reached,

apply this procedure recursively, slice by slice. E_2 at the right side of last slice automatically equalled to 0 or P_2 because the factor of safety is obtained through Equation 2.27.

3. Apply Equation 2.29 to calculate h_2 of the last slice, depends on $\Delta S = 0$, P_1 and h_1 of initial slice given, and E obtained in step 2. Equation 2.30 are applied for the 1st slice and Equation 2.31 for the slice of last instead of Equation 2.27. Until h_2 of the last slice is equal to $d_2/3$, δ is varied. Δ is varied until h_2 of the next-to-last slice from Equation 2.29 same as h_1 of slice of last from Equation 2.32 given $P_2 = 0$.

4. By $S = E \tan \delta$, the shear force between slices is computed and by difference of ΔS, $\Delta S = S_1 - S_2$, according to step 2 the values of E obtained and in step 3, δ. For $\Delta S = 0$, the first cycle of iteration is then completed.

5. Find new values of ΔS and FS by repeating steps 1 to 4. According to step 1, safety factor obtained and for step 4, ΔS value. With that, the second cycle of iteration is completed.

6. Until FS converges, the cycles is continued.

2.3 Factor of Safety (FS)

Safety factor (FS) for stability of slope is expressed as ratio of soil shear strength (resisting force) to maximum-armed shear stress (driving force) at potential failure surface. The soil strength consists of cohesion, internal friction angle. Gravity and other factors (e.g. removal of load at slope toe, additional loads at top of slope surface loads, seismic load, or seepage of water) contribute to the driving force in analysis of slope stability. However, slope fails when resisting force was smaller than the driving force (FS< 1). For this study, safety factor is the smallest value of FS among all potential slip surface's results obtained.

A particular FS for slopes is difficult to specify because it based on many factors. Consequently, it is subjective to decide on what factor of safety to be used. 1.15 to 1.5 is the usual range of factor of safety. FS < 1.1 to 1.2 are designed for tailing dams in the mining industry. As a general guide, FS < 1.3 is good for general slopes like a cut for highway. FS < 1.4 is common for a dam.

2.4 Slip Surface

On safety factor, numerous times of the effect of soil strength parameters was studied. However, seldom consideration on their effect on slip surface. Based on slope elemental material type, the surface of failure mode was different. It may be a circular, plane, logarithmic or curved or combination of all. Failure surface was mostly closed to the circle shape if the soil materials are homogeneous which was same case for this paper (Rahimi, 2013). The potential slip surface was explained as possible failure of surface for slope with varied FS. However, critical slip surface is the most critical failure surface together with minimum safety factor. By comparing several trial slip surfaces' safety factors, then the critical surface of failure of slope were determined. Usually, the critical slip surface was interpreted using software. According to Lin & Cao (2011), between these parameters and potential slip surface, there is a relationship and how the failure surface are affected by them is discussed.
Function of angle of Internal Friction φ, Cohesion c, Unit Weight γ, and slope height h is presented as:

$$\lambda = c/(\gamma h tan\varphi) \tag{2.34}$$

Where,
γ = Unit Weight, kN/m^3
c = Cohesion, kPa
φ = Internal Friction Angle, °

This paper considered that the failure surface remains the same if the Lambda value (λ) keeps constant, which proved earlier study (Jiang & Yamagami, 2008). $c/\tan\varphi$ and slip surface have a unique relation between them. Moreover, according to Lin & Cao (2012), the failure surface was made nearer by the smaller λ to surface of slope and deeper failure slip was indicated by greater λ.

2.5 Factors affecting slope stability

Stability of slope is mainly governed by slope factors of internal and external. Internal factors included soil strength at potential failure surface (e.g. cohesion and internal frictional angle) and slope geometry (e.g. slope height, slope inclination angle and slope shape). The external factors included the temperature and weathering changes, rainfall, earthquake, environment conditions of slope, tectonic stress, and artificial destruction (Wen, 2016).

2.5.1 Internal Factors

In general, the shear stress force increased causing the slope failure. In fact, the differences between driving forces (to cause slope instability) in creating failure and resisting forces respect to failure were slopes stability calculations. The soil mass stability opposed to potential failures were the safety factor (Das 2010). The parameters included unit weight, cohesion, internal friction angle, level of water surface, slope geometry, and existing stresses affected the slopes stability. Slip surface's shear resistance were affected by these parameters (Das 2010).

By assigning the soil a unit weight, gravitational force and sliding mass weight was used. The specified unit weight multiply cross sectional area of slice determined weight of slice in method of slice. Unit weight defined as ratio of soil's total weight to soil's total volume. Under soil engineering, unit weight is a soil property that was applied to resolve the issues related to earthwork. Specific weight is another naming for unit weight. Unit weight acted as main cause of driving forces. Driving force increased causing the slope to be more unstable (Cheng, 2003). Stability of slope was depended on the interaction between two types of forces, resisting forces and driving forces. Driving force generated motion of downslope, while resisting forces deterred motion. With that, during driving forces overcomed resisting forces, slope was unstable and resulted in mass wasting.

Within a soil, cohesion is the force that holds together like particles or molecules. It is ability of soil particles to attract or bind each other together. In the laboratory, Cohesion, c, was usually determined from the Direct Shear Test. Cohesion is the component of shear strength of a soil that is independent of interparticle friction. True cohesion came from electrostatic forces (lost through weathering) and cementing in soils. Apparent cohesion came from pore pressure response that was lost through time, negative capillary pressure (lost during wetting), and root cohesion (lost through fire of the contributing plants or logging). Cohesive soil was soil with a high clay content or fine grained soil, that had high cohesive strength. When dry, cohesive soil was hard to break up, and when submerged it exhibited significant cohesion. Cohesion is one of the resisting forces (Cheng, 2003). Due to the cohesion is a strength parameter, it will affect the safety factor. Resisting forces deter downslope movement that promoted by driving forces. Mass wasting were resulted when driving forces overcome resisting forces.

For a given soil at which shear failure occurred, internal friction angle is measurement of shear strength due to the friction between soil particles. It was determined through the Triaxial Stress Test and the Direct Shear Test. Resisting forces acted oppositely of driving forces. The slope material's shear strength was resistance to downslope movement (Cheng, 2003). Shear strength is a function of internal friction that is friction between grains within a material. The internal friction angle is a strength parameter that will affect the safety factor. With lower friction in soil, the slope stability became unstable and failure because resisting forces cannot deter downslope movement that promoted by driving forces.

Slope Geometry (e.g. slope height, slope inclination angle and slope shape) is one of the factors of internal factor. For added soil to the top part of slope, it was acted as overhead load. Overhead load will increase the driving force and causes the safety factor to decrease (Zulkifl, 2020). A rise in driving force that is the weight of failure surface caused increased in the surface of failure produced. In the meantime, more resisting force simultaneously are produced due to the arc length increased. In certain situation, some slope shape also acted as a resisting force. The safety factor increased by a more resisting force. Resisting force came from the angle for arc length decreases. This was due to only the resisting force which is the failure arc length increased and driving force that is mass of failure shape kept almost constant (Cheng, 2003). Therefore, the safety factor increased by increasing the arc length which simultaneously increased the resisting force. The moment of resisting force was larger than driving force, the slope stability increased, and failure were less likely to happen. Figure 2.9 shows the real life slope stability affected by slope geometry.

Figure 2.9: Real life Slope Stability affected by slope geometry (Kim, 2018).

2.5.2 External Factors

The external factors included the temperature and weathering changes, rainfall, earthquake, environment conditions of slope, tectonic stress, and artificial destruction. Human activity is the external cause of slope stability. Currently, changes in topography and natural vegetation are caused by improper use of slope. Digging, deforestation of natural vegetation and filling will have resulted in steepening of slope gradient. The slope collapse accident was accelerated due to loss of soil and water conservation function. When slopes were in more than their own and protection facilities can provided resistance situation, will caused increasing of downside force and brought slope failure. For example, on the crest of the hill that exerted on improper loading.

Other than that, the major external factors that caused slope instability and brought failure were rainfall, erosion of slope surface of slopes caused by flowing water, force caused by seepage water, sudden lowering of water adjacent to a slope and forces caused by earthquakes. Movement of soil from high points to low points were caused by all the forces listed above. Erosion of the surface that acted in the probable motion direction was the most important among all factors. Generally, in stability problems, the various effects of seeping or flowing water were very important, however these effects were not properly identified usually. There was a greater effect than commonly realized because seepage forces were caused by the seepage occurring within a soil mass. Removal of a certain soil weight are caused by erosion on the surface of a slope. It led to an increased stability as far as mass movement was concerned. Moreover, decreased the length of incipient surface of failure and increased height of slope are caused by erosion in the form of undercutting at the toe, thus the stability decreased. There was a decrease in the buoyancy of the soil when there was a free water surface adjacent to the slope and a lowering of the ground water. Thus, increase in the weight were caused by a decrease in the buoyancy of the soil. For example, in a reservoir happened a sudden drawdown of the water surface. The shearing stresses increased when weight increased. Depending on whether the soil can support compression which the increasing of load tends to cause, shearing stresses may or may not be in part counteracted (Stephen, 2013). The external factors that act on slopes were shown in Figure 2.10.

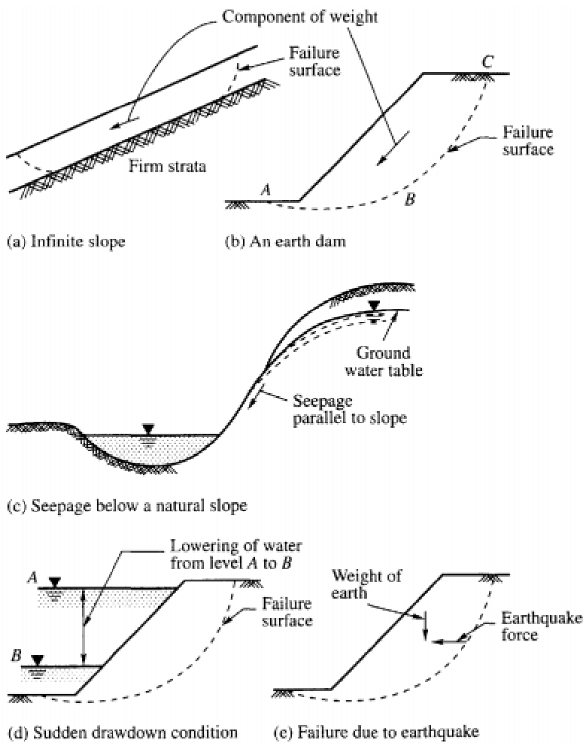

Figure 2.10: External factors that act on earth slopes (Stephen, 2013).

No volume changes occurred if a large mass of soil was saturated and low permeability. The strength increased may be inappreciable except at a slow rate and the load increased. Increase in the neutral pressure and decrease in intergranular pressure were accompanied by shear at constant volume. The entire soil mass turned into a liquefaction state and flows like a liquid caused failure. Due to forces of earthquake, the mass of soil was subjected to vibration condition. Sudden increased of water content was the most common external factor of slope stability. It was caused by event that converted water flow pattern on surface (e.g., heavy rain and rapid melting of snow or ice). Rapid melting can be caused by a volcanic eruption or suuden rise in temperature (e.g., in early summer or spring). Heavy rains were typically related to storms. Patterns of water flow changing were caused by human structures that constrain with runoff (e.g., parking lots, buildings, or roads), earthquakes, or previous slope failures that dam up streams. An example of this situation was the deadly 2005 debris flow in North Vancouver (Wang, 2020).

2.6 Parametric study

The influences of Shear Strength and parameters of Slope Geometry on stability of slope in terms of FS and critical slip surface (e.g. arc length “L”) by previous researches are discussed.

2.6.1 Influence of soil unit weight on safety factor and critical slip surfaces of slope

Wen (2013) conducted a research on the slope stability for soil with different Unit Weight, γ of soil on stability of slope. In the study, the unit weight of soil selected was varied from 15 to 23 kN/m^3 whereas other parameters were kept constant. Different analysis of slope stability methods (e.g. Fellinius, Bishop, Janbu, and Finite element) are adopted in this study. Figure 2.11 shows the schematic view of slope for this study. Table 2.1 displays FS computed by different slope stability analysis methods for soil with different unit weights. Figure 2.12 displays the graph of relationship between unit weight of soil and FS. Although FS resulted from all analysis of slope stability methods varied, trends are similar; FS of slope decreased when increased of soil unit weight. Unit Weight of a soil is expressed as ratio of the soil total weight to soil total volume. By assigning unit weight to soil, the sliding mass weight or gravitational force was used. The weight of slice was calculated by specified Unit Weight times cross-sectional area of slice (Wen, 2016). The increase of driving forces due to the higher soil unit weight had reduced the slope stability in term of factor of safety (Cheng, 2003). Janbu method had the highest factors of safety whereas Fellenius method had the lowest factors of safety for all unit weights. Bishop and finite element methods had slightly lower factor of safety compared to Fellenius method. The reduction rates of safety factor to soil unit weight are almost similar for all slope stability analysis methods. The unit weight affected the weight of the slice, w by referring to Equation 2.11 of Simplified Bishop method. Both the driving and resisting forces are affected by weight of slices. However, the increment rate of driving force due to the soil unit weight increase was higher compared to resisting force. Hence, the FS reduced with the increase of soil unit weight.

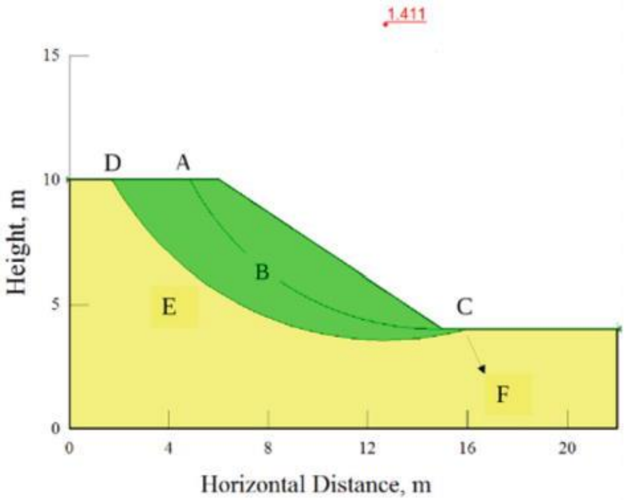

Figure 2.11: Schematic view of Slope (Wen, 2016).

Table 2.1: Relationship between Unit Weight of soil, γ and Factor of Safety, FS (Wen, 2013).

Calculation method	Safety Factor, FS								
	Unit weight of soil, γ (kN/m^3)								
	15	**16**	**17**	**18**	**19**	**20**	**21**	**22**	**23**
Fellenius	0.996	0.976	0.958	0.935	0.923	0.901	0.887	0.872	0.856
Bishop	1.058	1.034	1.012	0.997	0.977	0.964	0.938	0.919	0.901
Janbu	1.064	1.053	1.031	1.011	0.992	0.974	0.958	0.941	0.920
Finite element	1.052	1.037	1.017	1.002	0.982	0.970	0.943	0.926	0.906

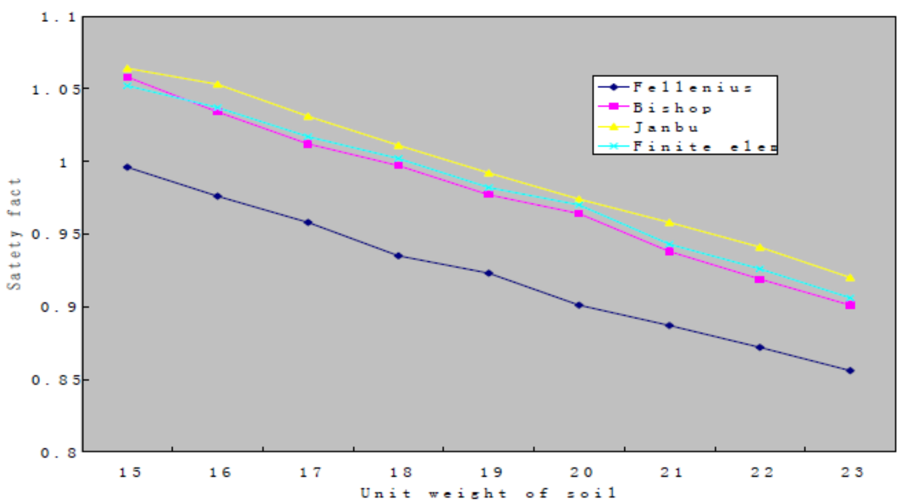

Figure 2.12: Relationship between unit weight of soil, γ and factor of safety, FS (Wen, 2013).

With increase of Unit Weight of soil, length of arc, L increased (Cheng, 2003). This trend is also applied to all the method used above. The larger value of arc length means the larger volume of slip surfaces. When Unit Weight of soil increased, failure surface became larger and deeper. With that, a larger soil weight above failure surface was resulted and hence the failure arc length was also increased. Less resisting force due to soil internal friction was produced due to the larger failure surface (Cheng, 2020). Smaller safety factor value was observed due to above reasons. By decrement of unit weight, the critical slip surface moved toward the slope's face. Hence, a smaller FS can be achieved by decreasing L (Wang, 2020).

2.6.2 Influence of soil cohesion on safety factor and critical slip surfaces of slope

Zulkifl (2020) conducted a numerical modelling by using 3 different computer programs (e.g. FLAC3D, ABAQUS, and Geo5) to study influence of cohesion on FS. Cohesion values selected in the study ranged from 15 kPa to 40 kPa. Figure 2.13 shows the effect of soil cohesion on FS of slope. Soil cohesion showed a remarkable effect on FS of slope, as shown in Figure 2.13. It was observed that FS of slope increased linearly with the soil cohesion. Factor of safety for slope with soil unit weight of 40 kPa was about twice of the slope with soil unit weight of 15 kPa. Within a soil, cohesion acts as a force that brings together molecules or like particles. Cohesion was usually affected by electrostatic force and cementing (Cheng, 2003). Since soil cohesion is one of the resisting forces in analysis of slope stability, result collected was satisfied with the theory (Cheng, 2003).

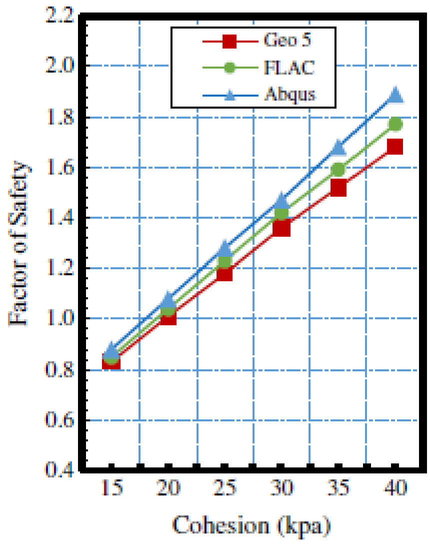

Figure 2.13: Effect of cohesion on the safety factor (Zulkifl, 2020).

Wang (2020) studied the effect of soil cohesion on FS and slip surface of slope by using SLOPE/W software. φ and γ chosen was 30 ° and 20 kN/m^3, respectively. Cohesion selected was ranging from 10 kN/m^2 to 20 kN/m^2. All-valid surfaces of failure and the summary of computed factor of safety were graphically portrayed in Figure 2.14. Larger cohesion had a considerable effect on FS of slope. There were big differences for all valid failure surfaces allocations when the cohesion force gets larger shown in Figure 2.14 (a-c). Moreover, Figure 2.14 shows that the safety factor and maximum depth of failure surface, D increased (8.5464 m, 10.309 m, 12.052 m) due to the cohesion is a parameter of strength. The increase of soil cohesion resulted in the increase of safety factor. It was also found that a larger local surface of slip was more likely to happen when soil cohesion was higher.

When c = 10 and c = 20 (kN/m^2), there are no major changes between safety factor and the failure surfaces allocations shown in Figure 2.14 (a, b). With that, 25 (kN/m^2) are used as the cohesion in Figure 2.14 (c). In Figure 2.14 (c), an increase of soil cohesion parameter caused failure surface and FS have a sudden increase.

In study of Wang (2020), the influence of cohesion on maximum failure length (L) was also studied. The arc failure surfaces for slope with different soil cohesions (e.g. small value, comparative large value, and large value) were as shown in Figure 2.14. The slip surfaces started from the entry point at the top of slope then passed through the slope and ended near to slope toe. The possible influence of soil Cohesion on Arc length was shown in Figure 2.14. Maximum failure arc length was 48.80 m, 50.20 m and 50.40 m recorded with the cohesion value of 15, 20 and 25 (kN/m^2) respectively. Failure arc length increased significantly when soil cohesion value increased. The critical slip surface become larger and deeper when the cohesion value increased. Critical surface of slip started from entry point at top of slope and pass through the slope and end at near the toe was the pattern of the arc of failure (Wang, 2020). For achieving an exact value for the Cohesion force, multiplied cohesion factor with Failure arc length. Weight of soil above surface of failure increased due to larger failure surface. FS increased when the arc length of failure surface increased due to the higher soil cohesion value. This showed that the cohesion which is the resisting force are more important that the driving force for this situation (Cheng,2003).

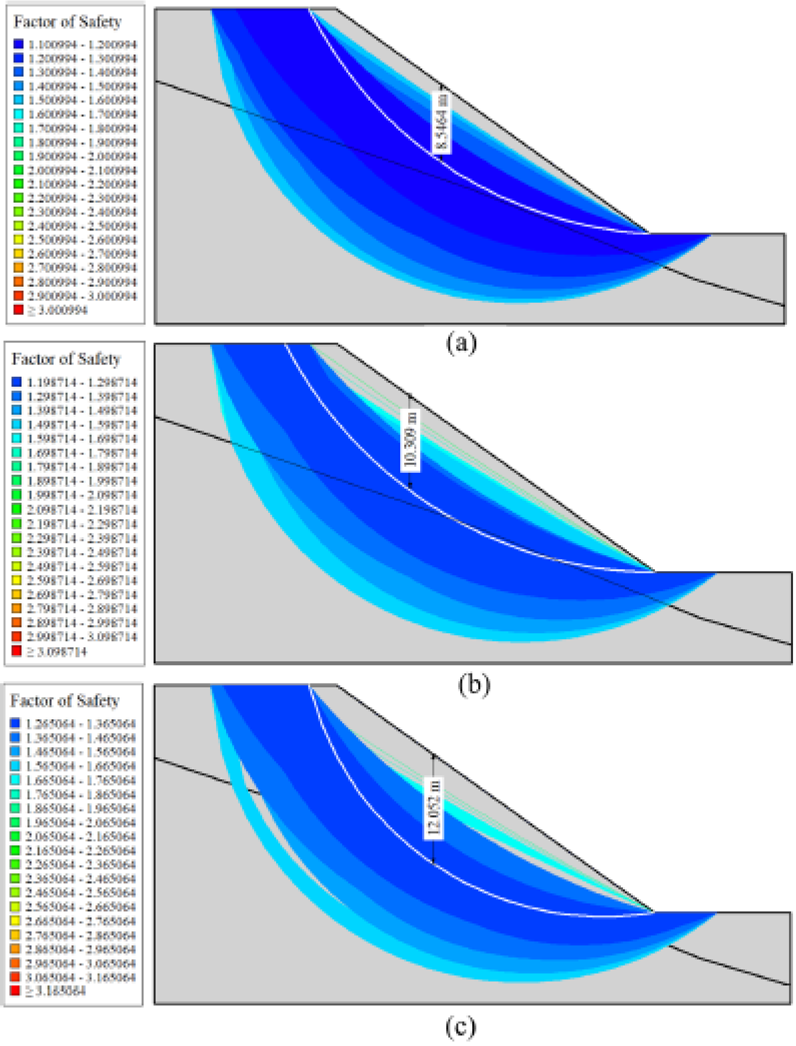

Figure 2.14: Display of multiple slip surfaces (a) small value of cohesion (b) comparatively large value of cohesion (c) large value of cohesion (Wang, 2020).

Wen (2013) also studied the influence of cohesion on slope stability of slope (in term of safety factor). The soil cohesion is varied from 11 to 19 kPa for this study. Different slope stability calculation methods are used (e.g Fellinius, Bishop, Janbu, and Finite element). Table 2.2 displays FS computed by different slope stability analysis methods for soil with soil cohesions. Figure 2.15 displays the graph of relation between cohesion of soil and safety factor. The FS of slope increased when cohesion increased as shown in Figure 2.15. Although FS obtained have several differences, but the trend of safety factor increments with soil cohesion was almost similar for all slope stability analysis methods applied. Fellenius method gave the lowest safety factor values for all cases. FS increased when the strength parameter values increased as soil cohesion is a strength parameter. Downslope movement of material were promoted by driving forces, whereas resisting forces deter the movement. So, the slope is more stable and when driving forces are resisted by higher resisting forces.

Table 2.2: Relationship between cohesion of soil, c and factor of safety, FS (Wen, 2013).

Calculation method	Safety Factor, FS								
	Cohesion, c (kPa)								
	11	12	13	14	15	16	17	18	19
Fellenius	0.943	0.981	1.021	1.061	1.099	1.137	1.178	1.217	1.259
Bishop	0.998	1.036	1.075	1.114	1.155	1.195	1.233	1.274	1.314
Janbu	1.011	1.050	1.089	1.131	1.169	1.209	1.251	1.289	1.331
Finite element	1.004	1.043	1.081	1.122	1.161	1.202	1.239	1.278	1.319

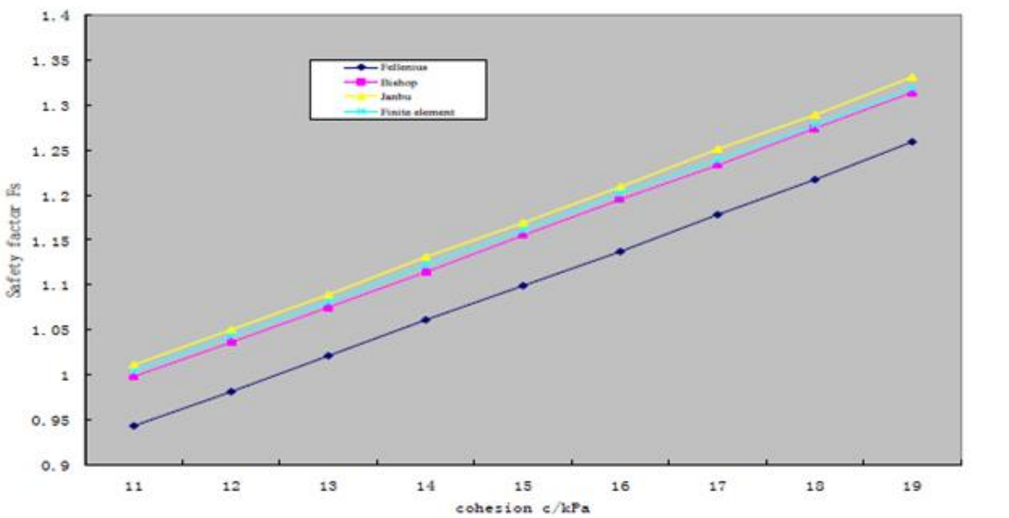

Figure 2.15: Relationship between cohesion of soil, c and factor of safety, FS (Wen, 2013).

With increase of cohesion of soil, the length of arc, L increased (Cheng, 2003). All the methods used above were having the similar trend. Larger value of arc length indicated the larger volume of soil above the slip surface. The resisting force and FS of slope also increased as the soil cohesion increased. The location and shape of critical surface of slip remained when soil cohesion increased. For searching the minimum value of safety factor, the driving force were increased. It can be reached by enlarging the failure area of slope. This gave rise to a greater failure arc length (L) and hence larger safety factor value (Cheng, 2003).

Bin (2016) also conducted a research on influence of cohesion on the slope stability. In this study, the soil cohesion was varied from 1 to 11 kPa meanwhile the friction angle of the soil remained unchanged. Table 2.3 shows results on FS from his study. Bin (2016) applied Bishop's method (BM), Fellenius's method (FM), and strength reduction method (SRM) in this study. E1 represents the relative error of strength reduction method compared to Fellenius method whereas E2 represents the relative error of strength reduction method compared to Bishop's method. The errors of strength reduction method compared with Fellenius's method fluctuates slightly with the rise of soil Cohesion. Maximum error of 10.19 % was observed for slope with cohesion of 3 kPa. For the relative error of strength reduction method compared to Bishop's method, it increased with the increase soil cohesion until the peak of 5 % at soil cohesion of 3 kPa. However the error decreased with the increased of soil cohesion afterwards. The minimum error was 3.43%.

Table 2.3: Safety factors for slope with different soil cohesion (Bin, 2016).

Slope (φ = 30) change c						
	1	**3**	**5**	**7**	**9**	**11**
FM	1.367	1.620	1.847	2.056	2.260	2.454
BM	1.430	1.700	1.938	2.162	2.370	2.569
SRM	1.487	1.785	2.029	2.262	2.463	2.657
E1%	8.780	10.190	9.850	10.020	8.980	8.270
E2%	3.990	5.000	4.700	4.630	3.920	3.430

The variation of safety factors and relative errors with the cohesive strength are shown in Figure 2.16 and Figure 2.17, respectively. FS resulted from strength reduction method were always larger compared to Bishop's method and Fellenius's method. For all methods applied, the safety factor increased with increase of cohesion. Relative error percentage of strength reduction method to Bishop's method was smaller compared to Fellenius's method.

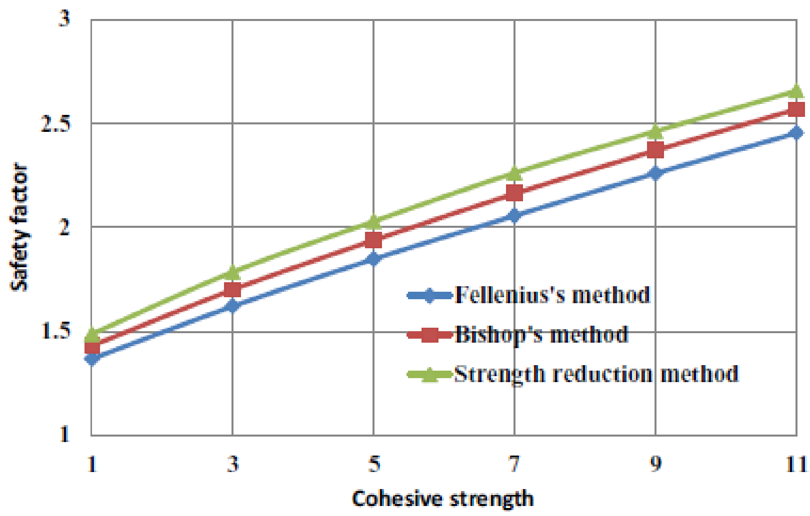

Figure 2.16: Safety factor versus cohesive strength (Bin, 2016).

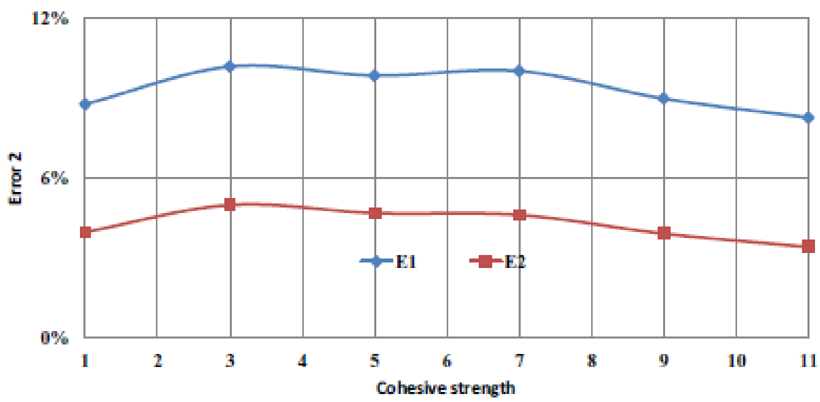

Figure 2.17: Relative error versus cohesive strength (Bin, 2016).

2.6.3 Influence of soil internal friction angle on safety factor and critical slip surfaces of slope

Based on research of Zulkifl (2020), 3 different softwares such as FLAC3D, ABAQUS, and Geo 5 are applied to study the influence of the angle of Internal Friction (φ) on FS. For studying effect, 15 to 40 ° of internal friction angle values were selected, but other parameters were remained unchanged. Especially for greater values of angle of internal friction, it had a notable effect on safety factor. The φ was directly proportional with FS and it is slightly upwards concave for the safety factor and internal friction angle curve as shown in Figure 2.18. For determining effect of φ and on FS, choosing a reference point was important for differentiation purposes. Failure surface of slip was affected with combination of φ and c. FS increased when cohesion and internal friction angle parameters increased due to their contribution to resisting forces in the slope stability analysis.

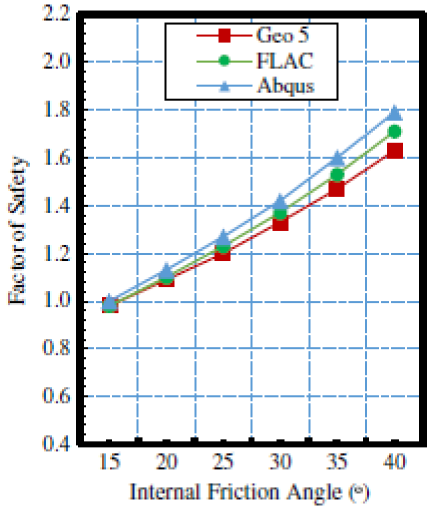

Figure 2.18: Effect of internal friction angle on the safety factor (Zulkifl, 2020).

Based on the study of Wang (2020), same slope model configuration is applied to analyze the effect of angle of Internal Friction, φ on FS, arc length, L, maximum depth, D, and all valid failure surfaces distribution range. The parameter of friction had a smaller influence on safety factor, slip surface and depth in contrast to cohesion parameters. The friction angle values were ranged from 20 ° to 35 °, and applying SLOPE/W software respectively. The Unit Weight and Cohesion was fixed at 20 kN/m^3 and 15 kPa, respectively. By considering different friction angles, the valid failure surface and the values of D for slope are as shown in Figure 2.19 (a-c). The safety factor and failure surface increased significantly as φ increased. However, depth of slip surface decreased with increase of φ, as shown in Figure 2.19. As shown in Figure 2.19 (a-b), local failures were resulted in first two cases (ϕ = 25 °, and ϕ = 30 °).

However, as shown in Figure 2.19 (c), no local failure occurred when internal friction angles of 35° was chosen for the soil. A larger safety factor was obtained because there was an increase of material resistance force when internal friction angle (a soil strength parameter) increased. It indicated that all failure surfaces were more likely to come into slope from point of entry and cross through slope toe during large value of φ. Comparatively, when the value of cohesion is small, the points of entry and exit were placed on crest and around toe of slope for local failures.

Possible failure surfaces distribution range increased as ange of soil friction increased, as shown in Figure 2.19 (c). Similar results are also observed by Ahmed (2017). The influence of φ on the failure arc length, L was shown in Figure 2.8. For slope with internal friction angles of 25°, 30° and 35°, the failure arc length (L) was 58.33 m. 48.88 m and 47.62, respectively. Higher soil φ produced shorter length of failure arc. Surface of failure (Failure Arc length) decreased with increase of the internal friction angle. Friction force was achieved by multiplying Failure Arc length with tangent of φ. Besides that, a larger value for the internal friction force and the smaller failure volume weight (smaller driving force) were resulted by smaller failure surface. Φ effect increased which is the resisting force was more dominant than the driving force. The critical slip surfaces were shallower for the slope with higher soil internal friction angle. The critical slip surfaces were more likely to come into slope from point of entry and pass through slope near toe for the soil with large internal friction angle (Wang, 2020). According to Jiang and Yamagami (2006), they stated that “In a homogeneous soil slope, when the unit weight, slope geometry, and pore water pressure distribution were given, the critical slip surface location was related only to $c/tan\ (\varphi)$ ratio of that slope for a particular method of slices”.

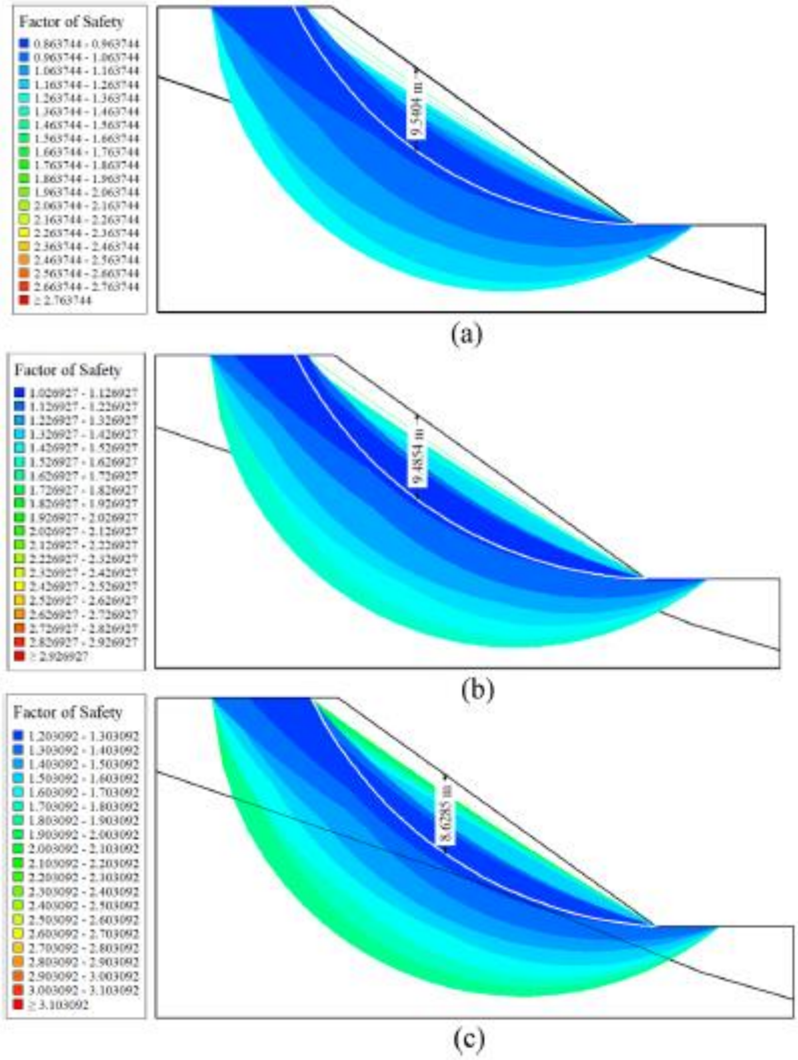

Figure 2.19: Display of multiple slip surfaces (a) small value of angle of internal friction (b) comparatively large value of angle of internal friction (c) large value of angle of internal friction (Wang, 2020).

Wen (2013) investigated the influence of ϕ on stability of slope. ϕ selected was varied from 16 ° to 24 °. Different analysis of slope stability methods were used, for example Fellinius, Bishop, Janbu, and Finite element methods. Table 2.4 shows the results of relationship between ϕ and safety factor, FS and Figure 2.20 displays the graph of relationship between ϕ and FS.

FS of slope increased when internal friction angle of soil increased, as shown in Figure 2.20. Due to the contribution of friction angle to the resisting force. For a given soil, angle of Internal Friction is the measurement of shear strength due to the friction between soil particles. Resisting forces act in the opposite direction of driving forces. The resistance to downslope movement is greatly based on shear strength of soil on slopes. Internal friction is friction between grains within a soil material. With lower friction in soil, the slope stability became unstable and failure (Wang, 2020).

Table 2.4: Relationship between internal friction angle of soil, ϕ and factor of safety, FS (Wen, 2013).

Calculation method	Safety Factor, FS								
	Internal Friction Angle, φ (°)								
	16	17	18	19	20	21	22	23	24
Fellenius	0.878	0.921	0.965	1.012	1.058	1.105	1.152	1.195	1.241
Bishop	0.912	0.955	1.003	1.045	1.092	1.137	1.183	1.225	1.268
Janbu	0.925	0.968	1.013	1.056	1.102	1.148	1.195	1.240	1.283
Finite element	0.920	0.963	1.005	1.050	1.096	1.143	1.188	1.235	1.281

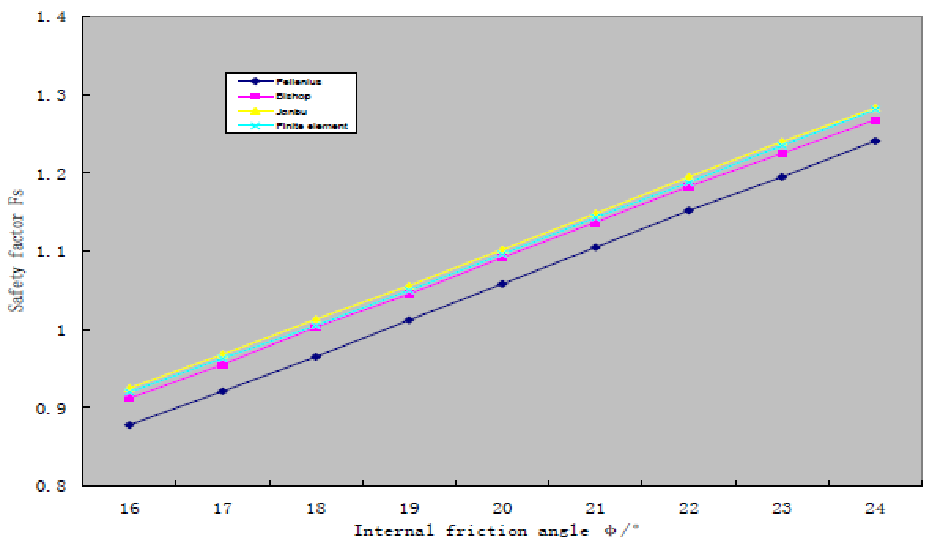

Figure 2.20: Relationship between internal friction angle of soil, ϕ and factor of safety, FS (Wen, 2013).

Bin (2016) conducted a study on the influence of internal friction angle on the FS. Similarly, FS were calculated with different soil internal friction angles from 15 ° to 40 °, as tabulated in Table 2.5. The error between strength reduction method and Fellenius's method decreased gradually as the internal friction angle increased;, with the minimum and maximum error of 7.34% and 8.85%, respectively. For the relative error between strength reduction method and Bishop's method, the maximum error was 4.24% for soil friction angle of 25 °. Then, the relative error reduced with increase of soil internal friction angle.

Table 2.5: Safety factor of slope under different soil friction angles (Bin, 2016).

Slope (c = 1 kPa) change φ						
	15	**20**	**25**	**30**	**35**	**40**
FM	0.706	0.913	1.180	1.370	1.630	1.920
BM	0.737	0.953	1.180	1.430	1.700	2.020
SRM	-	-	1.230	1.487	1.759	2.061
E1%	-	-	8.850	8.540	7.910	7.340
E2%	-	-	4.240	3.990	3.470	2.030

The variation of factor of safety and relative error due to increment of soil internal friction angle were shown in Figure 2.21 and Figure 2.22. FS obtained by Bishop's method and Fellenius's method were smaller compared to the strength reduction method. For all method applied, the safety factors increased with increase internal friction angle.

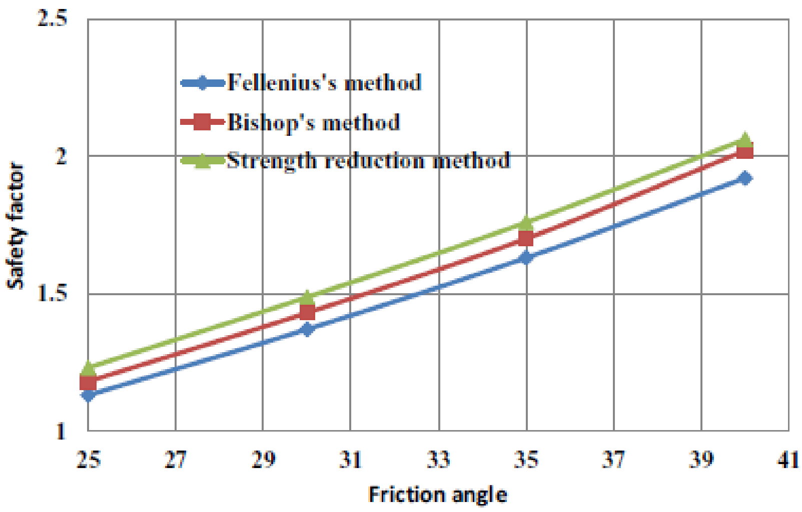

Figure 2.21: Safety factor versus soil friction angle (Bin, 2016).

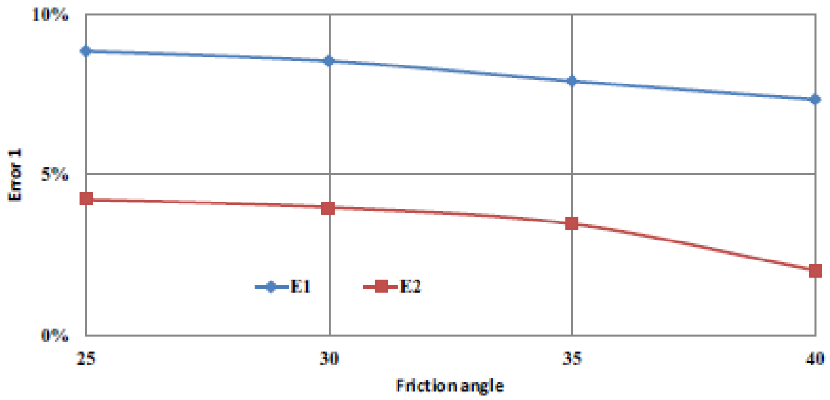

Figure 2.22: Relative error versus soil friction angle (Bin, 2016).

2.6.4 Influence of slope geometric parameters on safety factor and critical slip surfaces of slope

Effect of slope geometric parameters (Alpha α, Beta β) on safety factor were investigated by Zulkifl (2020). Figure 2.23 shows four different possible slope models of used in the research. The strength properties are kept constant with Cohesion value of 20 kPa, Unit weight of 20 kN/m^3, and angle of Internal Friction of 20 °. Case (a) and (c) are under the effect of “β” angle. While, case (b) and (d) are under effect of “α” angles.

Figure 2.24 displays the variation of safety factors with the β and α angles. For a given slope models, slope geometry had major impact on safety factor. Influence of β on safety factor for slope models (a) and (c) was shown in Figure 2.24 (a). A rapid increase was resulted, and can be said that β has a major impact on FS. Slope was more stable when β angle increased. The failure arc length increased with the increase of β angle. Hence, it resulted in higher resisting force that also increased the safety factor.

For the slope models (b) and (d), the effect of α angle on safety factor is shown in Figure 2.24 (b). However, until 35°, Zulkifl (2020) proved that effect of α on safety factor was very minor (FS of 1.20 to 1.25 only). After that, safety factor begins to decrease. This was due to the increase of skidding force when an overhead weight acted by the amount of surcharge material was increased.

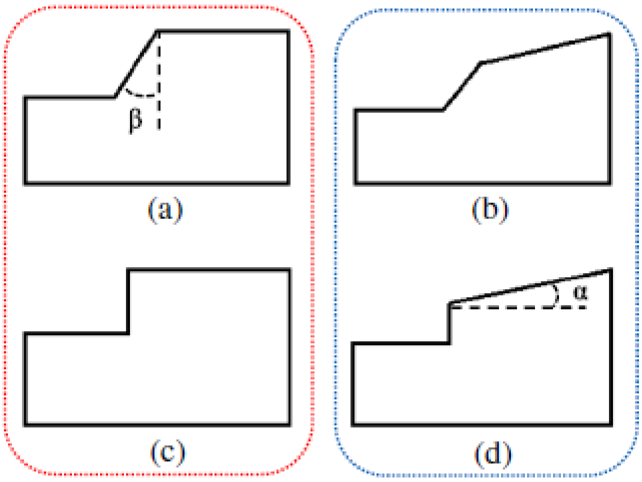

Figure 2.23: Possible slope models (Zulkifl, 2020).

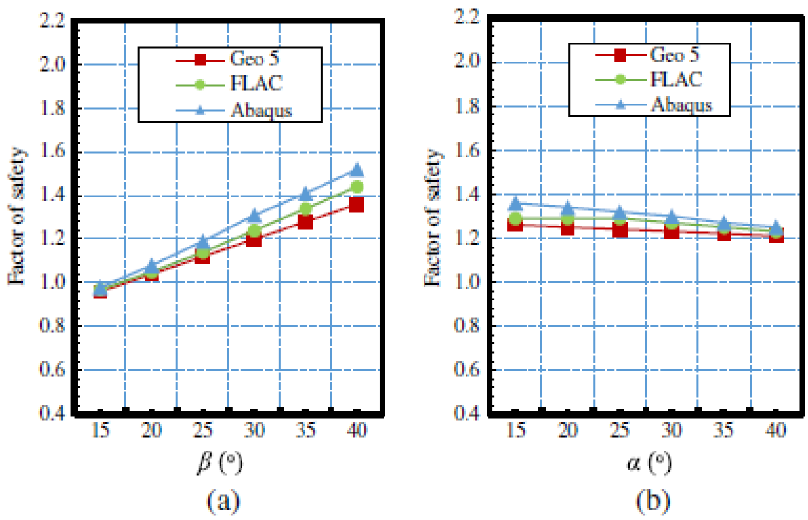

Figure 2.24: Effect of slope geometry on FS. (a) Effect of β. (b) Effect of α (Zulkifl, 2020).

Wen (2013) studied on influence of slope angle on stability of slope. Slope angle was defined as slope angle from horizontal surface, they were varied from 20 ° to 60 ° for the study. For better accuracy of data, other parameters were kept constant. Different calculation methods selected were Fellinius, Bishop, Janbu, and Finite element methods. Figure 2.25 shows the slope geometry schematic view of the study. Table 2.6 shows FS calculated based on different slope angles. The relationship between angle of slope and safety factor, FS were shown in Figure 2.26. The FS and stability increased when slope angle decreased, shown in Figure 2.26. Smaller slope angle represented greater slope gradient which meant that the slope is steeper. Slope angle of 30 ° produced factor of safety near to 1 for all calculation method. FS became less than 1 for slope angle exceeding 35 ° for Fellenius and Finite element methods. Meanwhile, FS became less than 1 for the slope angle exceeding 40 ° for Bishop and Janbu method. Although the different calculation methods resulted slightly different factor of safety values, they showed similar trends in which the safety factor increased with the reduction of slope angle.

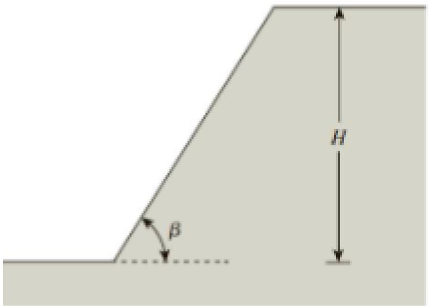

Figure 2.25: Slope Geometry (Wen, 2013).

Table 2.6: Relationship between slope angle and factor of safety (Wen, 2013).

Calculation method	**Safety Factor, FS**								
	Slope Angle, β (°)								
	60	**55**	**50**	**45**	**40**	**35**	**30**	**25**	**20**
Fellenius	0.741	0.783	0.824	0.869	0.915	0.962	1.012	1.082	1.152
Bishop	0.758	0.803	0.854	0.903	0.955	1.005	1.054	1.107	1.163
Janbu	0.765	0.806	0.857	0.903	0.957	1.007	1.056	1.108	1.165
Finite element	0.760	0.795	0.847	0.890	0.942	0.989	1.035	1.099	1.154

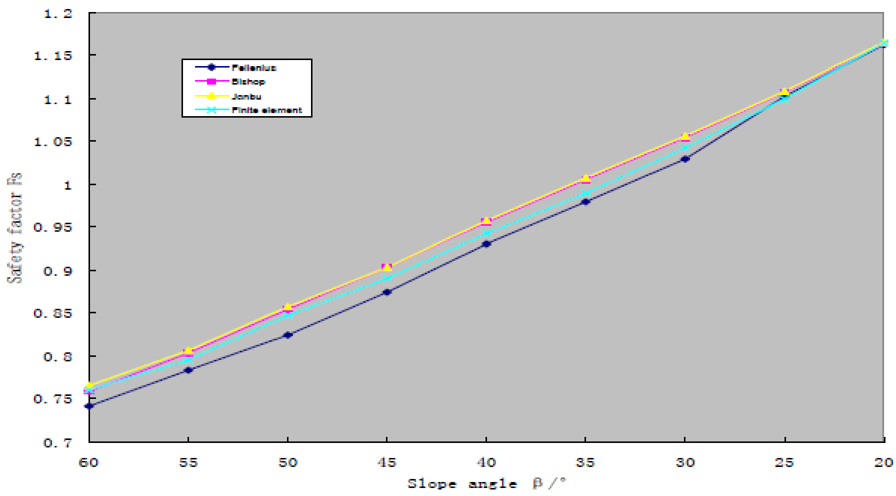

Figure 2.26: Relationship between slope angle and factor of safety (Wen, 2013).

According to Cheng (2003), the failure surface position did not change significantly by rising the α angle. The slope surface movement and the failure arc extension caused the increase in the failure arc length. Figure 2.27 shows schematic view of slope.

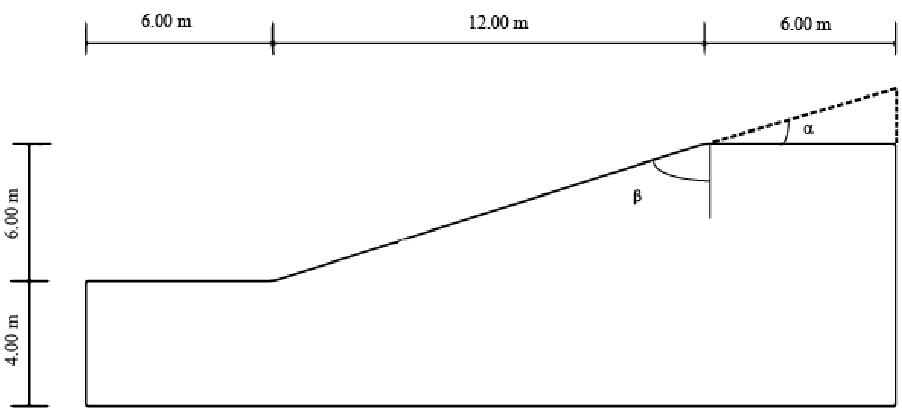

Figure 2.27: Schematic view of Slope (Cheng, 2003).

The possible slip surface, safety factor and type of slippage in the critical conditions are observed after the critical slope were simulated in the software (Farzin, 2019). For the given condition, SLOPE/W software calculated and drew up potential failure of slip to find FS. Software took the smallest possible FS as critical FS. Figure 2.28 shows the schematic representation of the simulated model and the studied parameters. The Cohesion (c) of 25 kPa, Unit weight (γ) of 15 kN/m^3, and Internal Friction angle (φ) of 14 ° were kept constant. Beta angle of 30 °, 45 ° and 60 ° were selected in the analysis. After the simulation, the factor of safety obtained was 2.142, 1.912 and 1.622. A comparative change in resistance and destructive forces were caused by change in slope geometric shape. Not only that, but various degrees of safety factor had also arisen. By increasing the slope angle, the safety factor was decreased. Steeper slopes resulted in smaller FS. Figure 2.29 shows FS and failure surface for the state.

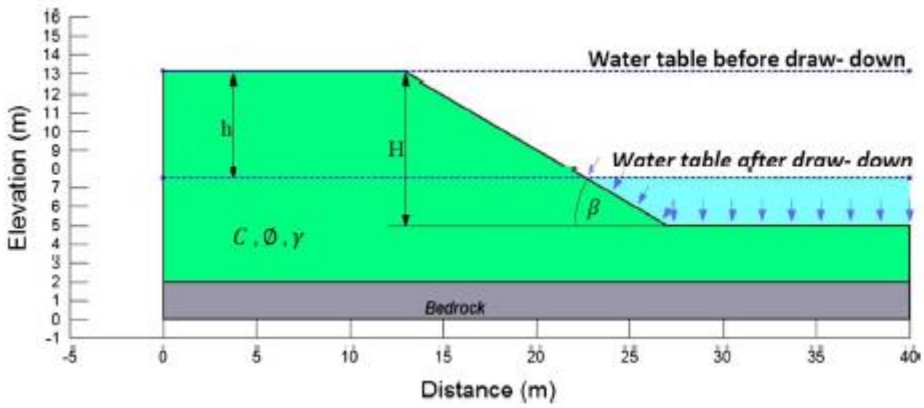

Figure 2.28: A schematic representation of the simulated model and the studied parameters (Farzin, 2019).

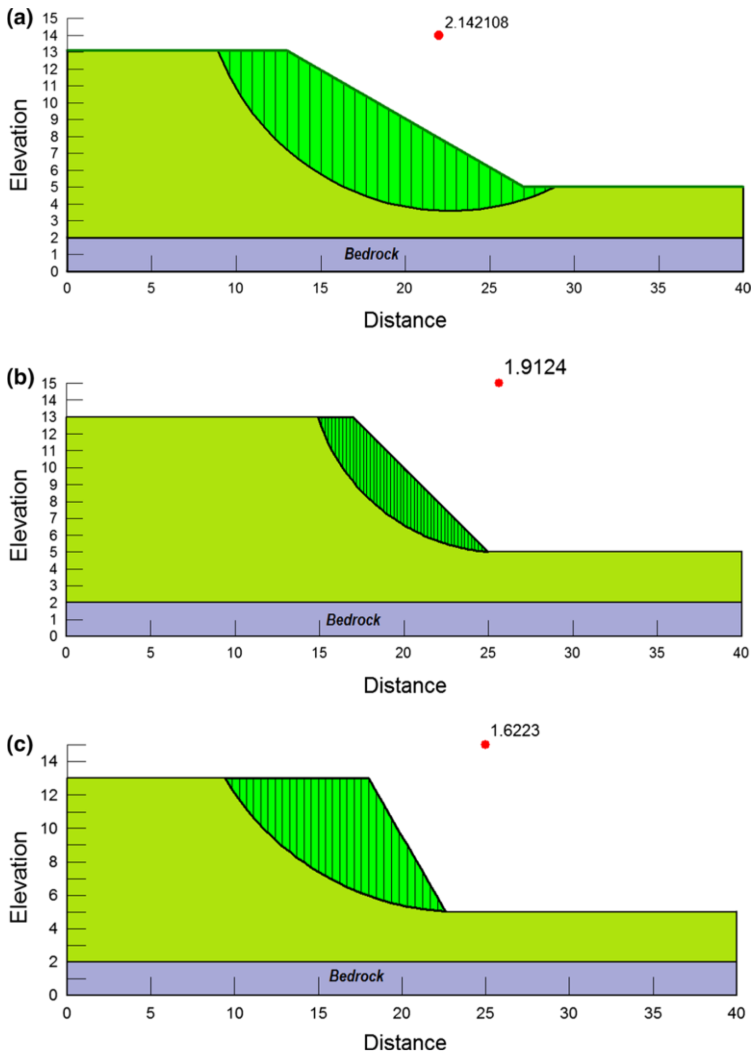

Figure 2.29: The FS and the type of slip circle for the state. (a) $\phi = 14^\circ$, C = 25 kPa, $\gamma = 15$ kN/m^3, $\beta = 30^\circ$, (b) $\phi = 14^\circ$, C = 25 kPa, $\gamma = 15$ kN/m^3, $\beta = 45^\circ$, (c) $\phi = 14^\circ$, C = 25 kPa, $\gamma = 15$ kN/m^3, $\beta = 60^\circ$ (Farzin, 2019).

2.6.5 Influence of lamda on safety factor and critical slip surfaces of slopes

Lin and Cao (2011) investigated the relationship between strength parameters and potential surface of failure. Moreover, studies for investigating the effect of strength properties such as (c, φ) on surface of failure are carried out by researchers (Wang, 2020). The function of angle of Internal Friction (φ), Cohesion (c), Slope height (h), and Unit weight (γ) are written as:

$$\lambda = c \; / \; (\gamma h tan\varphi) \tag{2.35}$$

Where,

φ: Angle of Internal Friction

c: Cohesion

h: Slope Height

γ: Unit Weight

λ (lambda) value keeps constant when cohesion and unit weight increase simultaneously and it is in a function of dimensionless for Equation 2.35. The surface of failure remained the same because of the constant value of λ. There is a special relationship between the c/tanφ and surface of slip (Jiang and Yamagami, 2006).

Influence of lambda on entry point distance

Based on study of Zulkifl (2020), for investigating effect of lambda (λ) on entry point (le), GEO5 software are applied. The definitions of slope failure surface exit point, entry point, and surface of failure entry point distance (le) are shown in Figure 2.17. The correlation between entry point distance (le) and lamda (λ) are displayed in Figure 2.18. From Figure 2.18, Zulkifl (2020) concluded that λ had an major effect on surface of failure entry point distance (le). When λ increased, entry point distance (le) increased significantly. From Figure 2.18, it was observed that the le and λ curve was slightly upwards convex. λ was a constant value and there was a logarithmic relationship between surface of failure entry point distance, le and λ. Zulkifl (2020) applied Equation 2.36 to calculate distance of entry point of failure surface by applying SPSS software from a non-linear regression.

$$l_e = 0.9ln\left(\frac{c}{\gamma h tan(\varphi)}\right) + 3.22 \qquad (2.36)$$

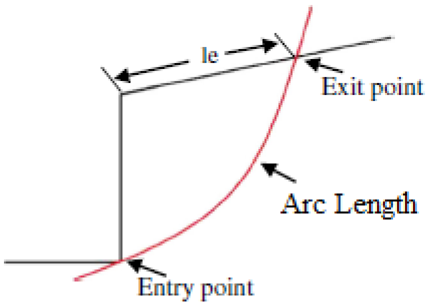

Figure 2.30: Distance of Entry point (le) and Failure Arc length (Zulkifl, 2020).

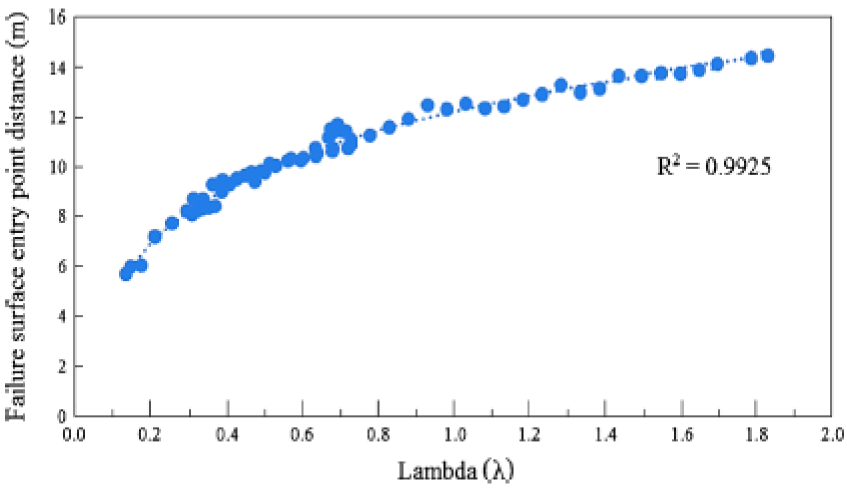

Figure 2.31: Effect of lambda λ on failure surface entry point distance le (Zulkifl, 2020).

Influence of lambda on length of failure arc

Zulkifl (2020) also adopted the same approach as for le for investigating the effect of λ on the failure arc length (L). Based on computed values, the relationship between failure arc length, L and dimensionless parameter lambda, λ for a given slope model is shown in Figure 2.32. The L versus λ curve was slightly downward concave and λ had an important influence on L. Zulkifl (2020) applied GEO5 software and proved that there was a logarithmic relationship between L and λ. Depended on slope properties, failure arc length were calculated by using Equation 2.37:

$$L = 0.77ln\left(\frac{c}{\gamma htan(\varphi)}\right) + 6.21 \quad (2.37)$$

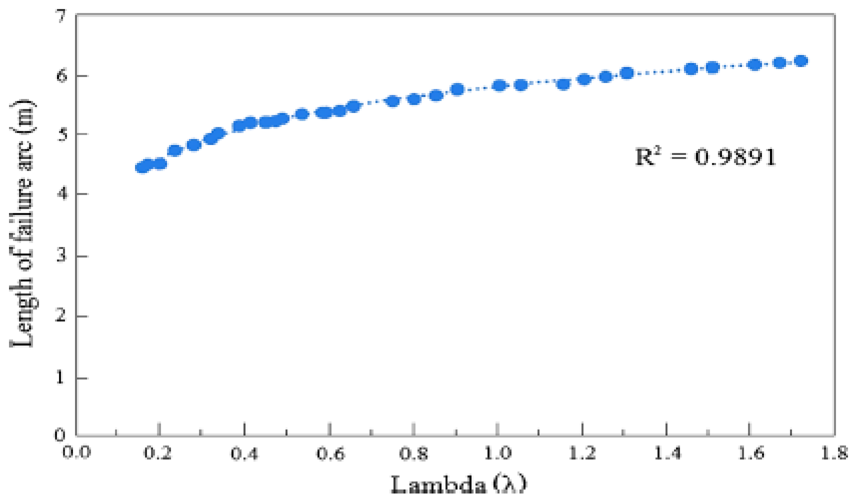

Figure 2.32: Relationship between lambda λ and the length of failure arc L (Zulkifl, 2020).

2.6.6 Relationship between failure arc length and factor of safety

Graph of safety factor with arc of failure length, L is shown in Figure 2.33. There was no co-relation between FS and failure arc length (Zulkifl, 2020). Hence, for validating the usefulness of the suggested method, Zulkifl (2020) applied various softwares (ABAQUS, GEO5, and FLAC3D) and the differences between the safety factor calculated were reasonable and small enough that was less than 5%. As compared to ABAQUS and FLAC3D, GEO5 was conservative and provided small value of safety factor. However, FLAC3D calculated only safety factor and did not define the surface of failure surface in detail. path For slope stability analysis, Zulkifl (2020) concluded that the search procedure is an convenient and effective method. Moreover, comparing to a real case, Table 2.7 shows surface of failure estimated, with the constant stress-based approach for a model was similar. For the failure surface, by applying Fellenius sophisticated method, an estimated excel spread sheet, which proved that proposed method was suitable for determining the surface of failure and slope stability (Fellenius, 1936).

Table 2.7: List of failure surface of a case calculation with corresponding forces (Zulkifl, 2020).

X (m)	Y (m)	Radius (m)	Max. depth (m)	Resistance S (kN/m)	Sliding T (kN/m)	FS
-1.0	444.0	28.200	4.000	765.01	764.34	1.000
-2.0	445.0	29.592	4.000	772.94	772.76	1.000
-3.0	446.0	30.977	4.000	779.28	778.49	1.001
-4.0	447.0	32.362	4.000	785.12	782.91	1.002
-5.0	452.0	37.101	5.000	856.49	851.75	1.005
0.0	443.0	26.802	4.000	758.75	754.02	1.006
-4.0	449.0	33.985	4.500	812.73	807.82	1.006
-5.0	450.0	35.382	4.500	819.56	814.66	1.006
-6.0	451.0	36.780	4.500	826.56	821.41	1.006
-3.0	448.0	32.591	4.500	805.95	800.55	1.006

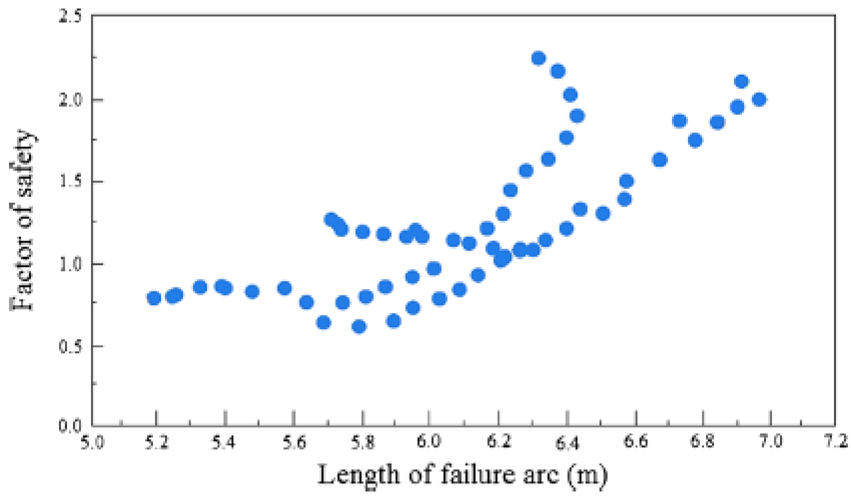

Figure 2.33: Relationship between FS and length of failure arc (Zulkifl, 2020).

2.7 Common software for slope stability analysis

For implementing in computer software, concepts for method of slices were easy to apply and those steps were not difficult at all. Moreover, the simpler methods were done on a spreadsheet. Therefore, after the implementation of computers, slope stability software became available widely. In the early 1980s, the introduction of powerful desktop personal computers allowed economically viable to produce commercial software products. In geotechnical engineering practice, such software products ready availability had brought to the daily use of LEM analysis of stability. Nowadays, several software such as GEO5, SLOPE/W, FLAC are available for analysis of slope stability purposes.

Modern LEM software made the possibility to solve higher complexity in analysing slope stability. With software, it is now possible to solve various linear and nonlinear shear strength models, complex stratigraphy, highly irregular pore-water pressure conditions, concentrated loads, almost any kind of slip surface shape, and structural reinforcement. Based on the method of slices, limit equilibrium formulations are also being used more and more on the stability analysis of structures such as nail or fabric reinforced slopes, tie-back walls, and even the sliding stability of structures subjected to high horizontal loading arising, such as, from ice flows. For analysing ever-increasingly complex problems, modern software is making it happens.

With software, the safety factor can be look beyond by graphical view of data applied in the calculations. For example, graphically view of parameters distribution along surface of slip and all each slice's detailed forces in the potential sliding mass. Software helped largely to recognize the technique's details. A deeper perception of method, especially dissimilarity between numerous methods available can be done by the graphical viewing of computed details due to vulnerability of limitations in formulations of limit equilibrium. For situation where normal stress along surface of slip was affected by gravity (weight of the slice), method of slices was initially conceived. Not only that, it included boosting in analysis went far beyond preliminary purposes. Knowing limitations was vital to understand and rely on results even though limitations do not necessarily prevent applying method in practice.

2.7.1 GEO5 software

GEO5 software is a program which provides slope stability analysis and solutions by using finite element and analytical analysis. The integrated modules include the analysis on stability of slopes, nailed slopes, reinforced slopes, rock stability, spread footing, abutment, gravity wall, gabions, and earth pressure. Swedish method of slices is used by GEO5 software for slope stability analysis. Analysis method available for GEO5 software are Bishop method, Spencer method and Morgenstern-Price method. The required input data for analysis are, slope geometry (inclination and height), soil profile, soil properties, phreatic line location, and water level adjacent to slopes.

Sample of a results from slope stability analysis using GEO5 is as shown in Figure 2.34. The minimum FS and critical slip surface are shown in the results.

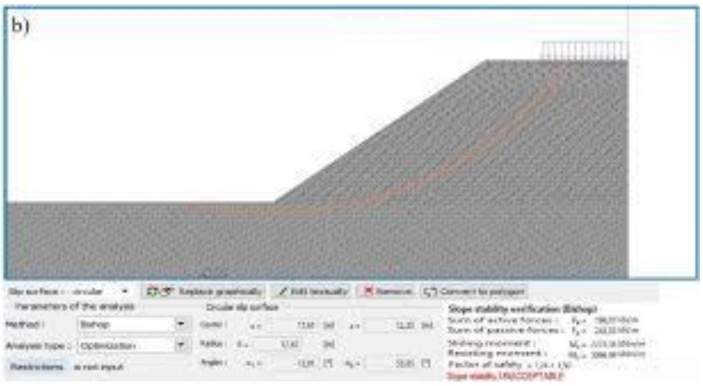

Figure 2.34: GEO 5 results of FS and critical slip surface (Wen, 2016).

For solving most geotechnical tasks, GEO5 is designed. It includes from the basic ones (e.g. slope stability, walls, verification of foundations), up to highly specialized programs (e.g. rock stability, building damage due to tunnelling, analysis of tunnels). Users can only choose the one they need, because definite structure type are solved by each GEO5 program. GEO5 is easy to apply because it composed of individual programs with common user interface. GEO5 provides analytical verification methods for effective and rapid structure designing and verification purposes. FEM program that structure was verified by method of finite element, there is a possibility for transferring the analytical model into it. The safety and objectivity are increased by comparison of two independent solutions. Moreover, for the use in third-party programs, GEO5 allow users to export in IFC and LandXML file (common BIM formats). It remains all soil parameters, elements description, and other object properties after transferred. It generates clear graphical outputs and text which can be easily edited based on users' needs. Directly printed from the program, output can be saved as PDF or exported to Microsoft Word. However, for highly specialized programs in GEO5 software, it was not easy to perform and does require studying guides and special training. However, GEO5 did offer few Training Materials, including user guides, engineering manuals, tutorials, and contextual help. Same to all software, the license of GEO5 is costly. With that, user can purchase only one program and buy additional ones later as required.

2.7.2 SLOPE/W software

With an objective being to determine an ultimate limit state, stability analysis is completed by SLOPE/W. It is to match Norwegian Standard NS 3480, Eurocode 7, and British Standard 8006 that are approaches of design. By applying partial factors onto loads characteristic and parameters of soil strength, stability analysis is completed. For safe design, an over-design factor that is Safety Factor (FS) must larger than or equal to 1.0. Eurocode 7 is the philosophy of limit state design implemented to show how stability analysis was conducted. (Bond and Harris, 2008; Orr and Farrell, 1999). However, adopting a philosophy of limit state design for all codes is the main principles. In SLOPE/W, all the methods in slope stability analysis are depended on formulations of limit equilibrium except for finite element method, that applied finite element computed stresses. SLOPE/W software provided analysis method such as Bishop method, Spencer method and Morgenstern-Price method, Janbu's Simplified method, etc. Like GEO5, the required input data for analysis are soil profile, soil properties, slope geometry (inclination and height), phreatic line location, and water level adjacent to slopes.

In SLOPE/W, there is an advantage like it has tools allowing users to show the detail forces on each slice and graph a list of different variables along surface of slip. With that, users can be more confident in judging the results. SLOPE/W opens the door to much wider types of analyses and more complex spectrum of problems which includes the use of finite element computed pore-water pressures and stresses in a stability analysis. It helps to deal with some limitations of purely formulations of limit equilibrium, but not only widen the analysis possibilities. There is certainly an increase in the capability of the program although this recently developed feature in SLOPE/W may be not needed. SLOPE/W are designed and developed for the purpose of stability analysis of earth structures. However, SLOPE/W is not designed for certain specific cases which is the disadvantages sometimes. For example, although SLOPE/W are applied to assess a gravity retaining wall's sliding stability and to find the wall's active earth forces, but SLOPE/W is not applied individually for designing retaining walls. Applying a general tool such as SLOPE/W sometimes requires careful thought that how to model a certain situation. However, it greatly expands the range of possible situations user can model compared to other software. With that, the general nature allows for much greater creativity.

Sample of a results from slope stability analysis using SLOPE/W is as shown in Figure 2.35. The minimum FS and critical slip surface are shown in the results.

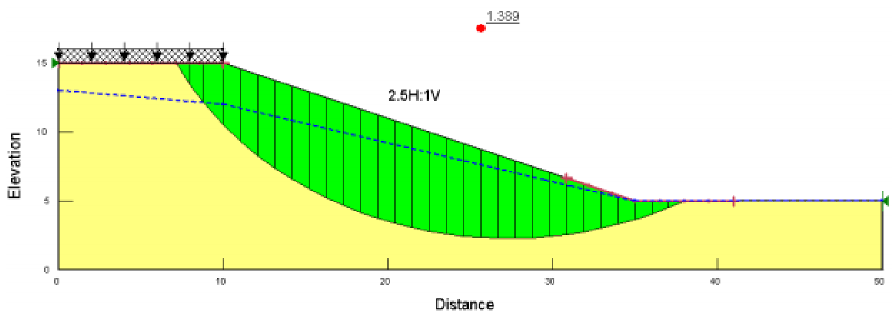

Figure 2.35: SLOPE/W calculated FS of the cut slope using characteristic values (Wang, 2020).

2.8 Summary

For analyzing the slope stability, several different methods are available to apply. It all depends on engineer to choose the method to apply (Albataineh, 2006). For a particular geotechnical situation, Limit Equilibrium Method were used to identify potential failure mechanisms and derived safety factors. The Limit Equilibrium Method was depending on two safety factor equations (equilibrium of moment (Fm) and equilibrium of horizontal force (Ff). Another name of Ordinary method of slices technique is "Fellenius' Technique". It satisfied the moment equilibrium but does not satisfy horizontal or vertical forces equilibrium. But, the resultant of inter-slices forces is ignored.

Acknowledged by all those engineering professions, the Simplified Bishop Method is most commonly used slope stability analysis method (Bishop, 1955). Simplified Bishop Method assumed rotation of a circular mass of soil caused the slope failure. The forces between the slices are also presumed acting from horizontal direction. Safety factor in simplified Bishop method was solved iteratively. Compared to FEM methods, the accuracy was also high with 5 percent of dissimilarity only. (Anderson and Richards 1987). Another clarified method is the Spencer method (Spencer, 1973). All the equations of equilibrium are satisfied. Depend on force equilibrium, the tangential force, T, the normal forces, E and N′, and safety factor, FS were determined. Safety factor (FS) for slope stability was expressed as ratio of soil shear strength (resisting force) to the maximum-armed shear stress (driving force) at potential failure surface. Safety factor is the smallest value of FS among all potential slip surface’s results obtained. The failure surface was mostly closed to the circle shape if the soil materials are homogeneous which was same case for this paper (Rahimi, 2013). Critical slip surface is most critical surface of failure together with minimum safety factor.

Stability of slope is mainly governed by slope factors of internal and external. Internal factors included soil strength at potential failure surface (e.g. unit weight, cohesion, and internal frictional angle) and slope geometry (e.g. slope height, slope inclination angle and slope shape). The external factors included the temperature and weathering changes, rainfall, earthquake, environment conditions of slope, tectonic stress, and artificial destruction (Wen, 2016). The influences of shear strength and parameters of slope geometry on the slope stability in terms safety factor and critical slip surface (e.g. arc length "L") by previous researches are discussed. Depended on the analysis of slope stability performed, the results were obtained. As driving force, unit weight (γ) increased, safety factor decreased (Wang, 2020). As resistance forces which is friction angle (φ) and cohesion (c) increased, safety factor increased (Wen, 2016). With the increment of Cohesion value (c) and Unit Weight (γ), Failure Arc length (L) value increased (Cheng, 2003). However, the length of failure arc (L) value was decreased with the increment of friction angle value (φ). Until a specific angle, the safety factor was not affected significantly by the increasing of the Alpha, α angle (Wen, 2016). Contrarily, safety factor was directly affected by increases of the Beta, β angle. From perspective of the length of failure arc, an increment of L happened when the Alpha, α angle increased. On the other hand, the length of failure arc did not affect significantly by the changes of the Beta, β angle (Wang, 2020).

For implementing in computer software, concepts in method of slices are easy to understand and steps are not difficult at all. Moreover, the simpler methods can even be done on a spreadsheet. Nowadays, several software such as GEO5 and SLOPE/W are available for slope stability analysis purposes. GEO5 software is a program which provides slope stability analysis and solutions by using finite element and analytical analysis. The required input data for analysis are, slope geometry (inclination and height), soil profile, soil properties, phreatic line location, and water level adjacent to slopes. In SLOPE/W, all the methods in slope stability analysis are depends on LEM exclusive of one method, the FEM, that applied finite element computed stresses.

CHAPTER 3

METHODOLOGY AND WORK PLAN

3.1 Introduction

The influence of soil strength and slope geometry parameters on slope stability are studied. Figure 3.1 shows the research methodology chart for this study.

This study mainly divided into two parts. Firstly, an excel spreadsheet was developed to investigate the effects of soil strength parameters (unit weight, cohesion, and internal friction angle) on the safety factors of slopes with fixed slip surface. Microsoft Excel (2019) under the Microsoft Office package that is a spreadsheet program was used to develop a spreadsheet for slope stability analysis with Simplified Bishop Method.

In the second part, numerical modelling using GEO5 software program with the license of education, Slope-Stability v16, was conducted to study the effect of both parameters of soil strength and slope geometry on minimum FS and critical surface of slip (location and arc length) of the slope. For simple determination, homogeneous soil was assumed in the slope stability analysis.

The latest student version of Automatic Computer-Aided Design (AutoCAD) software from the Autodesk Company was used to draw the critical slip surface obtained from GEO5 software program. Different graphs were generated for analysis purpose; to find the relationship between soil strength, slope geometry parameters, and safety factor together with length of failure arc. Finally, the study was concluded and written into a report.

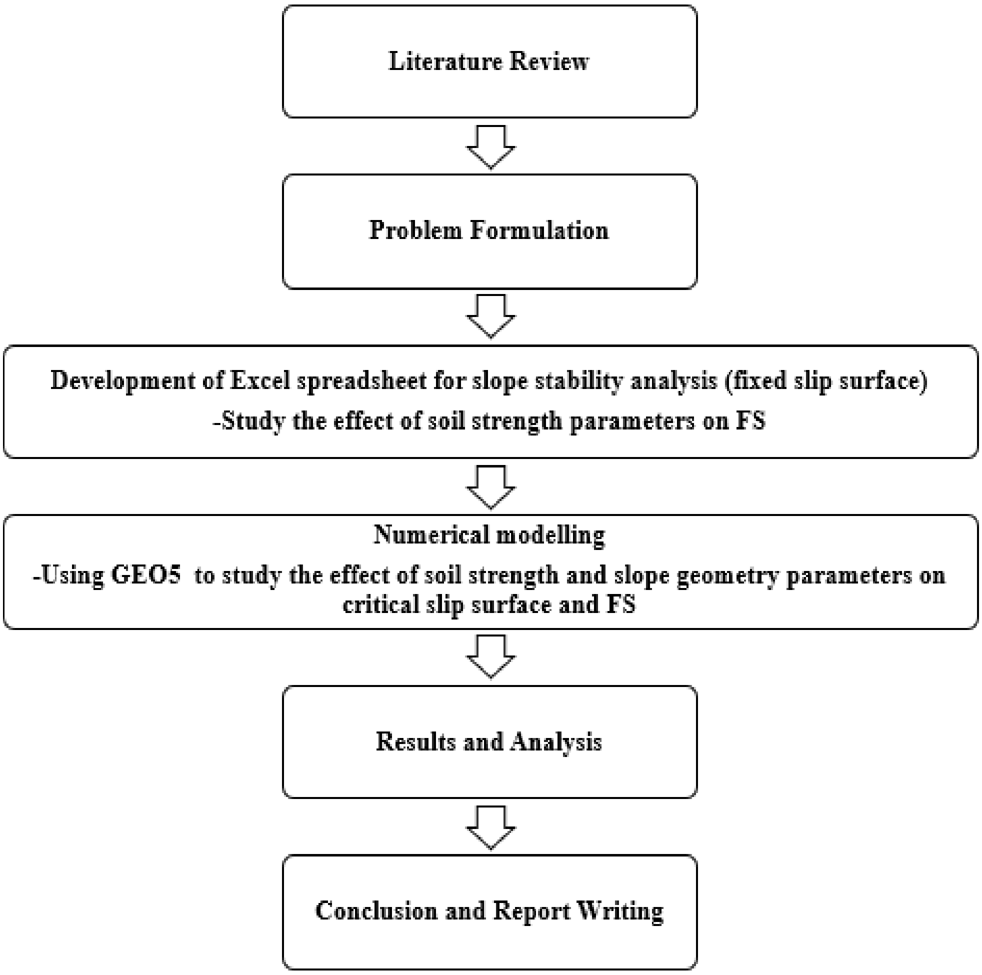

Figure 3.1: Research methodology chart.

3.2 Soil Strength and Slope Geometry Parameters

The soil strength parameters studied were soil γ, c, and φ whereas slope geometry parameters were Alpha and Beta angles. Alpha acts the overhead surcharge acting on slope and Beta is the steepness of slope. Table 3.1 shows the range of soil strength and slope geometry parameters chosen. According to previous researchers' studies, the range of parameters studied were chosen based on suitable value. According to Cheng (2020), by using accurate range of values, the results obtained will showed the trend of effects more obviously. If the value were out of this range, it tends to have differ results on some points.

The slope was assumed to be consisted of one type of soil. No multiple layers of soils were studied. Due to time limitation, no groundwater table effect was studied as the groundwater table is assumed far below the slope level.

Table 3.1: Soil Strength and Slope Geometry Parameters.

No.	Parameter	Range
1	Unit Weight, γ	15-25 kN/m^3
2	Internal Friction Angle, φ	14-22 °
3	Cohesion, c	15-30 kPa
4	Alpha angle, α	0-18 °
5	Beta angle, β	0-18 °

3.3 Slope Stability Analysis Using Excel Spreadsheet

A Excel Spreadsheet for slope stability analysis using Simplified Bishop Method was developed in this study. Then, it is used for the soil strength parametric study on the slope stability for fixed slip surface. Figure 3.2 shows the schematic view used for Excel Spreadsheet with fixed failure surface.

Figure 3.2: Schematic View for Excel Spreadsheet with fixed failure surface.

For the first step, as shown in Figure 3.3, soil type information was entered under “Soil data”, it could accommodate up to 6 soil types, together with SF tolerance and number of slices for calculation.

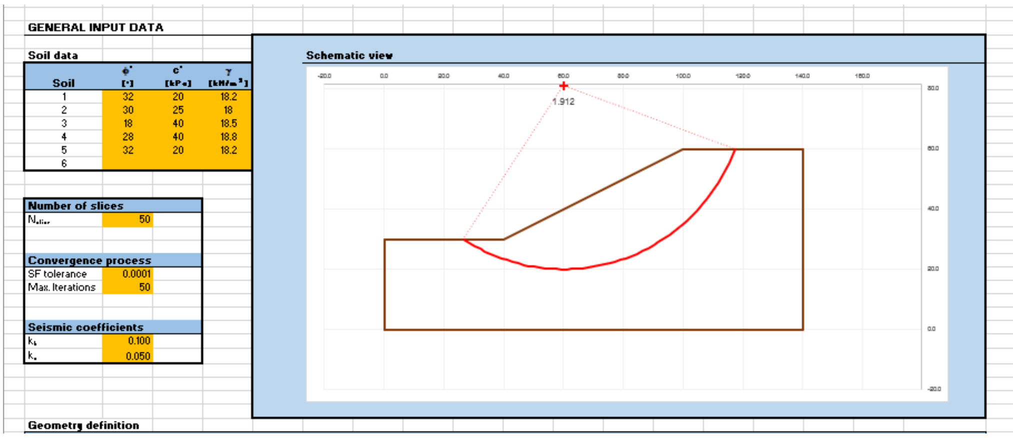

Figure 3.3: Spreadsheet KeyIN parameter.

As shown in Figure 3.4, under “Geometry definition”, the geometry of the soil layer was entered. For this spreadsheet, up to 5 layers of soil could be inputted, however, only 1 layer (homogeneous) were applied for ease of the study.

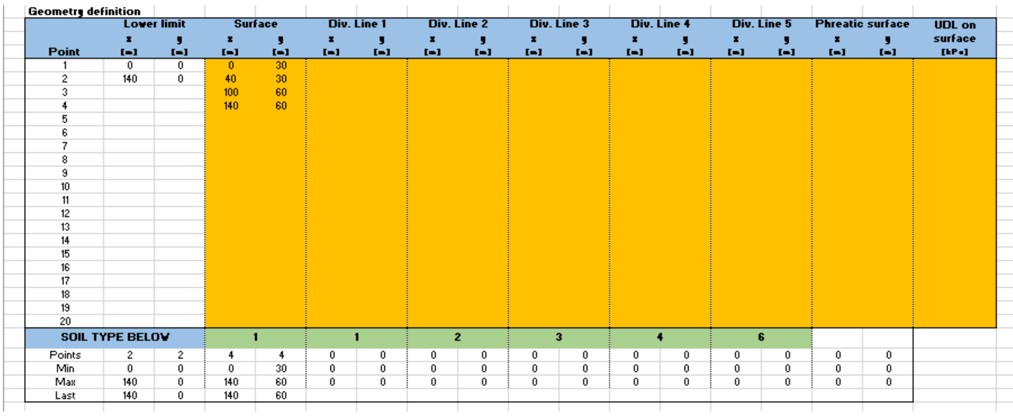

Geometry definition

Point	Lower limit x [m]	Lower limit y [m]	Surface x [m]	Surface y [m]	Div. Line 1 x [m]	Div. Line 1 y [m]	Div. Line 2 x [m]	Div. Line 2 y [m]	Div. Line 3 x [m]	Div. Line 3 y [m]	Div. Line 4 x [m]	Div. Line 4 y [m]	Div. Line 5 x [m]	Div. Line 5 y [m]	Phreatic surface x [m]	Phreatic surface y [m]	UDL on surface [kPa]
1	0	0	0	30													
2	140	0	40	30													
3			100	60													
4			140	60													
5																	
6																	
7																	
8																	
9																	
10																	
11																	
12																	
13																	
14																	
15																	
16																	
17																	
18																	
19																	
20																	
SOIL TYPE BELOW			1		1		2		3		4		6				
Points	2	2	4	4	0	0	0	0	0	0	0	0	0	0	0	0	
Min	0	0	0	30	0	0	0	0	0	0	0	0	0	0	0	0	
Max	140	0	140	60	0	0	0	0	0	0	0	0	0	0	0	0	
Last	140	0	140	60													

Figure 3.4: Spreadsheet KeyIN Geometry.

For the "Slip circle" part, the input were radius and coordinate of centroid. However, the slip surface was fixed for finding the relationship between soil strength parameters and safety factor. After that, “Solve” button was clicked to obtain the exact safety factor after few iterations was ran. The safety factor of the slope will be computed, as shown in the Figure 3.5, minimum safety factor. It was displayed at schematic view of slope in Figure 3.3.

INDIVIDUAL SLIP CIRCLE - SIMPLIFIED BISHOP METHOD

Slip circle data		
x_c	60.000	m
y_c	81.000	m
R	61.000	m
z_{min}	20.000	m

Update graph with slip circle

Intersection points with surface		
Point	x	y
1	26.534	30.000
2	117.271	60.000

Geometry		
Δx	90.74	m
Slices	50	
Δx_i	1.815	m

Safety factor iteration	
$SF_{initial}$	1.912
SF_{Bishop}	1.912
Iterations	4

Solve

Number of points

2.00

Horizontal ground?

0

Horizon	1	2	3	4	5	6	
Soil type	1	1	2	3	4	6	
γ	18.2	18.2	18	18.5	18.8	0	kN/m³
tanφ'	0.625	0.577	0.325	0.532	0.625	0.000	
c'	20	25	40	40	20	0	kPa

					Division lines levels						Geotechnical horizons heights					Weight	Seismic mom
Slice	x_i [m]	z_{bi} [m]	z_{ti} [m]	z_{1i} [m]	z_{2i} [m]	z_{3i} [m]	z_{4i} [m]	z_{5i} [m]	z_{wi} [m]	h_{1i} [m]	h_{2i} [m]	h_{3i} [m]	h_{4i} [m]	h_{5i} [m]	h_{6i} [m]	W_i [kN/m]	$k_s W_i y_{gi}/R$ [kN/m]
1	27.441	29.416	30.000	0.000	0.000	0.000	0.000	0.000	0.000	0.584	0.000	0.000	0.000	0.000	0.000	19.289	1.622
2	29.256	28.314	30.000	0.000	0.000	0.000	0.000	0.000	0.000	1.686	0.000	0.000	0.000	0.000	0.000	55.678	4.732
3	31.070	27.296	30.000	0.000	0.000	0.000	0.000	0.000	0.000	2.704	0.000	0.000	0.000	0.000	0.000	89.298	7.664
4	32.885	26.358	30.000	0.000	0.000	0.000	0.000	0.000	0.000	3.642	0.000	0.000	0.000	0.000	0.000	120.302	10.417
5	34.700	25.494	30.000	0.000	0.000	0.000	0.000	0.000	0.000	4.506	0.000	0.000	0.000	0.000	0.000	148.825	12.992
6	36.515	24.702	30.000	0.000	0.000	0.000	0.000	0.000	0.000	5.298	0.000	0.000	0.000	0.000	0.000	174.979	15.389
7	38.329	23.979	30.000	0.000	0.000	0.000	0.000	0.000	0.000	6.021	0.000	0.000	0.000	0.000	0.000	198.863	17.608
8	40.144	23.322	30.072	0.000	0.000	0.000	0.000	0.000	0.000	6.750	0.000	0.000	0.000	0.000	0.000	222.946	19.847
9	41.959	22.729	30.980	0.000	0.000	0.000	0.000	0.000	0.000	8.251	0.000	0.000	0.000	0.000	0.000	272.506	24.189
10	43.774	22.198	31.887	0.000	0.000	0.000	0.000	0.000	0.000	9.689	0.000	0.000	0.000	0.000	0.000	320.019	28.307
11	45.589	21.727	32.794	0.000	0.000	0.000	0.000	0.000	0.000	11.067	0.000	0.000	0.000	0.000	0.000	365.541	32.203
12	47.403	21.315	33.702	0.000	0.000	0.000	0.000	0.000	0.000	12.387	0.000	0.000	0.000	0.000	0.000	409.119	35.876
13	49.218	20.960	34.609	0.000	0.000	0.000	0.000	0.000	0.000	13.649	0.000	0.000	0.000	0.000	0.000	450.792	39.326
14	51.033	20.663	35.516	0.000	0.000	0.000	0.000	0.000	0.000	14.854	0.000	0.000	0.000	0.000	0.000	490.595	42.553
15	52.848	20.421	36.424	0.000	0.000	0.000	0.000	0.000	0.000	16.003	0.000	0.000	0.000	0.000	0.000	528.555	45.558
16	54.662	20.234	37.331	0.000	0.000	0.000	0.000	0.000	0.000	17.097	0.000	0.000	0.000	0.000	0.000	564.694	48.339

Figure 3.5: Spreadsheet Result.

To study the effect of soil strength parameters (e.g., γ, c, φ) on the safety, the processes were repeated by changing each of the parameter accordingly.

3.4 GEO5 software

From the GEO5 software package, student version of the "Slope Stability" software was used in this study. Its last version (16.3) was used for minimizing the problems of the software and possible bugs. Figure 3.6 shows the schematic view used for GEO5 software.

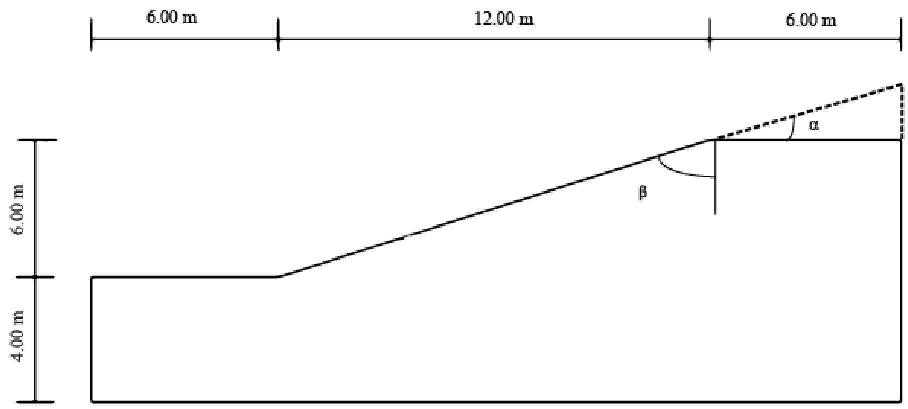

Figure 3.6: Schematic view for GEO5 software.

For the first step, as shown in Figure 3.7, coordinates of the slope was entered by applying the "Interface" tab, together with the "Add" button for each of the models.

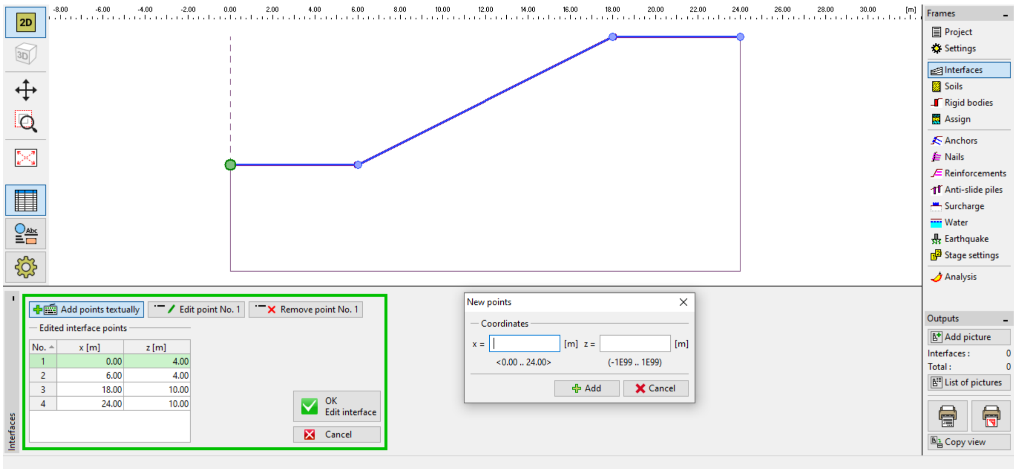

Figure 3.7: GEO5 Interface.

Next step, as shown in Figure 3.8, using "Add" button under "Soil" tab, the properties of the soil were entered. From the "Assign" tab, it was then assigned to the slope interface.

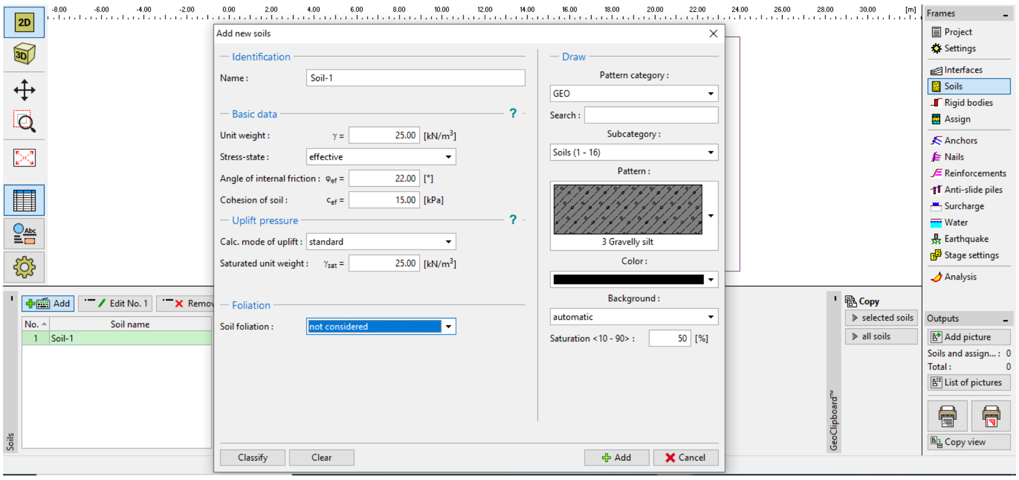

Figure 3.8: GEO5 Soil Properties.

In the "Slip Surface" part that was categorized below "Analysis" tab, input a first guess for the failure surface. Preliminary analysis was done by using "Analyze" button, after applying Simplified Bishop method, and changing "Analysis Type" to "Standard". After that, "Analysis Type" was adjusted to

"Optimization" and analysis were ran one more time for finding the critical failure surface and analyzing the slope. As shown in the Figure 3.9, minimum safety factor was found at critical surface of slip's detail and under "Analysis" section which came from "Slip Surface" section. The output information of critical surface of slip is coordinates of centroid and radius.

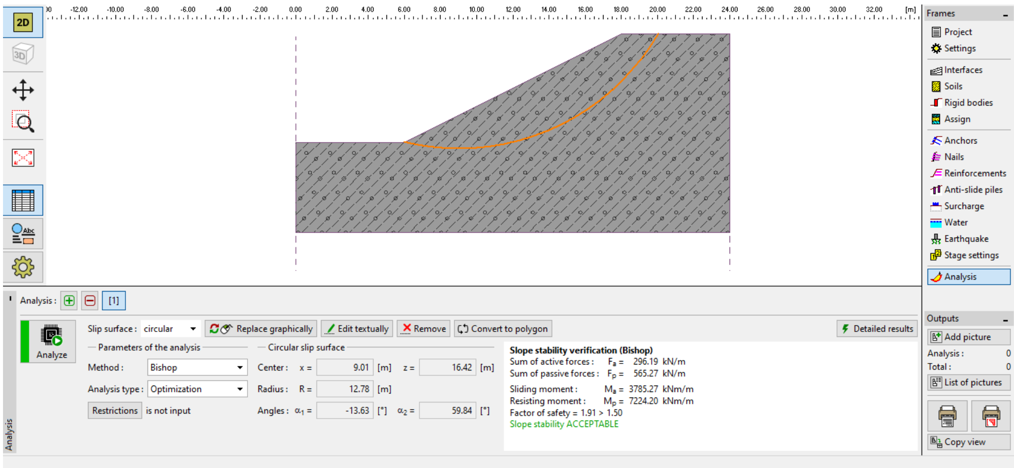

Figure 3.9: GEO5 Results.

3.5 Data and Analysis

From the Factor of Safety obtained from Excel spreadsheet, the graphs are plotted for showing the relationships between shear strength parameters (γ, c, φ) and FS. The graphs plotted are used to analyze the trend of line whether the relationship between parameters and FS is directly or inversely proportional. Figure 3.10 shows the sample of FS graph drawn for data from Excel spreadsheet.

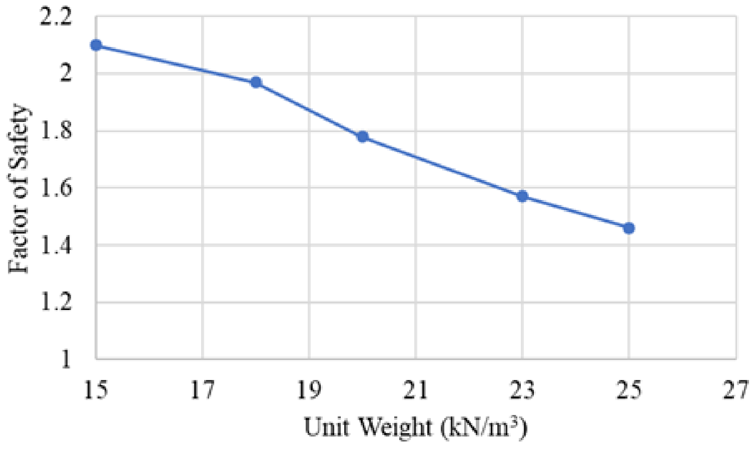

Figure 3.10: Sample of FS graph drawn for data from Excel spreadsheet.

From the Factor of Safety and critical slip surface obtained from GEO5 software, the graphs are plotted for showing the relationships between shear strength parameters (γ, c, φ) and slope geometry parameter (α, β) on FS and Length of Failure Arc, L. For drawing the critical slip surface of different model, the coordinates of centroid and radius from GEO5 are needed. The graphs plotted are used to analyze the trend of line whether the relationship between parameters and FS or Failure Arc Length is directly or inversely proportional. Figure 3.11 shows the sample of FS graph drawn for data from GEO5 and Figure 3.13 shows the sample of L graph drawn for data from GEO5. The sample of critical slip surface results of different models is shown in Figure 3.12.

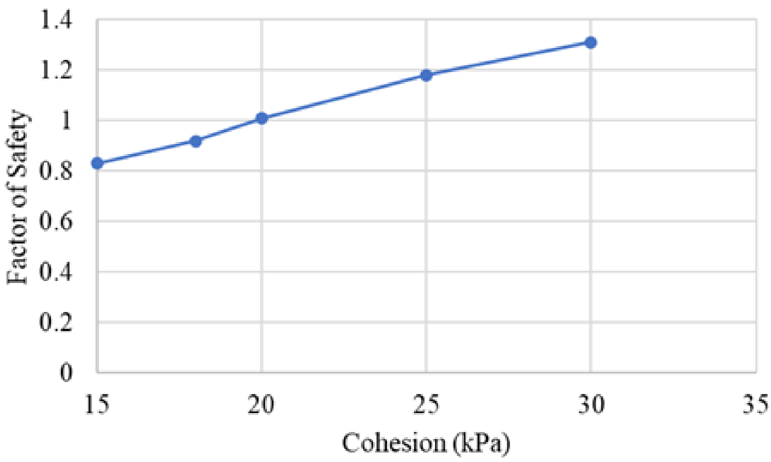

Figure 3.11: Sample of FS graph drawn for data from GEO5.

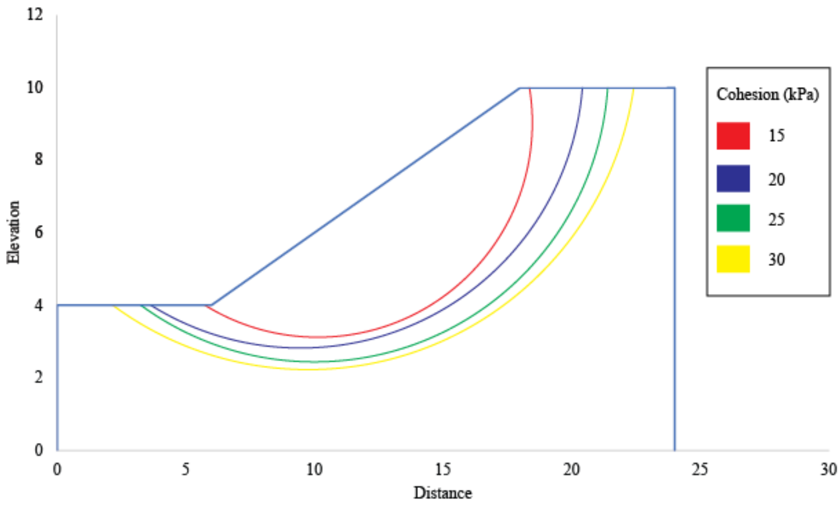

Figure 3.12: Sample of critical slip surface results of different models.

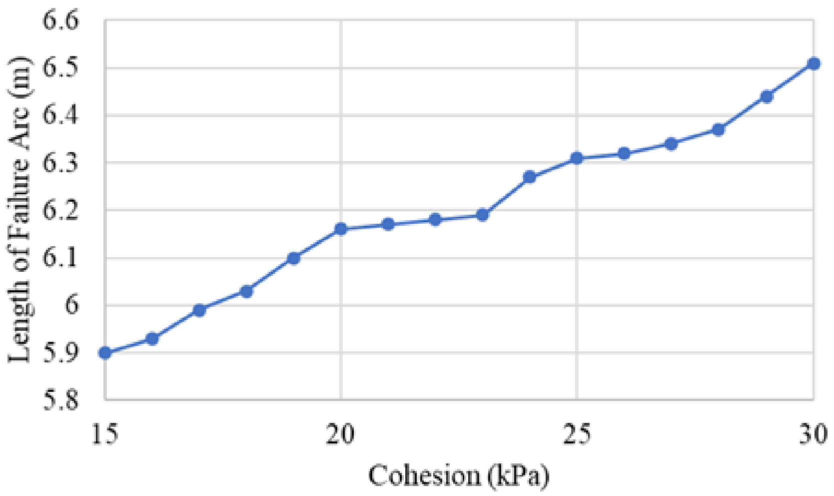

Figure 3.13: Sample of L graph drawn for data from GEO5.

3.6 Summary

The research methodology chart for this study is shown in this chapter. This study mainly divided into two parts. Firstly, an excel spreadsheet was developed to investigate the effects of soil strength parameters (unit weight, cohesion, and internal friction angle) on the safety factors of slopes with fixed slip surface. Simplified Bishop Method was used to create the slope stability analysis spreadsheet. Next, numerical modelling using GEO5 software program was conducted to study the effect of both parameters of slope geometry and soil strength on minimum FS together with critical slip surface (location and arc length) of the slope. The process taken are shown step by step. AutoCAD software from the Autodesk Company was used to draw the critical slip surface obtained from GEO5 software program. Different graphs were generated for analysis purpose using Microsoft Excel to find the relationship between soil strength, slope geometry parameters, and safety factor together with L. Parameters of soil strength studied were soil γ, c, φ whereas the slope geometry parameters were Alpha and Beta angles and the range of values are shown in this chapter. The schematic views of slope dimensions are displayed. For the limitation, the slope was assumed to homogeneous soil. Due to time limitation, no groundwater table effect was studied as the groundwater table is assumed far below the slope level.

CHAPTER 4

RESULTS AND DISCUSSION

4.1 Introduction

Based on each soil strength parameter (c, ϕ, and γ) and slope geometry parameter (α, β), two stages were studied both separately for slip surface and the safety factor in this chapter. For this purpose, few models had been studied in the first part, to find out the trend of changes in safety factor by parameters. Enough models were used, and were test in next part, with the intention to search for relationship between failure surfaces (length of failure arc) and parameters. Graph and figures had been drawn to display the influences of the parameters on failure surface (length of failure arc) and safety factor after generating and analyzing all the models. Furthermore, the causes of these different behaviors had been discussed to explain the trend.

4.2 Analyzing the Safety Factor by Excel Spreadsheet with Fixed Failure Surface

For this part of study, the spreadsheet were applied to analyze FS of slope with a fixed failure surface with different soil strength parameters. The relationship between soil strength parameter (γ, c, φ) and safety factor were determined. However, the limitation of spreadsheet was geometry parameter cannot be studied due to spreadsheet can only be used with a known critical surface. The schematic view of slope with fixed failure surface for this study are shown in Figure 4.1.

Figure 4.1: Schematic View of Slope with Fixed Failure Surface.

4.2.1 Effect of Unit weight, γ on the factor of safety, FS with Fixed Failure Surface

In this study, the soil unit weights were varied from 15 to 25 kN/m^3 whereas the soil cohesion and internal frictional angle was set at 30 kPa and 22 °, respectively. The failure surface was fixed for all cases. The FS reduced with the increase of the soil unit weight. Similar trend was obtained Wen (2013). Unit Weight of a soil is expressed as ratio of soil total weight to soil total volume. By assigning unit weight to soil, the sliding mass weight or gravitational force was used. The weight of slice was computed by specified Unit Weight times cross-sectional area of slice (Wen, 2016). The increase of driving forces due to the higher soil unit weight had reduced the slope stability in term of factor of safety (Cheng, 2003). Referring to Equation 2.11, the Unit Weight affected the slice weight, w. Weight of slices is affecting both the driving and resisting forces. However, the increment rate of driving force due to the soil unit weight increase was higher compared to resisting force. Hence, the FS reduced with the increase of soil Unit Weight. Effect of unit weight on FS is shown in Table 4.1.

Table 4.1: Effect of soil unit weight on FS.

Model No.	Unit Weight (kN/m³)	Internal Friction Angle (°)	Cohesion (kPa)	Factor of Safety
1	15	22	30	2.10
2	18	22	30	1.97
3	20	22	30	1.78
4	23	22	30	1.57
5	25	22	30	1.46

It was observed that FS reduced with increase of γ. By increasing the soil unit weight from 15 to 25 kN/m^3, the safety factor was reduced from 2.10 to 1.46. The FS for slope with γ of 25 kN/m^3 was only about 0.70 times of the FS for slope with γ of 15 kN/m^3. It was concludes that unit weight had a major effect on safety factor. The trend of safety factor decreasing with the increase of soil unit weight was quite same with the results obtained by Wen (2013). As the soil mass contributed to the main driving force, the safety factor was inversely proportional to the soil unit weight (Cheng,2003). Figure 4.2 shows the influences of soil γ on FS of slope with a fixed slip surface.

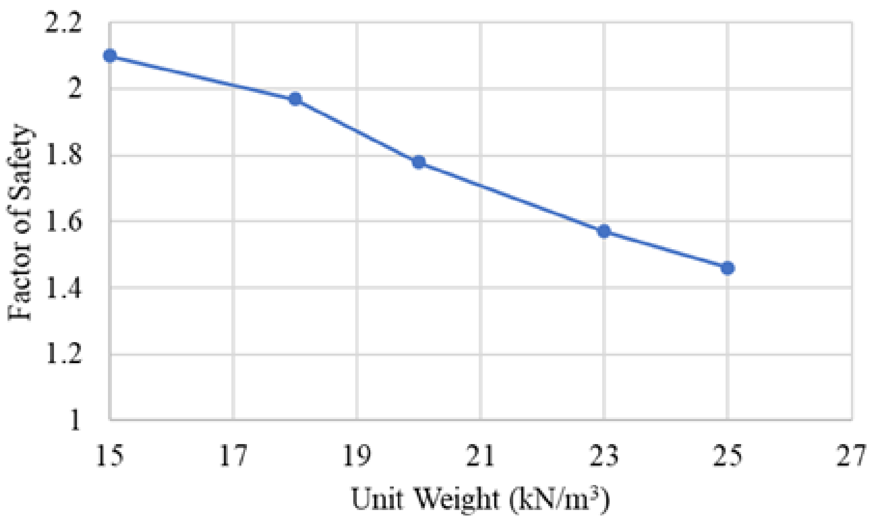

Figure 4.2: Effect of Unit Weight on the Factor of Safety.

4.2.2 Effect of Cohesion, c on the factor of safety, FS with Fixed Failure Surface

In order to study effect of soil Cohesion, c on FS of the slope, soil cohesion was varied from 30 to 15 kPa. Soil Unit Weight and angle of Internal Friction was set at 25 kN/m^3 and 22 °, the respectively. The failure surface was fixed for all cases. Table 4.2 shows the safety factors calculated using spreadsheet based on different soil cohesion values. According to Table 4.2, when the value of soil cohesion reduced, the safety factor decreased. The results obtained was tally with the studies by Zulkifl (2020) and Wen (2013) in which the safety factor increased with the increase of c. Within a soil, cohesion acts as a force that brings together molecules or like particles. Cohesion was usually affected by electrostatic force and cementing (Cheng, 2003). The result collected was satisfied with the theory since soil cohesion is one of the resisting forces in slope stability analysis as discussed earlier (Cheng, 2003). As soil cohesion is a strength parameter, FS increased when the strength parameter values increased. Downslope movement of material were promoted by driving forces, whereas resisting forces deter the movement. So, the slope is more stable and when driving forces are resisted by higher resisting forces. Effect of Cohesion on FS is shown in Table 4.2.

Table 4.2: Effect of Cohesion on FS.

Model No.	Unit Weight (kN/m^3)	Internal Friction Angle (°)	Cohesion (kPa)	Factor of Safety
1	25	22	30	1.27
2	25	22	25	1.10
3	25	22	20	0.98
4	25	22	18	0.90
5	25	22	15	0.81

Figure 4.3 shows the relationship between cohesion and safety factor. Value of FS increased when soil cohesion value increased. For soil cohesion

varied from 15 to 30 kPa, the slope safety factor was increased from 0.81 to 1.27, with a range of 0.46. The rapid increase of slope safety factor with the soil cohesion was also observed by Wen (2013). Effect of Cohesion,c on FS is shown in Figure 4.3.

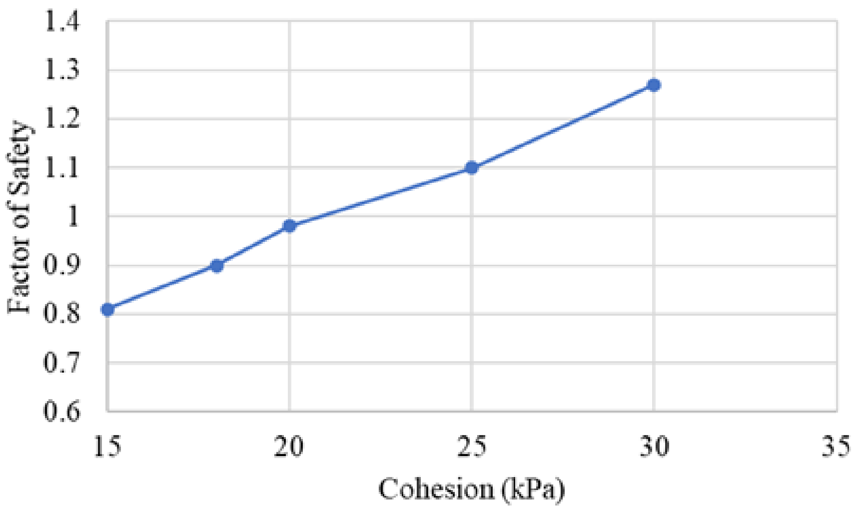

Figure 4.3: Effect of Cohesion, c on the Factor of Safety, FS.

4.2.3 Effect of Internal Friction Angle, φ on the factor of safety, FS with Fixed Failure Surface

For studying the slope stability for soil with different Internal Friction, φ was varied from 14 ° to 22 ° whereas the soil c and γ was fixed at 30 kPa and 25 kN/m^3, respectively. Range of internal friction angle was set based on the general value of friction angle for soil (Wang, 2020). The failure surface was fixed for all cases.

The factors of safety for slope with different soil internal friction angles are shown in Table 4.3. Figure 4.4 shows relationship between soil φ and FS. The value of FS increased with increase of soil φ as it was anticipated, due to the contribution of friction angle to the resisting force. For a given soil, internal friction angle is the measurement of shear strength due to the friction between soil particles. Due to the friction is a resisting force so FS increased when internal friction angle increased (Cheng, 2003). Resisting forces act in the opposite direction of driving forces. The resistance to downslope movement is greatly dependent on the shear strength of the soil on slope. Internal friction is the friction between grains within a soil material. With lower friction in soil, the slope stability became unstable and failure. The results obtained has same trend with the studies by Zulkifl (2020) and Wen (2013).

For increment of internal friction angle from 14 ° to 22 °, the safety factor was increased slightly from 1.05 to 1.20. It had a smaller effect on safety factor by comparing with cohesion parameters (Cheng, 2003). Similar trend was observed by Wen (2013). Effect of φ on FS is shown in Table 4.3 and Effect of φ on the FS is shown in Figure 4.4.

Table 4.3: Effect of φ on FS.

Model No.	Unit Weight (kN/m^3)	Internal Friction Angle (°)	Cohesion (kPa)	Factor of Safety
1	25	22	30	1.20
2	25	20	30	1.13
3	25	18	30	1.11
4	25	16	30	1.08
5	25	14	30	1.05

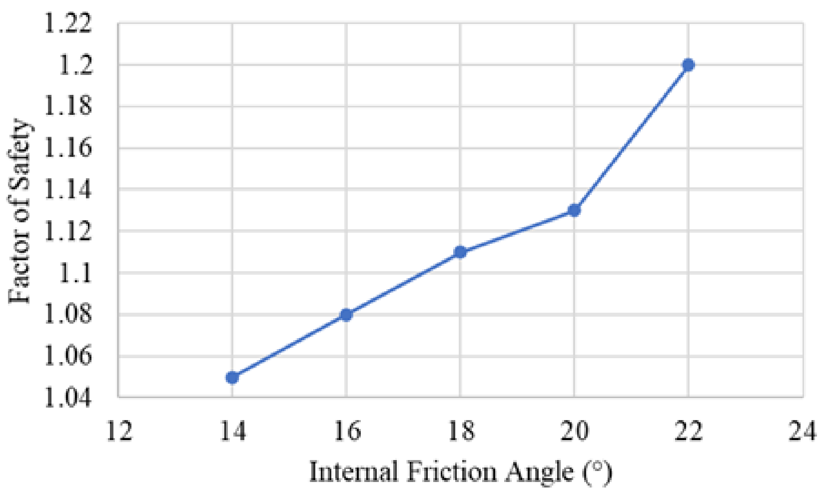

Figure 4.4: Effect of Internal Friction Angle on the Factor of Safety.

4.3 Effect of Soil Strength and Geometry Parameters on Minimum Safety Factor and Critical Slip Surface of Slope by GEO5

Slope modelling using GEO5 software program was conducted to study the influence of parameters of slope geometry together with soil shear strength on minimum FS and critical surface of slip. GEO5 software displayed minimum FS and critical slip surface, coordinates of centroid and radius for slip surface in the results obtained as shown in Figure 4.6 and Figure 4.7. Numerous slope models was studied by using GEO5 software to examine geometry of slope together with soil strength affected location of critical slip surface and the arc length of failure. The slip circles obtained from GEO5 were redrawn by using AutoCAD software to locate the entry point in the slope area and to find the arc length. To investigate the influence of each parameter on slip surface, the combination of results from software were drawn in one figure and table by using AutoCAD and Excel, respectively.The arc of failure length (L) and entry point were the side results for locating surface of slip. Critical slip surface were found by trial and error based on possible failure surface. For critical surface of slip, the minimum FS were shown together to show stability of the slope. The general slope model used in this study is as shown in Figure 4.5.

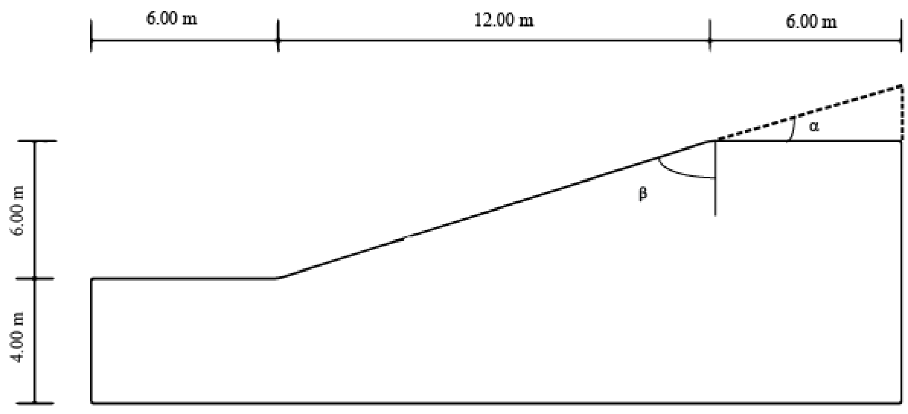

Figure 4.5: Schematic View of Slope Model Geometry.

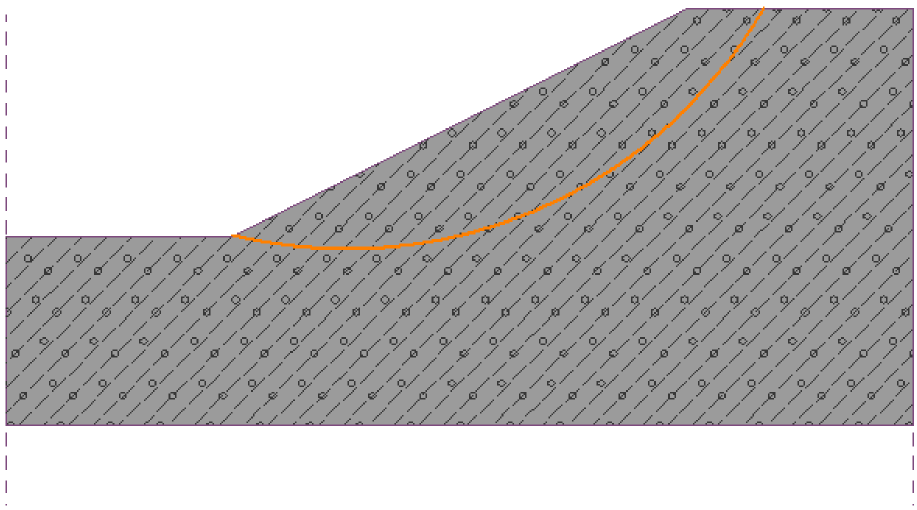

Figure 4.6: GEO5 Results of Critical Slip Surface for Each Single Model.

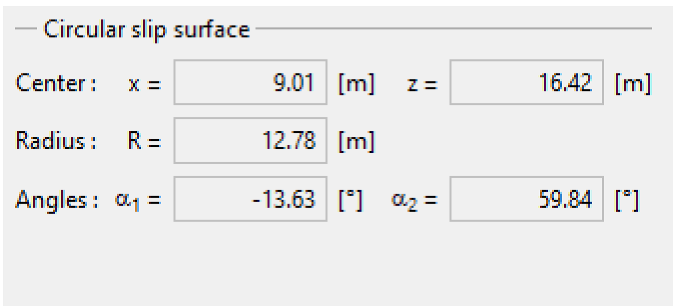

Figure 4.7: GEO5 Results of Centroid coordinate and Radius.

4.3.1 Effect of Unit weight, γ on the Minimum Safety Factor and Critical Slip Surface

To study influence of soil Unit Weight on FS, γ were varied from 15 to 25 kN/m^3. Soil cohesion and angle of Internal Friction was set at 30 kPa and 22 °, respectively.

The safety factor reduced with the increase of γ of the soil. According to Equation 2.11, the γ affected the slice weight, w. Both driving and resisting forces are affected by weight of the slices. However, the increment rate of driving force due to the soil unit weight increase was higher compared to resisting force. Hence, the safety factor reduced with increase of soil γ. Same as results of (Wen, 2013), the trend of results was similar. Although the safety factor value might vary for all the calculation method applied, Wen (2003) found that the trend was the same.

Figure 4.8 shows the influence of γ on FS of slope. It was observed that FS reduced with increase of soil γ. By increasing the soil unit weight from 15 to 25 kN/m^3, the safety factor was reduced from 2.29 to 1.55. The FS for slope with γ of 25 kN/m^3 was only about 0.50 times of the FS for slope with γ of 15 kN/m^3. It was concludes that unit weight had a major effect on safety factor. The trend of safety factor decreasing with the increase of soil unit weight was quite same with the results obtained by Wen (2013). As the soil mass contributed to the main driving force, the safety factor was inversely proportional to the soil unit weight (Cheng,2003). Effect of γ on FS is shown in Table 4.4 and Effect of γ on FS is shown in Figure 4.8.

Table 4.4: Effect of γ on FS.

Model No.	Unit Weight (kN/m^3)	Internal Friction Angle (°)	Cohesion (kPa)	Factor of Safety
1	15	22	30	2.29
2	18	22	30	2.05
3	20	22	30	1.81
4	23	22	30	1.68
5	25	22	30	1.55

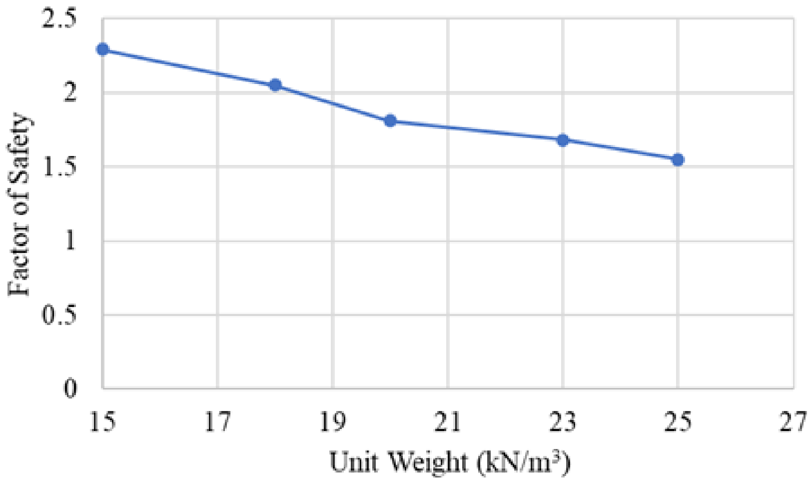

Figure 4.8: Effect of Unit Weight on the Factor of Safety.

To study the effect of γ on critical slip surface, γ was varied from 15 to 25 kN/m^3. The influence of γ on the failure surface is shown in Figure 4.9. A logical rule was followed by all the slip surfaces. The failure surface became larger and deeper as γ of the soil increased. With that, a larger soil weight above failure surface was resulted and hence the slip surface length was also increased. Less resisting force due to soil internal friction was activated due to the larger failure surface (Cheng, 2020). Smaller safety factor value was observed due to above reasons. Information of critical slip surface for slopes with different soil unit weight is shown in Table 4.5 and effect of γ on slip surface is shown in Figure 4.9.

Table 4.5: Information of Critical Slip Surface for Slopes with Different Soil Unit weight.

Model No.	Unit Weight (kN/m³)	Internal Friction Angle (°)	Cohesion (kPa)	Radius (m)	Entry Point Distance (m)	Length of Failure Arc (m)	Factor of Safety
1	15	15	15	7.54	2.23	5.28	1.02
2	16	15	15	7.87	2.35	5.37	0.97
3	17	15	15	7.96	2.40	5.49	0.93
4	18	15	15	8.03	2.47	5.50	0.89
5	19	15	15	8.35	2.48	5.54	0.82
6	20	15	15	8.65	2.52	5.61	0.77
7	21	15	15	8.89	2.60	5.68	0.73
8	22	15	15	8.98	2.68	5.71	0.68
9	23	15	15	9.24	2.73	5.74	0.65
10	24	15	15	9.47	2.74	5.78	0.61
11	25	15	15	9.78	2.79	5.80	0.59

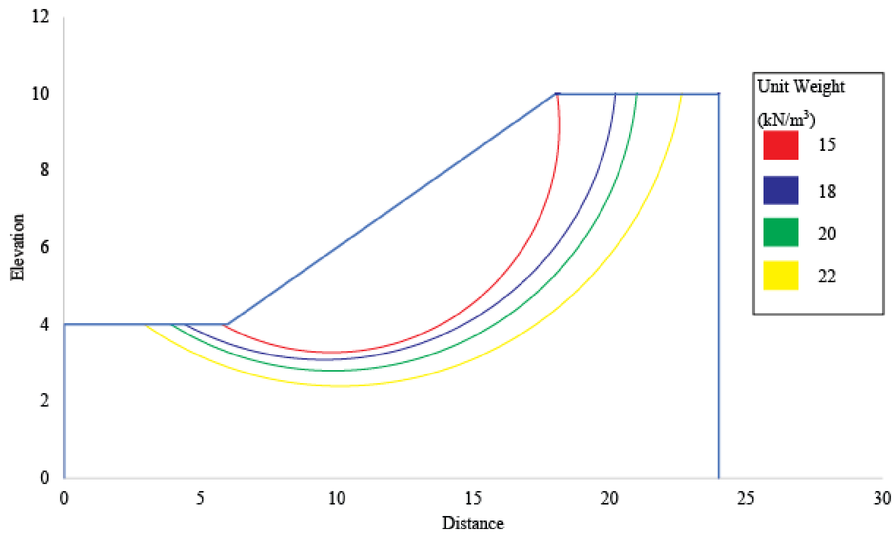

Figure 4.9: Effect of γ on Slip Surface.

The effect of soil unit weight on the failure surface arc length was studied in this section. A smaller safety factor was observed for slope with larger soil unit weight as shown in Figure 4.10. Critical slip surface moved toward slope's face by decrement of unit weight. Hence, a smaller safety factor can be achieved by decreasing L (Wang, 2020). Effect of γ on Failure Arc Length, L is shown in Figure 4.10.

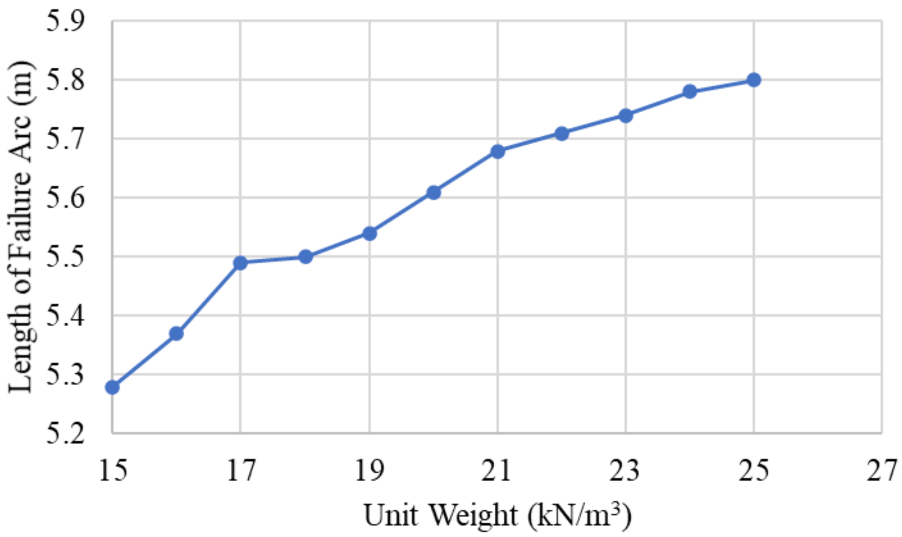

Figure 4.10: Effect of Unit Weight, γ on the Length of Failure Arc, L.

4.3.2 Effect of Cohesion, c on the Minimum Safety Factor and Critical Slip Surface

To study effect of soil cohesion on safety factor of the slope, Cohesion was set from 30 to 15 kPa. Unit Weight and Internal Friction angle of soil was set at 25 kN/m^3 and 22 °, respectively.

Table 4.6 shows the minimum safety factors for slopes with different soil cohesions. According to Table 4.6, when the value of cohesion reduced, the safety factor decreased. The results obtained was tally with the results from the study by Zulkifl (2020) in which the safety factor of slope increased when the soil cohesion increased. Similar findings were found by Wen (2013). Cohesion is the ability of soil particles to attract and hold each other together. Soil cohesion at the slip surface is one of the resisting forces. When the cohesion strength reduced, the ability soil to resist the driving forces reduced hence decreased the safety factor of the slope. If the soil cohesion was kept extensive, large slip surface were more likely to happen (Cheng, 2008).

Figure 4.11 shows the relationship between soil cohesion and safety factor of slope. For soil cohesion varied from 15 to 30 kPa, the safety factor was increased from 0.83 to 1.31, with the difference of 0.48. The trend of rapid increase was also observed by Wen (2013). Cohesive soil is soil with a high clay content with high cohesive strength. Cohesive soil does not crumble, and it is plastic when moist. Cohesive soil exhibits significant cohesion when submerged and is hard to break up when dry. As it was anticipated, FS increased when cohesion value that contributed to the resistant force was increased. Effect of c on FS is shown in Table 4.6 and Effect of c on FS is shown in Figure 4.11.

Table 4.6: Effect of c on FS.

Model No.	Unit Weight (kN/m^3)	Internal Friction Angle (°)	Cohesion (kPa)	Factor of Safety
1	25	22	30	1.31
2	25	22	25	1.18
3	25	22	20	1.01
4	25	22	18	0.92
5	25	22	15	0.83

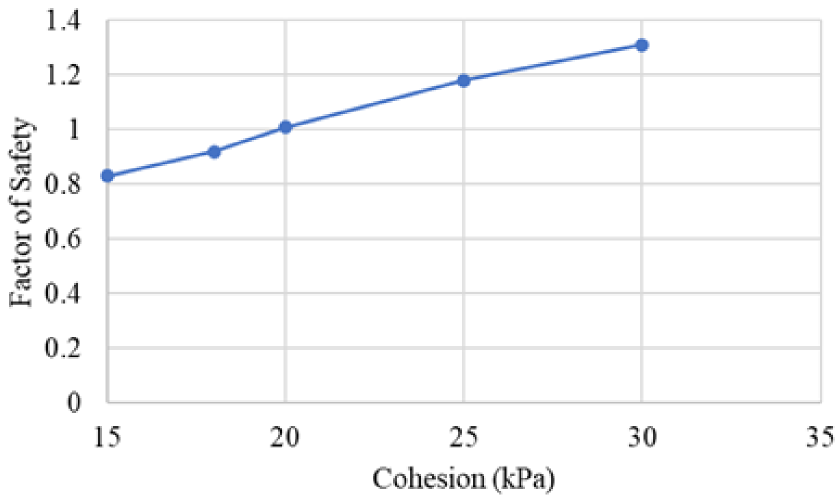

Figure 4.11: Effect of Cohesion on the Factor of Safety.

To study the effect of soil cohesion on critical slip surface, soil cohesion was varied from 15 to 30 kPa. The critical slip surface become larger and deeper when the cohesion value increased as shown in Figure 4.12. Critical slip surface started from the entry point at top of slope and pass through slope and end at near the toe was the pattern of the arc of failure (Wang, 2020). For achieving exact value of cohesion force, multiplied cohesion factor with length of failure arc. The increase of cohesion factor caused the arc length of failure surface increased (Wang, 2020). Besides that, the weight of soil above surface of failure increased due to larger failure surface. Next, the safety factor when the arc length of failure surface increased due to the higher soil cohesion value. This showed that the cohesion which is the resisting force are more important that the driving force for this situation (Cheng,2003). Information of Critical Slip Surface for Slopes with Different Soil Cohesions is shown in Table 4.7 and Effect of soil cohesion on Slip Surface is shown in Figure 4.12.

Table 4.7: Information of Critical Slip Surface for Slopes with Different Soil Cohesions.

Model No.	Unit Weight (kN/m^3)	Internal Friction Angle (°)	Cohesion (kPa)	Radius (m)	Entry Point Distance (m)	Length of Failure Arc (m)	Factor of Safety
1	15	15	15	7.49	2.92	5.9	1.08
2	15	15	16	7.67	2.97	5.93	1.14
3	15	15	17	7.70	3.05	5.99	1.21
4	15	15	18	7.89	3.13	6.03	1.26
5	15	15	19	8.03	3.23	6.1	1.33
6	15	15	20	8.12	3.24	6.16	1.39
7	15	15	21	8.23	3.26	6.17	1.45
8	15	15	22	8.45	3.27	6.18	1.50
9	15	15	23	8.67	3.29	6.19	1.56
10	15	15	24	8.97	3.33	6.27	1.63
11	15	15	25	9.03	3.38	6.31	1.69
12	15	15	26	9.12	3.40	6.32	1.75
13	15	15	27	9.21	3.44	6.34	1.81
14	15	15	28	9.45	3.47	6.37	1.87
15	15	15	29	9.67	3.52	6.44	1.93
16	15	15	30	9.78	3.56	6.51	2.00

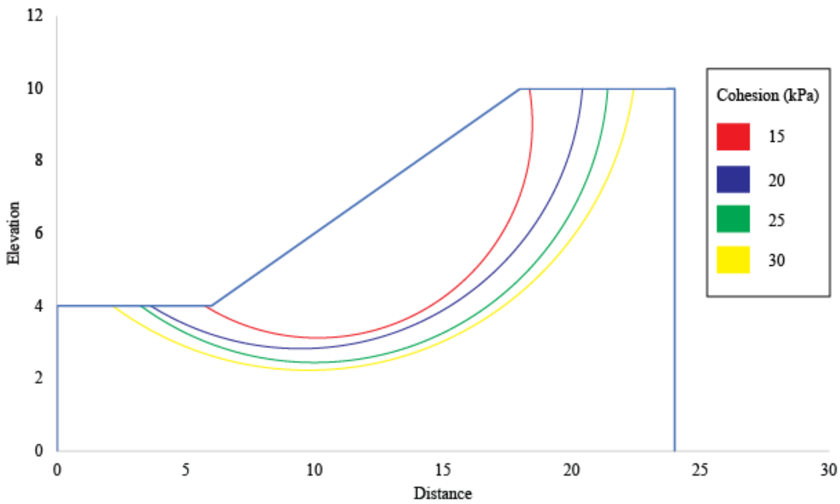

Figure 4.12: Effect of soil cohesion on Slip Surface.

Failure surface length increased by increasing the cohesion value as shown in Figure 4.13. Similar results were obtained in the study by Wang (2020) in which the cohesion increased the failure arc length. The resisting force and safety factor of slope also increased as the soil cohesion increased. This was because shape and location of the critical slip surface remained when soil cohesion increased. To achieve the main goal of analysis of slope stability which was to search for minimum value of safety factor. Hence, the driving force were increased. It can be reached by enlarging the failure area of slope. This gave rise to a greater failure arc length (L) and hence larger safety factor value (Cheng, 2003). Effect of c on Failure Arc length, L is shown in Figure 4.13.

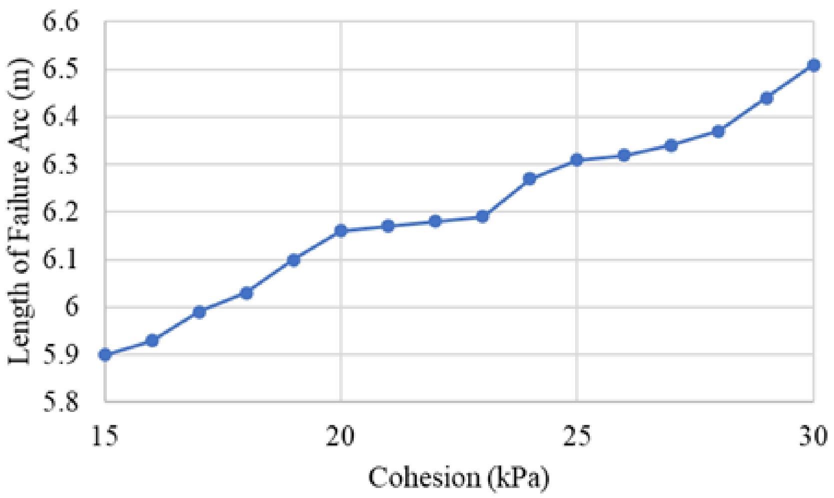

Figure 4.13: Effect of Cohesion, c on the Length of Failure Arc, L.

4.3.3 Effect of Friction Angle, φ on the Minimum Safety Factor and Critical Slip Surface

In this study, the soil cohesion was set at 30 kPa whereas the soil internal friction angles were varied from 22 to 14 °. The values of internal friction angle were selected based on the typical soil friction angle (Wang, 2020). Other than that, the unit weight was kept constant at 25 kN/m^3.

The decreased of soil internal friction caused the safety factor of slope to decrease as shown in Table 4.8. The soil internal friction angle is another component that contributed to resisting force in slope stability. Internal friction is a friction between grains within a material. With lower friction in soil, the slope stability became less stable. When the resisting force is smaller than driving force, failure of slope will happen. The results obtained has the same trend with the study by Zulkifl (2020) and Wen (2013).

The influence of φ on the FS was shown. The value of FS increased as φ increased. Figure 4.14 shows relationship between φ and FS, it was concavely increasing. For φ varied from 14 to 22 °, FS of slope was from increased from 1.11 to 1.25. The increment of 0.14 was considered small and played less effect on safety factor. It had a smaller effect on safety factor compared to the cohesion parameters (Cheng, 2003). Similar trend was obtained by Wen (2013). Effect of φ on FS is shown in Table 4.8 and Effect of φ on the FS is shown in Figure 4.14.

Table 4.8: Effect of φ on FS.

Model No.	Unit Weight (kN/m³)	Internal Friction Angle (°)	Cohesion (kPa)	Factor of Safety
1	25	22	30	1.25
2	25	20	30	1.17
3	25	18	30	1.16
4	25	16	30	1.12
5	25	14	30	1.11

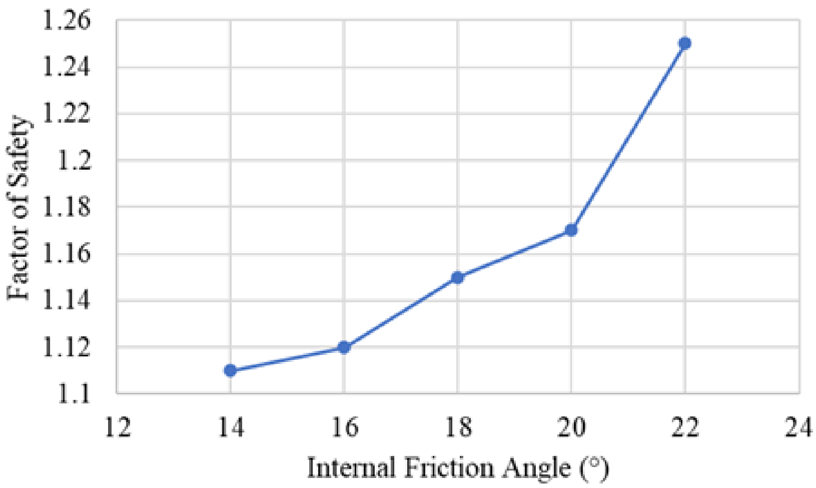

Figure 4.14: Effect of Internal Friction Angle on the Factor of Safety.

To study effect of φ on critical slip surface, φ was varied from 14 to 22 °. The influence of φ on critical surface of slip is shown in Figure 4.15. Surface of failure (failure arc length, L) decreased with increase of internal friction angle. Friction force was achieved by multiplying L with tangent of internal friction angle. Besides that, a larger value for φ force and smaller weight of failure volume (smaller driving force) were resulted by smaller failure surface. In contrast, FS increased with decrease of slip surface (failure arc length) and increase of φ. This concluded that the increase in φ effect which is the resisting force was more dominant than the driving force. The critical slip surfaces were shallower for the slope with higher soil internal friction angle. The critical slip surfaces were more likely to enter slope from point of entry and pass through slope near toe for the soil with large internal friction angle (Wang, 2020). Comparatively, when the value of cohesion was small, points of entry and exit located around toe and on crest for local failures of the slope (Wang, 2020). The results were further confirmed with the results published by Ahmed (2017). When the internal friction angle increased, all the failure surfaces moved to the left and became smaller. Information of Critical Slip Surface for Slopes with Different Soil Internal Friction Angle is shown in Table 4.9 and Effect of φ on Critical Slip Surface is shown in Figure 4.15.

Table 4.9: Information of Critical Slip Surface for Slopes with Different Soil Internal Friction Angle.

Model No.	Unit Weight (kN/m^3)	Internal Friction Angle (°)	Cohesion (kPa)	Radius (m)	Entry Point Distance (m)	Length of Failure Arc (m)	Factor of Safety
1	15	14	15	9.88	2.87	5.84	1.01
2	15	15	15	9.54	2.84	5.81	1.04
3	15	16	15	8.99	2.81	5.78	1.09
4	15	17	15	8.56	2.76	5.76	1.11
5	15	18	15	8.34	2.71	5.71	1.12
6	15	19	15	8.06	2.69	5.69	1.13
7	15	20	15	7.95	2.66	5.66	1.14
8	15	21	15	7.78	2.59	5.59	1.15
9	15	22	15	7.52	2.54	5.57	1.16

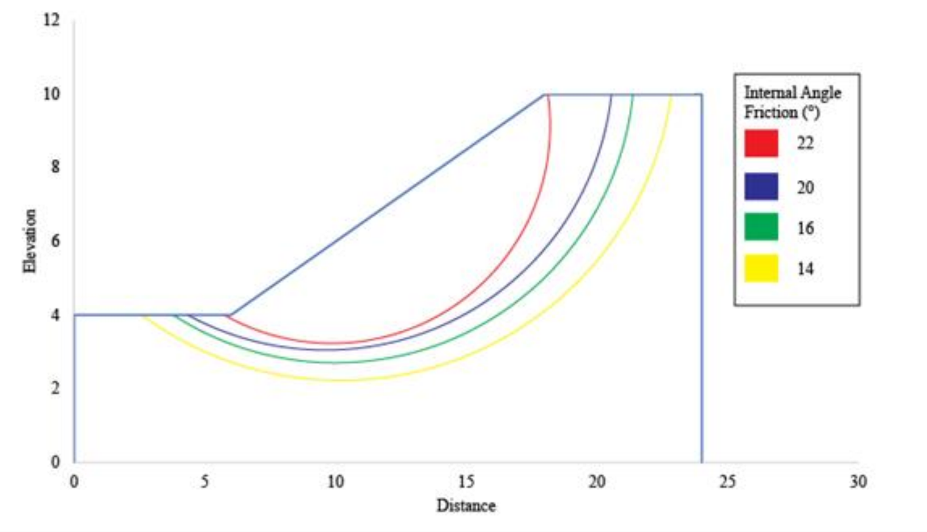

Figure 4.15: Effect of φ on Critical Slip Surface.

It can be anticipated that arc length of failure surface, L decreased with increment of φ, phi based on the same clarification in previous section. However the arc length of failure surface and soil internal frictional angle was inversely related as shown in Figure 4.16. According to Jiang and Yamagami (2006), they stated that "In a homogeneous soil slope, when the unit weight, slope geometry, and pore water pressure distribution were given, the critical slip surface location was related only to $c/tan\ (\varphi)$ ratio of that slope for a particular method of slices". This study presented that the failure arc length is in an inversely proportional with angle of internal friction. Effect of φ on Failure Arc Length, L is shown in Figure 4.16.

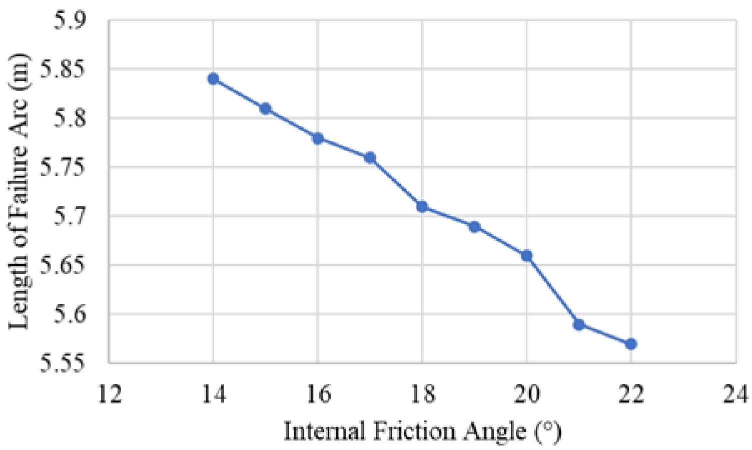

Figure 4.16: Effect of Internal Friction Angle, φ on the Length of Failure Arc, L.

4.3.4 Effect of Slope Geomtery on the Minimum Safety Factor and Critical Slip Surface

Using constant parameters of soil strength: γ = 25 kN/m^3, c = 30 kPa, and φ = 22 °, different slope shapes had been analyzed for investigating the influence of geometry of slope on FS. Two slope angles α, and β had been varied to study influence of slope geometry on FS based on schematic view of slope in Figure 4.17. The possible slope geometry is shown in Figure 4.18.

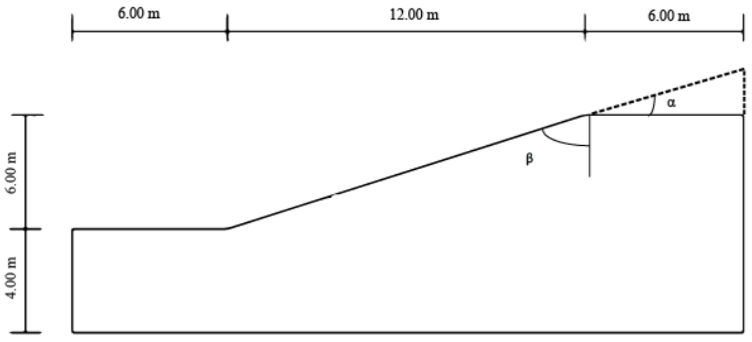

Figure 4.17: Schematic View of Slope Model Geometry.

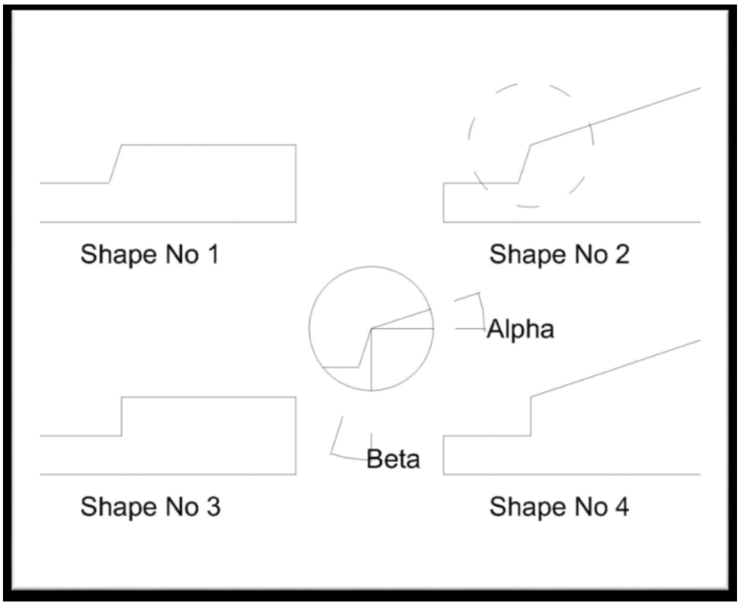

Figure 4.18: Possible slope geometry

The increase of the slope angle (Alpha) reduced the FS and slope stability. This was due to overhead load was acted by amount of added soil to top part of slope. Overhead load will increase the driving force and causes the safety factor to decrease (Zulkifl, 2020). When the driving force increased while the resisting force remained, the slope stability was decreased causing the safety factor to decrease. The slope was less stable in decreasing the slope angle (Beta). The smaller the beta, the steep the slope. The safety factor increased by a more resisting force. Resisting force came from the angle for arc length decreases (Zulkifl, 2020). The effect of slope geometry on FS is shown in Table 4.10.

Not much difference was observed on the safety factor by changing the alpha angle from 2° to 18° . The safety factor varied from 1.19 to 1.11 only with difference of 0.08 as shown in Figure 4.19. The results obtained was tally with the results obtained by Zulkifl (2020). On the slope surface, increasing of alpha angle added an extra overhead surcharge to the slope that contributed to the driving forces. It also generated a rise in driving force because of higher weight of soil above surface of failure. However, resisting force was also increased because of longer failure arc length when the soil area above failure surface was increased. With the simultaneous increase of resisting and driving forces, the effect of alpha angle on the safety factor was minima (Zulkifl, 2020). The increase in driving force became larger compared to the resisting force for alpha angle larger than 16 °. When the driving force became larger than resisting force, resisting force started to unable to withstand driving force and therefore, a more noticeable decrease was observed on the safety factor value (Cheng, 2003). Effect of α on Safety Factor, FS is shown in Figure 4.19.

Table 4.10: Effect of Alpha, α and Beta, β on Factor of Safety, FS.

Model No.	α (°)	β (°)	Failure Surface				Factor of Safety
			Center		Radius (m)	Length of Arc (m)	
			X (m)	Y (m)			
1	18	0	4.81	21.27	10.28	7.28	1.11
2	16	0	3.45	23.79	10.27	7.27	1.15
3	14	0	3.12	23.89	10.26	7.25	1.16
4	12	0	3.29	23.55	10.25	7.24	1.16
5	10	0	2.54	24.34	10.23	7.22	1.18
6	8	0	5.08	20.61	10.21	7.20	1.18
7	6	0	5.12	21.75	10.20	7.19	1.19
8	4	0	2.53	24.00	10.18	7.14	1.19
9	2	0	1.75	24.31	10.17	7.10	1.19
10	0	0	1.37	24.81	10.15	6.96	1.20
11	0	2	2.95	23.36	10.14	6.67	1.25
12	0	4	4.04	22.54	8.82	6.32	1.28
13	0	6	4.16	22.11	8.34	6.13	1.29
14	0	8	5.44	19.94	5.71	6.04	1.33
15	0	10	5.43	20.98	6.57	5.95	1.37
16	0	12	5.19	21.24	6.88	5.79	1.40
17	0	14	6.15	20.22	5.47	5.65	1.45
18	0	16	6.28	20.10	5.33	5.43	1.47
19	0	18	5.78	20.37	5.67	5.25	1.50

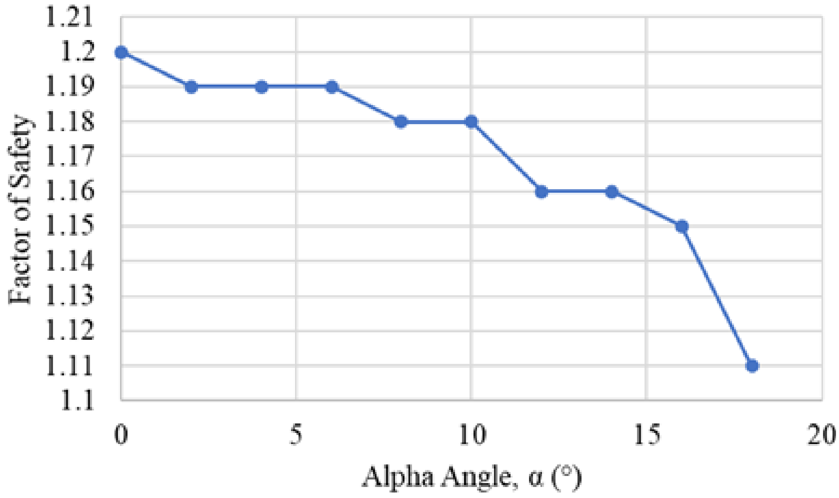

Figure 4.19: Effect of α on Safety Factor, FS.

Safety factor increased significantly with the increase Beta angle as shown in Figure 4.20. The resisting force increased due to increase of the arc length of failure surface but the driving force was kept almost constant as the shape and location of failure surface had not much changes when the beta angle increased (Cheng, 2003). The greater beta angle also showed that the slope was less steep. Hence, the safety factor increased when beta angle increased. When resisting force is larger than driving force, the slope has higher stability and failure is less likely to happen. Compared to the Alpha angle, Beta angle was more significant effects on the safety factor of slope (Zulkifl, 2020). Effect of β on Safety Factor, FS is shown in Figure 4.20.

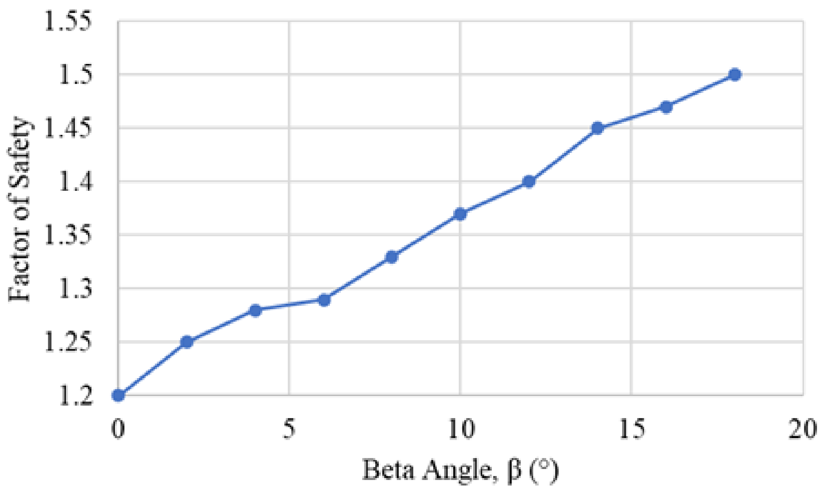

Figure 4.20: Effect of β on Safety Factor, FS.

The angles α and β selected for the slope geometry are shown in Table 4.11, varied from 0 ° to 18 °. Other soil strength parameters were kept constant (cohesion = 15 kPa, internal friction angle = 15°, and unit weight = 15 kN/m^3). Information of Critical Slip Surface for Slopes with Different Alpha and Beta angle is shown in Table 4.11.

Table 4.11: Information of Critical Slip Surface for Slopes with Different Alpha and Beta angle.

Model No.	α (°)	β (°)	Failure Surface				Factor of Safety
			Center		Radius (m)	Length of Arc (m)	
			X (m)	Y (m)			
1	18	0	4.81	21.27	10.28	7.28	1.11
2	16	0	3.45	23.79	10.27	7.27	1.15
3	14	0	3.12	23.89	10.26	7.25	1.16
4	12	0	3.29	23.55	10.25	7.24	1.16
5	10	0	2.54	24.34	10.23	7.22	1.18
6	8	0	5.08	20.61	10.21	7.20	1.18
7	6	0	5.12	21.75	10.20	7.19	1.19
8	4	0	2.53	24.00	10.18	7.14	1.19
9	2	0	1.75	24.31	10.17	7.10	1.19
10	0	0	1.37	24.81	10.15	6.96	1.20
11	0	2	2.95	23.36	10.14	6.67	1.25
12	0	4	4.04	22.54	8.82	6.32	1.28
13	0	6	4.16	22.11	8.34	6.13	1.29
14	0	8	5.44	19.94	5.71	6.04	1.33
15	0	10	5.43	20.98	6.57	5.95	1.37
16	0	12	5.19	21.24	6.88	5.79	1.40
17	0	14	6.15	20.22	5.47	5.65	1.45
18	0	16	6.28	20.10	5.33	5.43	1.47
19	0	18	5.78	20.37	5.67	5.25	1.50

In Figure 4.21, critical slip surface became bigger and deeper as the alpha angle increased. The failure arc extension caused the increase in the failure arc length (Zulkifl, 2020). From Figure 4.22, it was observed that the failure arc length increased significantly from 6.96 m to 7.28 m for alpha angle of 0 to 18 ° compare to Beta angle. The skidding force increased, when an overhead weight acted by the amount of surcharge material increased (Zulkifl, 2020). Skidding force is a sliding force, typically sideways on slippery ground causing the arc length increased. When the alpha angle increased, the critical slip became larger and deeper. Figure 4.21 and Figure 4.22 shows influence of slope angle (α) on critical slip surface and failure arc length, respectively.

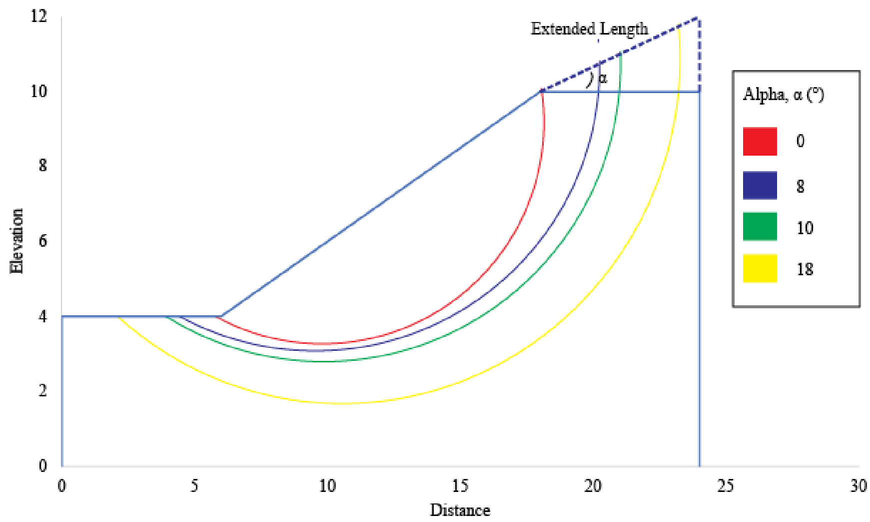

Figure 4.21: Effect of Alpha, α on length of Arc, L.

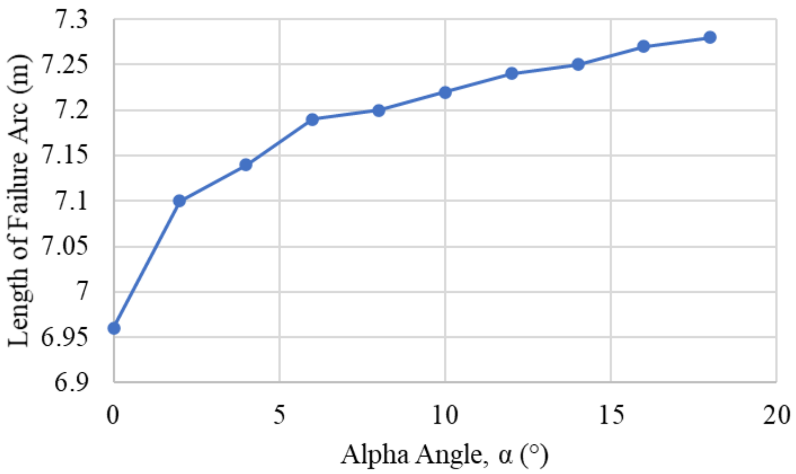

Figure 4.22: Effect of Alpha Angle, α on Length of Failure Arc, L.

Increase of beta angle, β caused critical slip surface to be smaller and shallower and this made the arc of failure arc to be lengthened as shown in Figure 4.23. A slightly shorter failure arc length was generated. It can be said that β had a major impact on safety factor compared arc length. The slope was more stable when the β angle increased as the gradient of slope reduced with the increase of beta angle. As the failure arc length was decreased due to higher β angle, higher resisting forces was and therefore increased the safety factor of slope (Zulkifl, 2020). Resisting forces act in the opposite way of driving forces, that increase the stability of slope. Effect of Beta, β on Length of Arc, L is shown in Figure 4.23 and Effect of β on Failure Arc Length, L is shown in Figure 4.24.

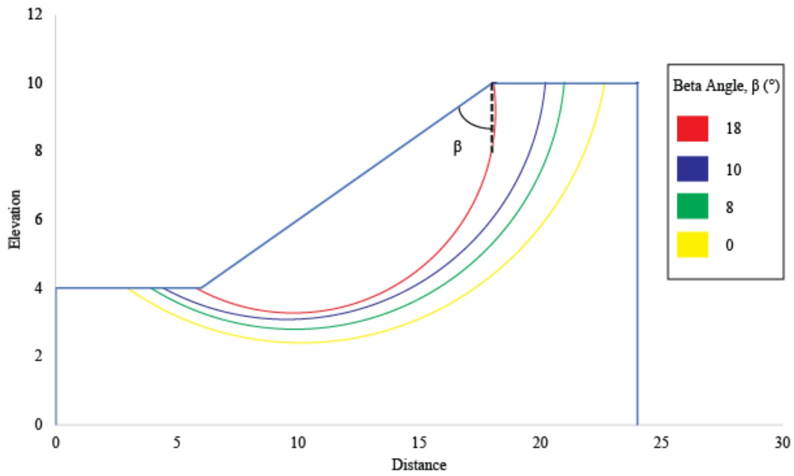

Figure 4.23: Effect of Beta, β on Length of Arc, L.

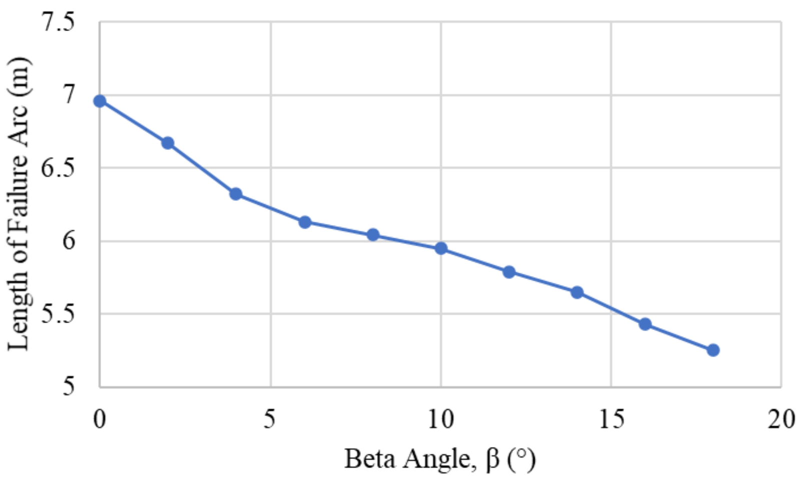

Figure 4.24: Effect of Beta Angle, β on Length of Failure Arc, L.

4.4 Combined Effect of Strength Parameter on the Factor of Safety and Critical Slip Surface

Lin and Cao (2011) studied the relationship between strength parameters and potential failure surface. The function of angle of Internal Friction (φ), Cohesion (c), Slope height (h), and Unit weight (γ) were written as:

$$\lambda = c \,/\, (\gamma \, h \tan \varphi) \tag{4.1}$$

Where,

λ = Lambda

c = Cohesion, kPa

γ = Unit Weight, kN/m^3

φ = Angle of Internal Friction, °

λ was in a function of dimensionless for Equation 4.1. There is a special relationship between the c/tanφ and surface of slip (Jiang and Yamagami, 2006). Hence, the combined effect of strength parameters on the minimum FS and critical surface of slip was investigated.

4.4.1 Effect of Cohesion, c, and Unit Weight, γ (with fixed lambda) on the Factor of Safety and Slip Surface

A research on the slope stability for soil with different γ and c on FS was studied. Here, the unit weight and cohesion were rose together, and the ratio was kept constant. The results described that the slip surface whose function was defined as λ was resulted by the combination of c and γ and refer to Equation 4.1. The values for both unit weight and cohesion were varied from 15 to 25. Whereas the soil friction angle was kept constant at 15 °. Information of Critical Slip Surface for Slopes with Different Soil Unit Weights and Cohesions is shown in Table 4.12.

Table 4.12: Information of Critical Slip Surface for Slopes with Different Soil Unit Weights and Cohesions.

Model No.	Unit Weight (kN/m^3)	Internal Friction Angle (°)	Cohesion (kPa)	Radius (m)	Entry Point Distance, l (m)	Length of Failure Arc (m)	Factor of Safety
1	15	15	15	7.49	2.88	5.86	1.08
2	16	15	16	7.49	2.88	5.86	1.08
3	17	15	17	7.49	2.88	5.86	1.08
4	18	15	18	7.49	2.88	5.86	1.08
5	19	15	19	7.49	2.88	5.86	1.08
6	20	15	20	7.49	2.88	5.86	1.08
7	21	15	21	7.49	2.88	5.86	1.08
8	22	15	22	7.49	2.88	5.86	1.08
9	23	15	23	7.49	2.88	5.86	1.08
10	24	15	24	7.49	2.88	5.86	1.08
11	25	15	25	7.49	2.88	5.86	1.08

Figure 4.25 indicated that the factor of safety remained constant as the λ value remained. The safety factor remained at 1.08 for all the models. The constant λ was due to the constant increase of both the cohesion and unit weight as represented in Equation 4.1 (Cheng, 2003). The Combined Effect of c and γ on the FS is shown in Figure 4.25.

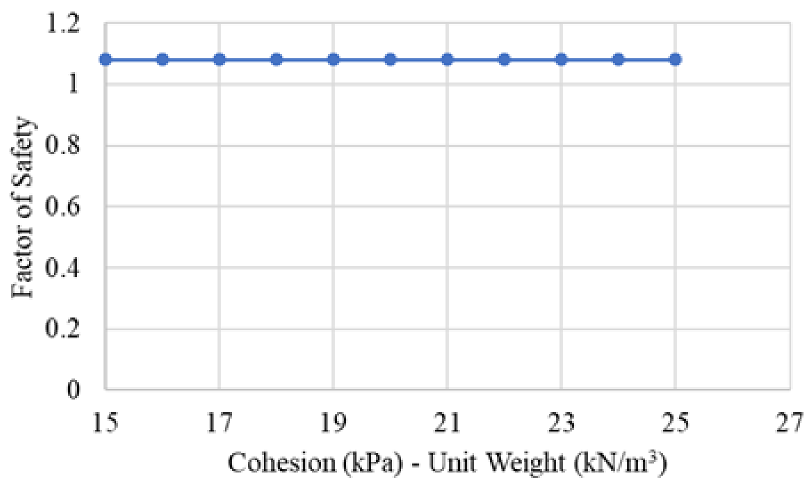

Figure 4.25: The Combined Effect of Cohesion, c and the Unit Weight, γ on the Factor of Safety.

As shown in Figure 4.27, length of failure arc was a constant of the lambda is set at 0.75 for slope with different soil unit weight and unit weight increased together respectively causing the λ to be constant although the value of both were increasing. A constant λ are led by a constant ratio of unit weight over cohesion. Unit weight acted as the driving force while the cohesion acted as the resisting force. Resisting forces acted in the opposite way of driving forces. The downslope movement of unit weight are resisted by soil cohesion which is a contributor to the resisting force. When both forces cancelled out each other, λ value was kept constant. The length of failure arc was remained at 5.86 m. Figure 4.26 shows the combined effect of cohesion, c and unit weight, γ with fixed lambda on critical surface of slip. It was found that slopes had similar critical surface of slip. According to Lin & Cao (2011), this represented a constant value for L with same critical slip surface for the constant λ. The Combined Influence of c and γ on surface of slip is shown under Figure 4.26 and The Combined influence of c and γ on L is shown in Figure 4.27.

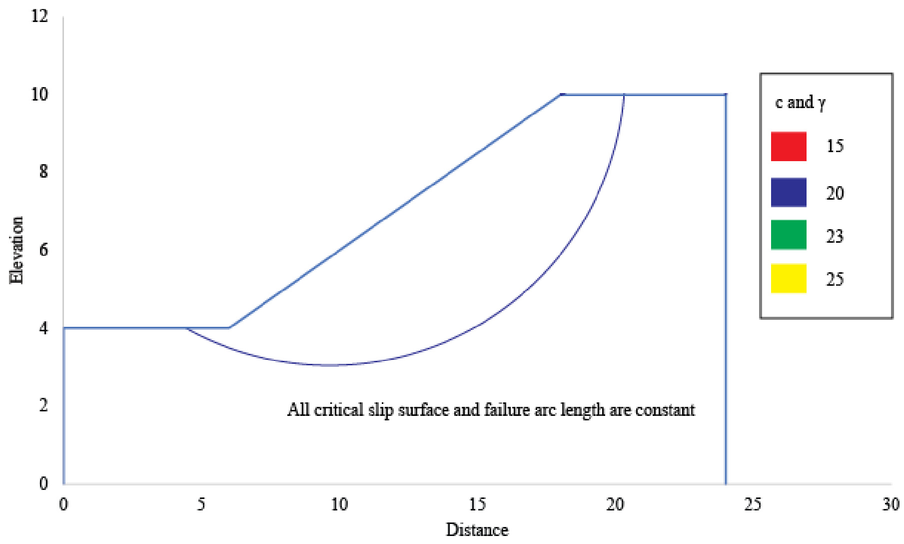

Figure 4.26: The Combined Effect of Cohesion, c and Unit Weight, γ on the Slip Surface.

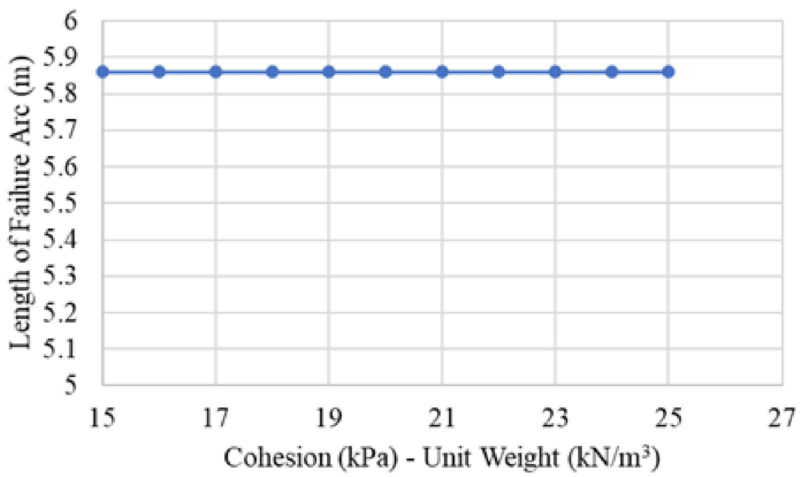

Figure 4.27: The Combined Effect of Cohesion, c and Unit Weight, γ on the Length of Failure Arc, L.

4.4.2 Effect of Internal Friction Angle, φ, and Unit Weight, γ on the Safety Factor and Slip Surface

Soil Unit Weight and angle of Internal Friction varied from 15 to 22 whereas soil cohesion was kept constant at 15 kPa. In this part, by increasing both φ and γ, the value of tan (φ) * γ increased. Figure 4.28 shows the safety factor versus tan (φ) * γ. Information of Critical Slip Surface for Slopes with Different Soil Unit Weights and Internal Friction Angle is shown in Table 4.13.

Table 4.13: Information of Critical Slip Surface for Slopes with Different Soil Unit Weights and Internal Friction Angles.

Model No.	Unit Weight (kN/m^3)	Internal Friction Angle (°)	Cohesion (kPa)	tan (φ) * γ	Radius (m)	Entry Point Distance, l (m)	Length of Failure Arc (m)	Factor of Safety
1	15	15	15	4.02	7.51	2.87	5.89	1.09
2	16	16	15	4.59	7.82	2.84	5.81	1.04
3	17	17	15	5.20	7.98	2.61	5.61	0.97
4	18	18	15	5.85	8.12	2.51	5.54	0.92
5	19	19	15	6.54	8.34	2.31	5.36	0.88
6	20	20	15	7.28	8.78	2.08	5.17	0.85
7	21	21	15	8.06	9.32	1.94	5.07	0.83
8	22	22	15	8.89	9.75	1.66	4.85	0.81

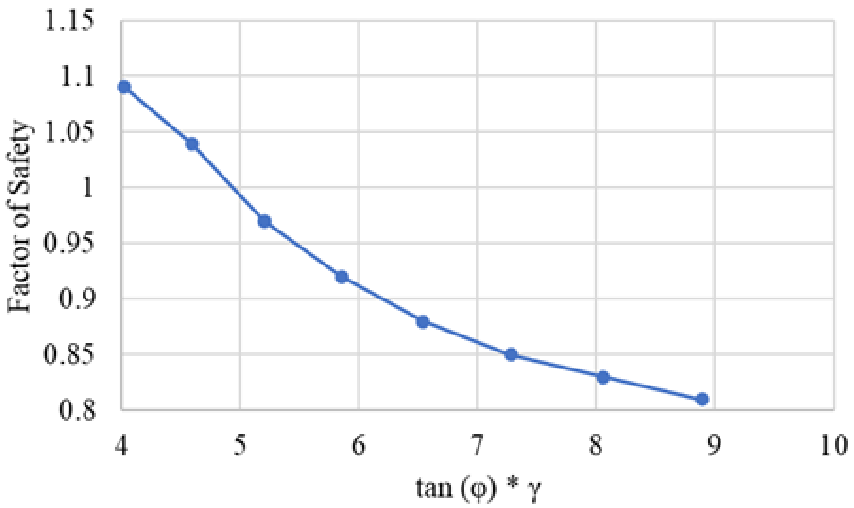

Figure 4.28: The Combined Effect of Internal Friction Angle and the Unit Weight, tan (φ) * γ on the Factor of Safety.

By increasing value of tan (φ) * γ, reduction in FS value was resulted as shown in Figure 4.28. This was due to reduction of resisting force due to the decrease of length of failure arc as the critical slip surface became smaller (Cheng, 2008). The length of failure arc decreased concavely when the tan (φ) * γ were increased. The λ values and entry length decreased together when the tan (φ) * γ values increased causing FS and length of failure arc to decrease (Zulkifl, 2020).

Figure 4.30 shows the effect of different angle of internal friction and unit weight on failure arc length. A decrease in the failure arc length was observed with the increasing of the $\gamma * tan\ \varphi$ value. This was very relevant when taking into consideration the λ value. λ decreased by increasing tan (φ) * γ value. Therefore, smaller failure arc length was caused by smaller λ and smaller entry length. Figure 4.29 shows the combined effect of φ and γ, tan (φ) * γ on critical slip surface. It found that when λ decreased, the critical slip surface became shallower and moved nearer to the slope surface. Besides, when the tan (φ) * γ increased, the failure surface area moved to the left and become smaller. The Combined Effect of φ and γ, tan (φ) * γ on Slip Surface is shown in Figure 4.29 and The Combined Effect of φ and γ, tan (φ) * γ on L is shown in Figure 4.30.

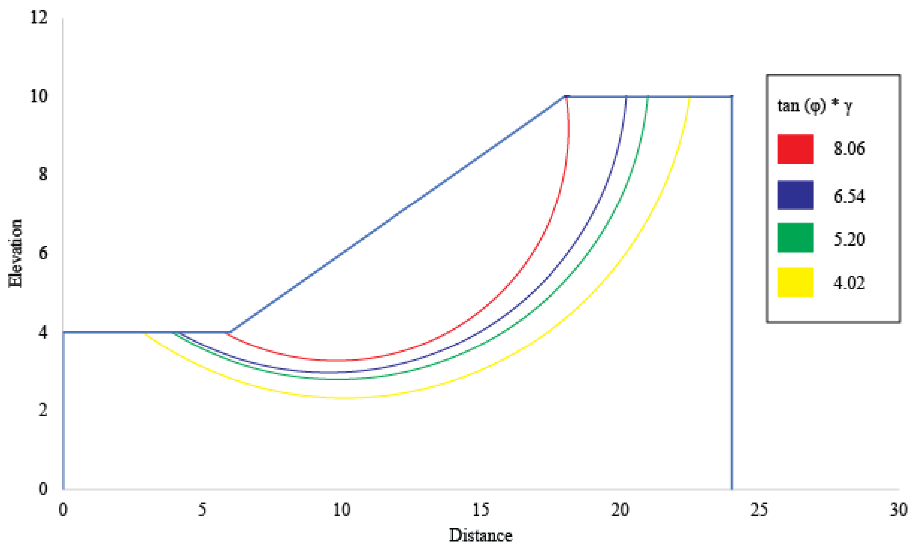

Figure 4.29: The Combined Effect of Internal Friction Angle and the Unit Weight, tan (φ) * γ on the Slip Surface.

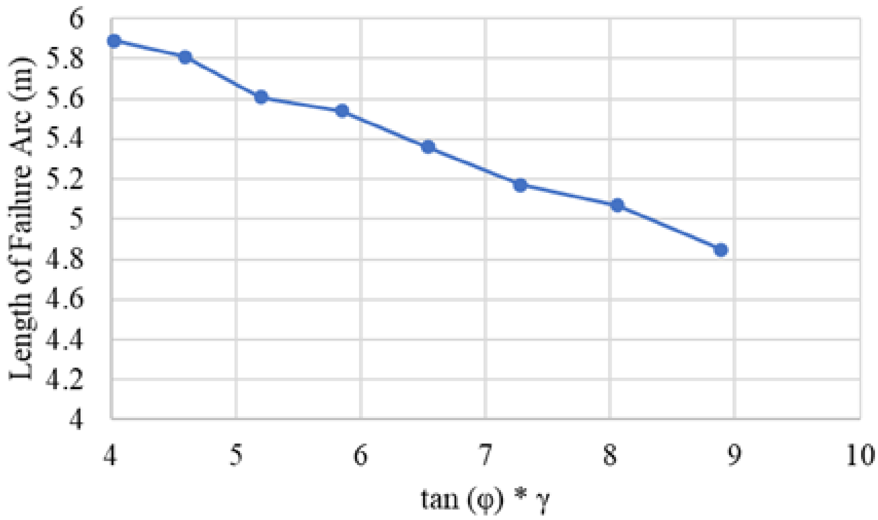

Figure 4.30: The Combined Effect of Internal Friction Angle and the Unit Weight, tan (φ) * γ on the Length of Failure Arc, L.

4.4.3 Effect of Internal Friction Angle, φ, and Cohesion, c on the Safety Factor and Critical Slip Surface

Unit Weight was remained unchanged at 15 kN/m^3, but other parameters were differed from 15 to 22. Figure 4.28 shows relationship between safety factor and $c\ and\ tan\ (\varphi)$. The relationship between these two parameters were described as *c/ tan (φ)* (Zulkifl, 2020). An increase in FS was resulted from increase of both of shear strength parameters which contributed to the resisting forces (Cheng, 2003). Information of Critical Slip Surface for Slopes with Different Soil Internal Friction Angles and Cohesions is shown in Table 4.14 and The Combined Effect of φ and c, c/ tan (φ) on the FS is shown in Figure 4.31.

Table 4.14: Information of Critical Slip Surface for Slopes with Different Soil Internal Friction Angles and Cohesions.

Model No.	Unit Weight (kN/m^3)	Internal Friction Angle (°)	Cohesion (kPa)	c/ tan (φ)	Radius (m)	Entry Point Distance, l (m)	Length of Failure Arc (m)	Factor of Safety
1	15	15	15	55.98	7.52	2.34	5.41	1.08
2	15	16	16	55.80	7.87	2.58	5.57	1.16
3	15	17	17	55.60	7.97	2.84	5.81	1.30
4	15	18	18	55.40	8.12	3.01	5.91	1.45
5	15	19	19	55.18	8.23	3.01	5.94	1.60
6	15	20	20	54.95	8.67	3.02	5.96	1.76
7	15	21	21	54.71	9.03	3.03	5.97	1.90
8	15	22	22	54.45	9.76	3.08	6.03	2.05

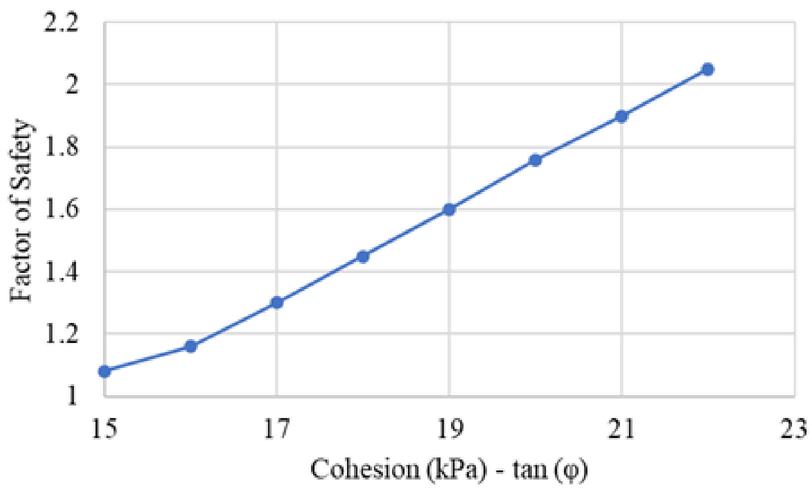

Figure 4.31: The Combined Effect of Internal Friction Angle and Cohesion, c/ tan (φ) on the Factor of Safety.

Figure 4.33 demonstrates the combination influence of c and φ on L. Although the length of arc decreased with increasing value of $c/tan\ \varphi$, however, L value was almost constant at relatively constant $c/tan\ \varphi$ (54.45 – 55.98 kPa) value as shown in Figure 4.33. The length of arc was kept at 5.41 to 6.03 m and with a range of 0.62 m, which were considered constant. The arc length kept constant due to constant $c/tan\ \varphi$ that brought to a relatively constant λ (Cheng, 2003). A relatively constant critical slip surface was caused by constant λ as well. Although the value was almost constant, however the factor of safety was increased as both cohesion and internal friction angle are resisting force. Within a soil, cohesion acts as a force that brings together molecules or like particles. Cohesion was usually affected by electrostatic force and cementing (Cheng, 2003). Internal friction angle is the measurement of shear strength due to the friction between soil particles. As c and φ are strength parameters, FS increased when the strength parameter values increased. Downslope movement of material were promoted by driving forces, whereas resisting forces deter the movement. So, the slope is more stable and when driving forces are resisted by higher resisting forces. However, the increase of both parameters caused the critical slip surface and arc length to reduce. Figure 4.32 shows the combined effect of φ and c, c/ tan (φ) on critical slip surface. When the c/ tan (φ) decreased, the slip surface became larger and deeper. The Combined Effect of φ and c, c/ tan (φ) on L is shown in Figure 4.33.

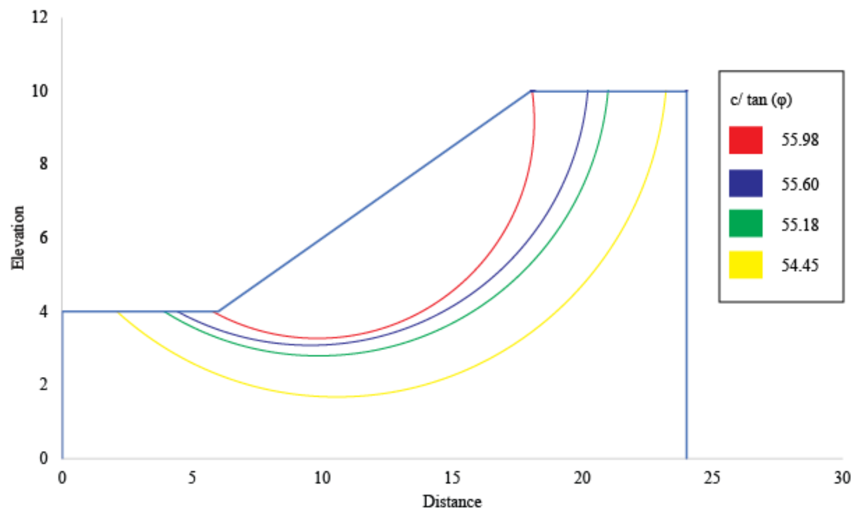

Figure 4.32: The Combined Effect of Internal Friction Angle and Cohesion, c/ tan (φ) on the Slip Surface.

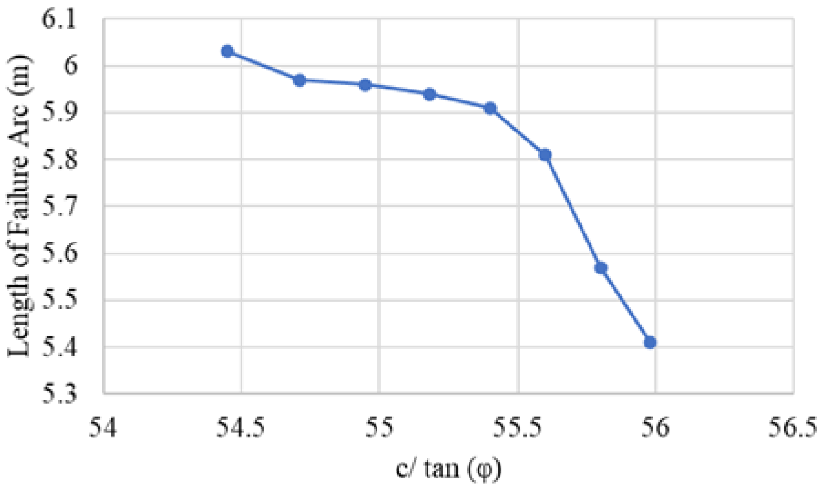

Figure 4.33: The Combined Effect of Internal Friction Angle and Cohesion, c/ tan (φ) on the Length of Failure Arc, L.

4.5 Summary

To investigate the effects of strength parameters on safety factor in slopes including soil specific weight (γ), soil cohesion (c), angle of internal friction (φ) and geometric parameters of slope including alpha (α) and beta (β) angle. An Excel Spreadsheet are developed for slope stability analysis to investigate the effects of soil strength on safety factor of slope with fixed slip surface. φ and c as resisting forces increased causing safety factor increased. Unit weight (γ), as driving force increased causing safety factor decreased.

Applying GEO5 software programs, the effect of parameters of geometry together with soil strength on minimum FS and critical slip surface are studied. As driving force, unit weight (γ), was inversely proportional to safety factor. As resistance forces which is friction angle (φ) and cohesion (c), were directly proportional to safety factor. The length of failure arc (L) value increased, and critical slip surface became larger and deeper with the increment of cohesion value (c) and unit weight (γ). However, the length of failure arc (L) value was decreased, and critical slip surface became smaller and shallower with the increment of friction angle value (φ).

Until a specific angle, the safety factor was not affected significantly by the increasing of the Alpha, α angle. This is because extra overhead surcharge to the slope that contributed to the driving forces. However, resisting force was also increased because of longer failure arc length when the soil area above failure surface was increased. Contrarily, safety factor was directly affected by increases of the Beta, β angle. The greater beta angle also showed that the slope was less steep and more stable. From perspective of the length of failure arc and critical slip surface, an increment of L happened, and critical slip surface became larger and deeper when the Alpha, α angle increased. The skidding force increased when an overhead weight acted by the amount of surcharge material increased. On the other hand, the length of failure arc and critical slip surface did not affect significantly by the changes of the Beta, β angle. The combined effect of strength parameters on the minimum FS can be studied by function of $\lambda = c / (\gamma h \tan\varphi)$. Constant safety factor was achieved with constant lambda value (λ). With that, same went to the constant slip surface that resulted by constant lambda value (λ).

CHAPTER 5

CONCLUSIONS AND RECOMMENDATIONS

5.1 Conclusions

The main objective of the study was to investigate the effects of strength parameters on safety factor in slopes including soil specific weight (γ), soil cohesion (c), angle of internal friction (φ) and geometric parameters of slope including alpha (α) and beta (β) angle. Not only that, but an Excel Spreadsheet was also developed for slope stability analysis using Simplified Bishop Method to investigate the influences of parameters of soil strength on FS of slope with fixed slip surface. Few models were numerically simulated using GEO5 software program, and the results were demonstrated as graphs to find the relationship. The following conclusions were drawn.

From the slope stability analysis using Excel Spreadsheet with fixed critical slip surface, the following conclusions were made. Soil unit weight (γ), which is contributor to the force of driving, was inversely proportional to FS. Friction angle (φ) and cohesion (c) as the contributors to the resistance forces, were directly proportional to safety factor.

From the slope stability analysis using GEO5 software program, the following conclusions were made. As a contributor to driving force, the soil unit weight (γ), was inversely proportional to safety factor of slope. As the contributors to the resistance forces, soil friction angle (φ) and cohesion (c), were directly proportional to safety factor. The length of failure arc (L) increased, and critical slip surface became larger and deeper with the increment of soil cohesion value (c) and unit weight (γ). However, the length of failure arc (L) value was decreased, and critical slip surface became smaller and shallower with the increment of soil internal friction angle value (φ). Until a specific angle, the safety factor was not affected significantly by the increasing of the Alpha, α angle. Contrarily, safety factor was directly affected by increase of the Beta, β angle. From perspective of the length of failure arc and critical slip surface, an increment of L was observed, and critical slip surface became larger and deeper when the Alpha, α angle increased. On the other hand, the length of failure arc and critical slip surface did not affect significantly by the changes of the Beta, β angle. Constant safety factor and critical slip surface was achieved with constant lambda value (λ). A greater value of failure arc length (L) and a deeper and larger slip surface were resulted by a greater lambda value (λ). On the other hand, a shorter failure arc length and shallower slip surface was resulted by smaller lambda value (λ). To make it clear, safety factor and failure arc length (L) did not exist any relationship. By applying below formula, the failure arc length (L) was mathematically correlated with lambda (λ).

5.2 Recommendations for future work

Only a limited range of parameters of soil strength were investigated due to time limitation in this study. Furthermore, only the factors had an impact on the failure arc length had been researched due to the restriction of the accessible software programs.

For further studies, the following analysis can be brought about which is correlated to the study. A greater range of parameters of the soil strength are modeled and analyzed. The level of ground water table is to be taken into consideration, as well as considering pore-air pressure effect in unsaturated soils. More variables regarding the geometry of slope are to be considered (e.g., height of slope). Lastly, proposed to improve the excel by adding the function of automatically locating the critical slip surface and finding the minimum Fs (by using Python software program).

REFERENCES

Abramson, L. W. (2002). *Slope stability and stabilization methods*: John Wiley & Sons Inc.

Albataineh, N. (2006). *Slope stability analysis using 2D and 3D methods*. The University of Akron.

Alkema, D., & Hack, H. (2011). *Stability assessment of man-made slopes, A case study in Yen Bai*. (Master of Science), University of Twente.

Anagnosti, P. (1969). *Three-dimensional stability of fill dams*.

Anderson, M., & Richards, K. (1987). Modelling slope stability: the complimentary nature of geotechnical and geomorphological approaches. *Slope Stability: Geotechnical Engineering and Geomorphology*. John Wiley and Sons., 1-9.

Aryal, K. (2008). Differences between LE and FE methods used in slope stability evaluations. *Paper presented at the The 12th International Conference of International Association for Computer Methods and Advances in Geomechanics (IACMAG).*

Azadmanesh, M., & Arafati, N. (2012). A Comparison on Slope Stability Analysis of Aydoghmoosh Earth Dam by Limit Equilibrium, Finite Element and Finite Difference Methods. *IJCEBM*, 115-124.

Azzouz, A., Baligh, M., & Ladd, C. (1981). Three-dimensional stability analyses of four embankment failures. *Paper presented at the Proceedings of the 10th International Conference on Soil Mechanics and Foundation Engineering, Volume 3*, Stockholm.

Azzouz, A. S., & Baligh, M. M. (1983). *Loaded areas on cohesive slopes. Journal of Geotechnical Engineering*, 109(5), 724-729.

Baker, R. (1980). Determination of the critical slip surface in slope stability computations. *International journal for numerical and analytical methods in geomechanics*, 4(4), 333-359.

Baker, R., & Leshchinsky, D. (1987). Stability analysis of conical heaps. *Soils and Foundations*, 27(4), 99-110.

Baligh, M. M., & Azzouz, A. S. (1975). End effects on stability of cohesive slopes. *Journal of the Geotechnical Engineering Division*, 101(11), 1105-1117.

Baligh, M. M., Azzouz, A. S., & Ladd, C. C. (1977). *Line loads on cohesive slopes*.

Bojorque, J., De Roeck, G., & Maertens, J. (2008). Comments on 'Two-dimensional slope stability analysis by limit equilibrium and strength reduction methods' by Y.M. Cheng, T. Lansivaara and W.B. Wei [*Computers and Geotechnics 34 (2007)* 137–150]. *Computers and Geotechnics,* 35(2), 305-308.

Bolton, H., Heymann, G., & Groenwold, A. (2003). Global search for critical failure surface in slope stability analysis. *Engineering Optimization,* 35(1), 51-65.

Boutrup, E., & Lovell, C. (1980). Searching techniques in slope stability analysis. *Engineering Geology,* 16(1), 51-61.

Bromhead, E. (1992). *The stability of slopes*: Taylor & Francis.

Carter, R. (1971). Computer oriented slope stability analysis by method of slices. *MSCE Thesis,* Purdue University.

Cavoundis, S. (1987). On the ratio of factors of safety in slope stability analyses. *Geotechnique*, 37(2), 207-210.

Celestino, T., & Duncan, J. (1981). Simplified search for non-circular slip surface. *Paper presented at the Proceedings of the 10th International Conference on Soil Mechanics and Foundation Engineering*, Stockholm, Sweden.

Chen, R., & Chameau, J.-L. (1983). Three-dimensional limit equilibrium analysis of slopes. *Geotechnique,* 33(1), 31-40.

Cheng, Y. (2003). Location of critical failure surface and some further studies on slope stability analysis. *Computers and Geotechnics*, 30(3), 255-267.

Cheng, Y. (2008). Reply to "Comments on 'Two-dimensional slope stability analysis by limit equilibrium and strength reduction methods' by YM Cheng, T. Lansivaara and WB Wei," by J. Bojorque, G. De Roeck and J. Maertens. *Computers and Geotechnics*, 35(2), 309.

Cheng, Y., Lansivaara, T., & Wei, W. (2007). Two-dimensional slope stability analysis by limit equilibrium and strength reduction methods. *Computers and Geotechnics*, 34(3), 137-150.

Cheng, Y., & Lau, C. (2008). *Slope stability analysis and stabilization: new methods and insight*: Psychology Press.

Cheng, Y., Li, L., Chi, S.-c., & Wei, W. (2007). Particle swarm optimization algorithm for the location of the critical non-circular failure surface in two-dimensional slope stability analysis. *Computers and Geotechnics,* 34(2), 92-103.

Cheng, Y., Li, L., Lansivaara, T., Chi, S., & Sun, Y. (2008). An improved harmony search minimization algorithm using different slip surface generation methods for slope stability analysis. *Engineering Optimization*, 40(2), 95-115.

Cho, S. E., & Lee, S. R. (2001). Instability of unsaturated soil slopes due to infiltration. *Computers and Geotechnics*, 28(3), 185-208.

Das, B. M. (2010). Principles of geotechnical engineering: *Cl-Engineering*.

Duncan, J. M. (1996). State of the art: limit equilibrium and finite-element analysis of slopes. *Journal of Geotechnical Engineering*, 122(7), 577-596.

Duncan, J. M., & Wright, S. G. (2005). *Soil strength and slope stability*: John Wiley & Sons, Incorporated.

Gens, A., Hutchinson, T., & Cavounidis, S. (1988). Three-dimensional analysis of slides in cohesive soils. *Geotechnique*, 38(1), 1-23.

Giger, M. W., & Krizek, R. J. (1976). Stability of vertical corner cut with concentrated surcharge load. *Journal of the Geotechnical Engineering Division*, 102(1), 31-40.

Goh, A. T. (1999). Genetic algorithm search for critical slip surface in multiple-wedge stability analysis. *Canadian Geotechnical Journal*, 36(2), 382-391.

Griffiths, D., & Lane, P. (1999). Slope stability analysis by finite elements. *Geotechnique*, 49(3), 387-403.

Griffiths, D., & Lu, N. (2005). Unsaturated slope stability analysis with steady infiltration or evaporation using elasto-plastic finite elements. *International journal for numerical and analytical methods in geomechanics*, 29(3), 249-267.

Hack, R., Alkema, D., Kruse, G. A., Leenders, N., & Luzi, L. (2007). Influence of earthquakes on the stability of slopes. *Engineering geology*, 91(1), 4-15.

Hovland, H. J. (1979). Three-dimensional slope stability analysis method. *Journal of Geotechnical and Geoenvironmental Engineering*, 105(ASCE 14549 Proceeding), 693-695.

Hungr, O. (1987). An extension of Bishop's simplified method of slope stability analysis to three dimensions. *Geotechnique*, 37(1), 113-117.

Jiang, J.-C., & Yamagami, T. (2006). Charts for estimating strength parameters from slips in homogeneous slopes. *Computers and Geotechnics*, 33(6), 294-304.

Jiang, J.-C., & Yamagami, T. (2008). A new back analysis of strength parameters from single slips. *Computers and Geotechnics*, 35(2), 286-291.

Jibson, R. W. (2011). Methods for assessing the stability of slopes during earthquakes—A retrospective. *Engineering Geology*, 122(1), 43-50.

Khabbaz, H. F., Behzad, Nucifora, C. (2012). Finite Element Methods against Limit Equilibrium Approaches for Slope Stability Analysis. *Geomechanical Society and New Zealand Geotechnical Society*, 5.

Leshchinsky, D., & Baker, R. (1986). Three-dimensional slope stability: end effects. *Soils and Foundations*, 26(4), 98-110.

Leshchinsky, D., Baker, R., & Silver, M. (1985). Three-dimensional analysis of slope stability. *International Journal for Numerical and Analytical Methods in Geomechanics*, 9(3), 199-223.

Leshchinsky, D., & Huang, C.-C. (1992). Generalized three-dimensional slope-stability analysis. *Journal of Geotechnical Engineering*, 118(11), 1748-1764.

Li, K. S., & White, W. (1987). Rapid evaluation of the critical slip surface in slope stability problems. *International Journal for Numerical and Analytical Methods in Geomechanics*, 11(5), 449-473.

Lin, H., & Cao, P. (2011). Potential slip surfaces of slope with strength parameters. *Advanced Materials Research*, 243, 3315-3318.

Lin, H., & Cao, P. (2012). Limit Equilibrium Analysis for the Relationships Among Slope c, phi and Slip Surface. *Electronic Journal of Geotechnical Engineering*, 17, 185-195.

Malkawi, A. I. H., Hassan, W. F., & Sarma, S. K. (2001). Global search method for locating general slip surface using Monte Carlo techniques. *Journal of Geotechnical and Geoenvironmental Engineering*, 127(8), 688-698.

Matsui, T., & San, K. (1992). Finite element slope stability analysis by shear strength reduction technique. *Soils and Foundations*, 32(1), 59-70.

McCombie, P., & Wilkinson, P. (2002). The use of the simple genetic algorithm in finding the critical factor of safety in slope stability analysis. *Computers and Geotechnics*, 29(8), 699-714.

Michalowski, R. (1989). Three-dimensional analysis of locally loaded slopes. *Geotechnique*, 39(1), 27-38.

Namdar, A. (2011). Geometry in Slope Modeling and Design. *e -Journal of Science & Technology* (e-JST)(22), 9-21.

Nguyen, V. U. (1985). Determination of critical slope failure surfaces. *Journal of Geotechnical Engineering*, 111(2), 238-250.

Revilla, J., & Castillo, E. (1977). The calculus of variations applied to stability of slopes. *Geotechnique*, 27(1), 1-11.

Seed, R. B., Mitchell, J. K., & Seed, H. B. (1990). Kettleman hills waste landfill slope failure. II: stability analyses. *Journal of Geotechnical Engineering*, 116(4), 669-690.

Sengupta, A., & Upadhyay, A. (2009). Locating the critical failure surface in a slope stability analysis by genetic algorithm. *Applied Soft Computing*, 9(1), 387-392.

Siegel, R. A. (1975). *Computer analysis of general slope stability problems: Indiana Department of Transportation and Purdue University*.

Spencer, E. (1967). A method of analysis of the stability of embankments assuming parallel inter-slice forces. *Geotechnique*, 17(1), 11-26.

Swan, C. C., & Seo, Y. K. (1999). Limit state analysis of earthen slopes using dual continuum/FEM approaches. *International journal for numerical and analytical methods in geomechanics*, 23(12), 1359-1371.

Ugai, K. (1985). Three-dimensional stability analysis of vertical cohesive slopes. *Soils and Foundations*, 25(3), 41-48.

Ugai, K. (1988). Three-dimensional slope stability analysis by slice methods. *Paper presented at the Proceedings of the Sixth International Conference on Numerical Methods in Geomechanics* (Vol. 2, pp. 1369-1374).

Wang, L. (2020). The Effects of Various Factors on Slope Stability. *Science and Engineering Inverstigations* Vol. 4 (6), 22-35.

Wen, S. (2016). Analysis of influence of factors of slope stability. *Applied Mechanics and Materials* Vols 256-259, 34-38.

Whitman, R. V., & Bailey, W. A. (1967). Use of computers for slope stability analysis. *Journal of Soil Mechanics & Foundations Div*.

Wright, S. G. (1969). *A study of slope stability and the undrained shear strength of clay shales*. University of California, Berkeley.

Wright, S. G., Kulhawy, F. H., & Duncan, J. M. (1973). Accuracy of equilibrium slope stability analysis. *Journal of the Soil Mechanics and Foundations Division*, 99(10), 783-791.

Xing, Z. (1988). Three-dimensional stability analysis of concave slopes in plan view. *Journal of Geotechnical Engineering*, 114(6), 658-671.

Zolfaghari, A. R., Heath, A. C., & McCombie, P. F. (2005). Simple genetic algorithm search for critical non-circular failure surface in slope stability analysis. *Computers and Geotechnics*, 32(3), 139-152.

Zulkifl, A. (2020). Study of critical failure surface influencing factors for slope. *Critical Slip surface*, 34(2), 300-323.